

New Fluorescent Probes for ATP and other Phosphates

Dissertation zur Erlangung des Doktorgrades der Naturwissenschaften

(Dr. rer. nat.)

an der

Fakultät für

**– Chemie und Pharmazie –
der Universität Regensburg**



vorgelegt von

Thomas Lang

aus Regensburg

im Mai 2012

Die vorliegende Arbeit wurde in der Zeit von Mai 2009 bis April 2012 unter Anleitung von Herrn Prof. Dr. O. Wolfbeis am Institut für Analytische Chemie, Chemo- und Biosensorik der Universität Regensburg angefertigt.

Promotionsgesuch eingereicht am: 14.05.2012

Kolloquiumstermin: 06.06.2012

Prüfungsausschuss

Vorsitzender: Prof. Dr. J. Daub

Erstgutachter: Prof. Dr. O. S. Wolfbeis

Zweitgutachter: Prof. Dr. K. Zeitler

Drittprüfer: Prof. Dr. H. Brunner

Acknowledgements

First of all I would like to thank **Prof. Dr. O. S. Wolfbeis** for the great opportunity and experience of working at his institute.

Furthermore, I want to thank PD Dr. **Michael Schäferling** for acting as my supervisor.

A lot of people have contributed greatly in various ways to this work. From the very beginning **Thomas Hirsch** was a tremendous source of help and encouragement. **Matthias Stich** and **Martin Link** instantly made me feel at home. The latter patiently trying to “learn me his experience” (Yogi Berra). Ceaselessly, **Péter Kele** allowed me to benefit from the genius of the Pannonians. **Do’minique Grögel** was always open to discussions. **Daniela Achatz** and **Gisela Hierlmeier** are way too nice for their own good. I want to express my deep appreciation for what you all have been doing and for your friendship.

Moreover I want to thank **Judith, Raphaela, Joachim, Franzi, Steffi, Frau Stoiber, Reham** and **Sayed, James, Bobbel**, and each and every member of the Institute of Analytical Chemistry, Chemo- and Biosensors including the **mass spec department**, our (former) apprentice **Martin Rappl**, and my bachelor students, especially **Uwe Käfer**.

Good connections to other institutes are always important. Hence, **Hannes Krauss, Klaus Harrar, Thomas Ehrenschwender, Dominik Frank, Ludwig Pils, Diana Drettwan** and **Christine Thoms** duly deserve to be mentioned here.

Lunch is also important, so are the people who voluntarily offer their company, thank you for doing just that!

I hope my friends know how grateful I am for everything - for them!

I lack the words, however, to express how grateful I am and to describe how much my parents, **Renate** and **Pius Lang** have contributed to making this work possible and to making me the person I am (faults are definitely not theirs to blame). Thank you so much!

Without deviation from the norm, progress is not possible!

Frank Vincent Zappa

Dedicated to *Marc Studtmann*

Inhaltsverzeichnis

1. Introduction	8
2. Background.....	17
2.1 Viologens as New Phosphate-sensitive Fluorescent Probes	17
2.2 NIR Dye as New Phosphate-sensitive Fluorescent Probe.....	28
3. Experimental.....	37
3.1 Materials and Methods.....	37
3.1.1 Instrumental Set Up	37
3.1.2 Chemicals.....	38
3.1.2 Synthesis	39
4. Viologen-Type Probes for Phosphates.....	49
4.1 Results and Discussion	49
4.1.1 HPTS with TEAPB as fluorescent probe for the detection of ATP and other phosphates.....	51
4.1.2 APTS with TEAPB as fluorescent probe for the detection of ATP and other phosphates.....	56
4.1.3 HPTS with TEABB as fluorescent probe for the detection of ATP and other phosphates.....	61
4.1.4 APTS with TEABB as fluorescent probe for the detection of ATP and other phosphates.....	67
4.1.5 HPTS with TEAPeB as fluorescent probe for the detection of ATP and other phosphates.....	72
4.1.6 APTS with TEAPeB as fluorescent probe for the detection of ATP and other phosphates.....	78
4.2 Summary	83
5. Cyanine-Type Probe for Phosphates	90
5.1 Results and Discussion	90
5.1.1 [Zn(FEW-L)]: Absorption-Based sensing of ATP and other phosphate species	92
5.1.2 [Zn(FEW-L)]: Emission-Based sensing of ATP and other phosphate species...	97
5.1.3 [Zn(FEW-L)]: Optimization of composition of the complex	101
5.2 Conclusion	103
6. Summary	107
6.1 English	107
6.2 Deutsch	108

7. Curriculum Vitae	109
8. List of Publications.....	111

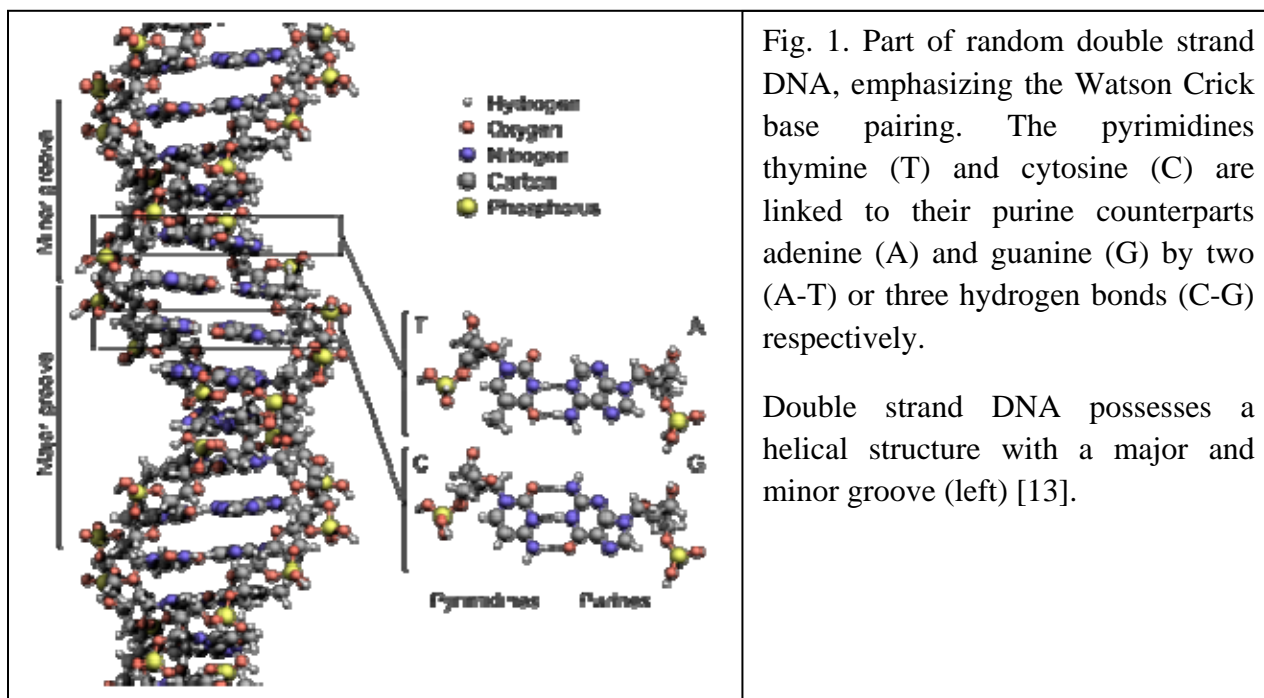
1. Introduction

“In hoc signo vinces!” or “Ἐν τούτῳ νικά!” are the famous words addressed to Constantine the Great by God himself in the wake of the Battle of the Milvian Bridge according to Lactantius (Latin) [1, 2] or Eusebios of Caesarea (Greek) [2, 3]. This event, which sees its 1700th anniversary this year, Constantine becoming the protégée of the Christian god, had a tremendous impact on the course of world history and science. On the one hand the Christian Roman Empire retained a big portion of the strength and power of its pagan predecessor and grew extremely resilient in the east, surviving well into the 15th century [4, 5]. On the other hand, the unfortunate symbiosis of church and state put a hold to freedom of expression and thought, interrupting scientific progress for one millennium.

Atomic hypothesis, for instance, was postulated by Democritus, Leucippus and Epicurus as early as the 4th century BCE [6]. One of the latter’s most dedicated pupils, Lucretius, expressed in his famous work *De rerum natura* that life is merely based on, and governed by, the movement, association and dissociation of atoms [7, 8]. It took well over 1500 years before John Dalton [9] would pick such theories up again and thus enabled science to continue where it had been forced into silence. A generation after atomic hypothesis had reemerged, Friedrich Miescher discovered a substance he labeled “nuclein” which happened to be crude DNA. After further examination he concluded that it must be distinct from proteins, as it contains no sulphur and does not undergo typical reactions. He also found out that phosphor, in the form of phosphoric acid, formed an essential part and gained a vague idea of its true structure [10]. Miescher and many other contemporaries, however, thought, while deeming “nuclein” to be very interesting, that it was too simple a compound to play a crucial part in genetics. Thus proteins were believed to be responsible for heredity. Hence progress in that field stalled.

It was as late as 1952 when most doubts were dismissed by the Hershey-Chase experiment, using radioactive labeling [11]. Now DNA was rightfully regarded as the driving force behind heredity. Thus, after 2000 years, Lucretius, who was called insane by Christian historians of the Dark Ages [8], was rehabilitated: life is indeed to a very large extent a matter of atoms, their association and dissociation.

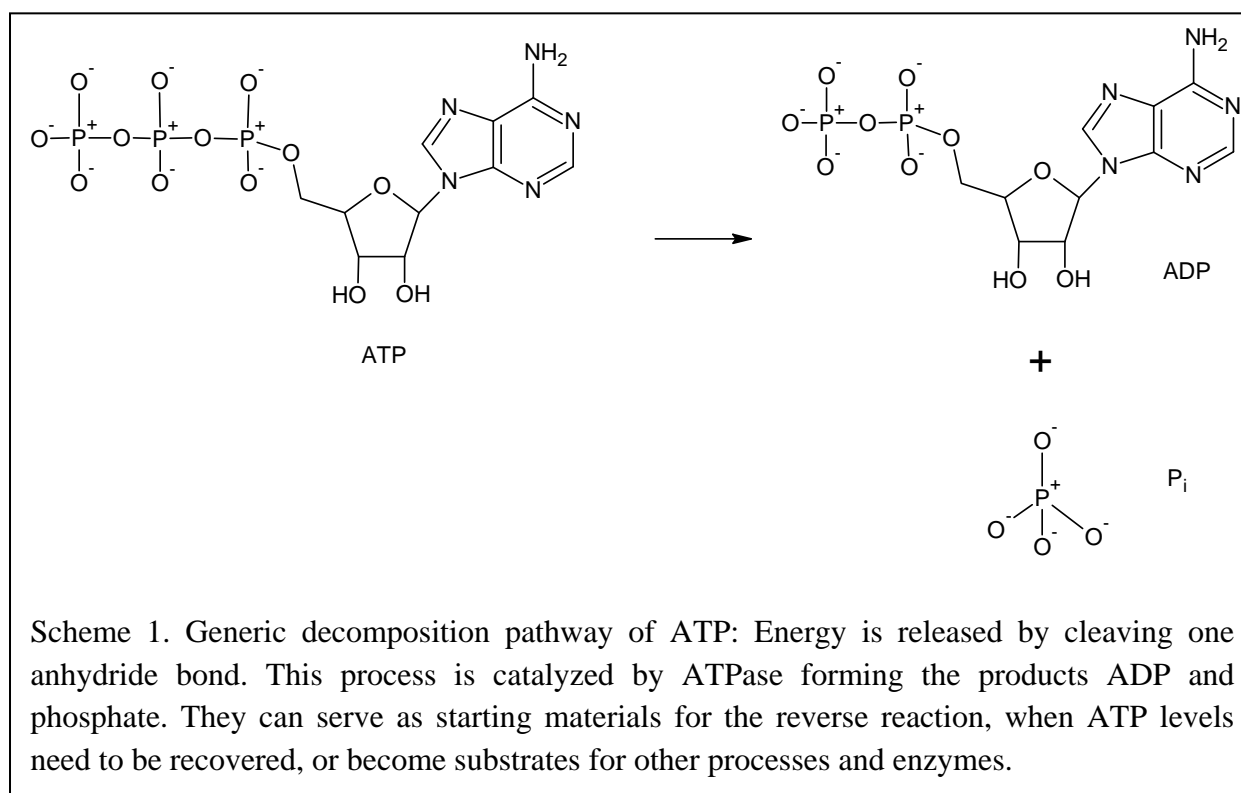
Early and important basic information on the structure of DNA was provided by Phoebus Levine and William Astbury. Yet it was not until 1953 when Rosalind Franklin (X-ray), James Watson and Francis Crick came up with the correct solution: a helical structure of two strands consisting of a backbone of sugars, linked by phosphate esters, and carrying bases which link these two strands by hydrogen bonds (Fig.1). Watson and Crick presented the first



model of this base pairing in DNA with the help of Chargaff's experimental results [12]. A DNA strand consists of nucleotides: phosphate ester, sugar (deoxyribose) and base. These bases are aromatic compounds: purines such as adenine and guanine possess ten cyclic conjugated π -electrons according to Hückel's rule ($4n+2$; $n=2$) over two rings, while the pyrimidine-based thymine and cytosine constitute of a single ring of six electrons ($n=1$). Hence π -stacking and other π - π interactions are important factors of stability in the 3-D structure of DNA [14].

Nucleotides do not merely constitute a structural element of DNA but together with nucleosides they serve as substrates or products in enzymatic processes as well. Adenosine mono-, di-, and triphosphate (AMP, ADP, ATP), guanine mono-, di-, and triphosphate (GMP, GDP, GTP), cyclic adenosine and cyclic guanine monophosphate (cAMP, cGMP), phosphate (P_i) and pyrophosphate (diphosphate, PP_i) are most prominently featured in such reactions [15-24]. The various enzymes involved therein can be divided into several categories: Phosphotransferases or kinases [25] in particular catalyze phosphorylations, phosphatases [26] cleave esters, and phosphorylases [27] are responsible for phosphorolysis. The cell cycle

is regulated by cyclin-dependent kinases (CDKs) [28] while G protein-coupled receptor kinase plays a key role in signal transduction [29, 30]. Furthermore, ATPases decompose ATP (Scheme 1) in order to provide energy for important processes and reactions. P-type



ATPases, for instance, control and enable the transport of certain ions across biological membranes against gradient between the extra- and intracellular spaces.

One such enzyme is H^+/K^+ ATPase which is crucial in the production of gastric acid [31]. Furthermore, sarco/endoplasmic reticulum Ca^{2+} ATPase (SERCA) is transferring Ca^{2+} ions after muscle relaxation [32], Cu^{2+} is transported by ATP7B, the Wilson disease protein [33]. Additionally, there are several such enzymes like ATP13A2 [34] which deal with less common or more complex, organic ions [35-37]. Finally, Na^+/K^+ -ATPase is an important part of the cell membrane as it regulates the ionic gradient of cell by maintaining a relatively low level of sodium inside and a relatively high concentration of sodium outside [38].

Apparently, these enzymes are abundant, versatile, diverse and crucial to many processes inside the human body or organisms in general. Hence it is a great goal in biology to gain insight into the principles according to which they are working and how they can be controlled, inhibited or stimulated, rendering them a substantial drug target. Monitoring alterations in phosphate concentrations can provide essential information for the better

understanding of the working mechanism of these enzymes. Thus detection of phosphates is an important analytical task.

Various sensing schemes have been reported which harness amperometry, or electrochemistry in general, (capillary) electrophoresis, and (ion) chromatography [39, 40]. Procedures derived from protocols focused on the Taussky-Shorr [41] reagent (including ammonium molybdate) are still widely used. However, this approach is rather complicated and sensitive to many external influences like pH. Other fluorescent setups apply enzymes and/or organic dyes but these methods, too, suffer from the same drawbacks [40]. Another way of monitoring phosphate concentrations, with ATP in particular, is radioactive labeling with ^{32}P . This very sensitive method suffers from the poor reputation of radiochemistry which entails a legislation that demands high and expensive standards of quality management, operational safety and waste-disposal to be maintained [42]. Lanthanide complexes, especially these of europium and terbium, have become a convenient alternative though. Numerous sensing schemes have been designed which are based on such compounds [39, 40, 43, 44]. Complexes based on ruthenium, aluminum, cadmium, copper and zinc have been reported [42, 43, 45, 46]. Furthermore sensors utilizing aptamers [47], carbon nanotubes [48], and polythiophene [49, 50] and polyamine probes have been published [51].

As could be seen, the field of available phosphate-sensitive probes offers a large pool of compounds and schemes for a variety of applications. Yet there are disadvantages that need to be taken into account: cross-sensitivity, complicated set-ups which are expensive and require trained personnel, limit of detection, toxicity in biological matrices or *in vivo* studies, pH-dependence of probe, and many more [39, 40, 43, 46, 51].

Hence, new probes are expected not to suffer from the shortcomings of these current probes. Accordingly, the design and screening of new fluorescent probes for the detection of ATP and other phosphates is an important task and the main objective of this work. It is focused on possible application for enzymatic assays for ATPase, GTPase, protein kinases and adenylyl cyclase.

- [1] Laktanz, A. Städele, *Laktanz – Die Todesarten der Verfolger / De Mortibus Persecutorum*, Brepols, Turnhout, **2003**
- [2] S. N. C. Lieu, D. Montserrat, *From Constantine to Julian, Pagan and Byzantine Views*, Routledge, New York, **1996**
- [3] Eusebius von Caesarea, H. A. Gärtner, H. Kraft, P. Haeuser, *Kirchengeschichte*, Wissenschaftliche Buchgesellschaft, Darmstadt, **2006**
- [4] S. Mitchell, *A history of the Later Roman Empire*, Blackwell, Malden, Oxford & Carlton, **2009**
- [5] A. Cameron, *The Byzantines*, Blackwell, Malden, Oxford & Carlton, **2006**
- [6] C. Bailey, *The Greek Atomists and Epicurus*, Russell & Russell, Kent, **1964**
- [7] Lukrez; K. Büchner, *De Rerum Natura / Welt aus Atomen*, Reclam, Stuttgart, **1973**
- [8] G. B. Conte, J. B. Solodow, D. Fowler, G. W. Most, *Latin Literature*, John Hopkins, Baltimore & London, **1994**
- [9] F. Greenway, *John Dalton and the Atom*, Cornell University Press, Ithaca, **1966**
- [10] R. Dahm, *Friedrich Miescher and the Discovery of DNA*, Dev Biol, **2005**, 278, 274-288
- [11] A. Hershey, M. Chase, *Independent function of Viral Protein and Nucleic in Growth of Bacteriophage*, J Gen Physiol, **1952**, 1, 39-56
- [12] J. Watson, D. Crick, *Molecular Structure of Nucleic Acids*, Nature, **1953**, 171, 737-738
- [13] http://en.wikipedia.org/wiki/File:DNA_Structure%2BKey%2BLabelled.pn_NoBB.png
(accessed on 04-05-2012)
- [14] P. Yakovchuk, E. Protozanova, M. D. Frank-Kamenetskii, *Base-stacking and base-pairing contributions into thermal stability of the DNA double helix*, Nucleic Acids Res, **2006**, 34, 2, 564-574
- [15] C. M. Spangler, C. Spangler, M. Göttle, Y. Shen, W.J. Tang, R. Seifert, M. Schäferling, *A fluorimetric assay for real-time monitoring of adenylyl cyclase activity based on norfloxacin*, Anal Biochem, **2008**, 381, 86-93

- [16] F. Facchiano, A. Facchiano, A. M. Facchiano, *The role of transglutaminase-2 and its substrates in human disease*, Front Biosci, **2006**, 11, 1758-73
- [17] J. R. Knowles, *Enzyme-Catalyzed Phosphoryl Transfer Reactions*, Ann Rev Biochem, **1980**, 49, 877-919
- [18] K. Hibino, T. Shibata, T. Yanagida, Y. Sako, *Activation Kinetics of RAF Protein in the Ternary Complex of RAF, RAS-GTP, and Kinase on the Plasma Membrane of Living Cells*, J Biol Chem, **2011**, 286, 36460-36468
- [19] C. P. Vellano, F. Shu, S. Ramineni, C. K. Yates, G. G. Tall, J. R. Helper, *Activation of the Regulator of G Protein Signaling 14–Gai1-GDP Signaling Complex Is Regulated by Resistance to Inhibitors of Cholinesterase-8A*, Biochemistry, **2011**, 50, 752-762
- [20] G. S. Ahluwalia, J. L. Grem, Z. Hao, D. A. Cooney, *Metabolism And Action Of Amino Acid Analog Anti-Cancer Agents*, Pharmac Ther, **1990**, 46, 243-271
- [21] R. Abramovitch, E. Tavor, J. Jacob-Hirsch, E. Zeira, N. Amariglio, O. Pappo, G. Rechavi, E. Galun, A. Hnigman, *A Pivotal Role of Cyclic AMP-Responsive Element Binding Protein in Tumor Progression*, Cancer Res, **2004**, 64, 1338-1346
- [22] F. Polleux, T. Morrow, A. Ghosh, *Semaphorin 3A is a chemoattractant for cortical apical dendrites*, Nature, **2000**, 404, 567-574
- [23] S. Y. Breusegem, H. Takahashi, H. Giral-Arnal, X. Wang, T. Jiang, J. W. Verlander, P. Wilson, S. Miyazaki-Anzai, E. Sutherland, Y. Caldas, J. T. Blaine, H. Segawa, K. Miyamoto, N. P. Barry, M. Levi, *Differential regulation of the renal sodium-phosphate cotransporters NaPi-IIa, NaPi-IIc, and PiT-2 in dietary potassium deficiency*, Am J Physiol Renal Physiol, **2009**, 297, 350-361
- [24] S. K. Kim, D. H. Lee, J. Hong, J. Yoon, *Chemosensors for Pyrophosphate*, Accounts Chem Res, **2009**, 42, 23-31
- [25] K. R. Hallows, R. Alzamora, H. Li, F. Gong, C. Smolak, D. Neumann, N. M. Pastor-Soler, *AMP-activated protein kinase inhibits alkaline pH- and PKA-induced apical vacuolar H⁺-ATPase accumulation in epididymal clear cells*, Am J Physiol Cell Physiol, **2009**, 296, 672–681

- [26] Y. Ma, I. Szostkiewicz, A. Korte, D. Moes, Y. Yang, A. Christmann, E. Grill, *Regulators of PP2C Phosphatase Activity Function as Abscisic Acid Sensors*, *Science*, **2009**, 324, 1064-1068
- [27] S. K. Dasa, U. K. Sokhia, S. K. Bhutiaa, B. Azaba, Z. Sua, D. Sarkara, P. B. Fishera, *Human polynucleotide phosphorylase selectively and preferentially degraded microRNA-221 in human melanoma cells*, *PNAS*, **2010**, 11948-11953
- [28] J. W. Harper, P. D. Adams, *Cyclin-Dependent Kinases*, *Chem Rev*, **2001**, 2511-2526
- [29] J. A. Pitcher, N. J. Freedman, R. J. Lefkowitz, *G Protein-Coupled Receptor Kinases*, *Annu Rev Biochem*, **1998**, 67, 653-692
- [30] D. M. Rosenbaum, S. G. F. Rasmussen, B. K. Kobilka, *The structure and function of G-protein-coupled receptors*, *Nature*, **2009**, 459, 356-363
- [31] H. Luo, J. Wang, W. Deng, N. Huang, K. Zuo, *Bisabolangelone, a gastric H⁺/K⁺-ATPase inhibitor: homology modeling and docking study*, *Med Chem Res*, **2011**, 2, 9780-9784
- [32] J. V. Møller, C. Olesen, A. L. Winther, P. Nissen, *The sarcoplasmic Ca²⁺-ATPase: design of a perfect chemi-osmotic pump*, *Q Rev Biophys*, **2010**, 43, 501-566
- [33] P. C. Bull, G. R. Thomas, J. M. Rommens, J. R. Forbes, D. W. Cox, *The Wilson disease gene is a putative copper transporting P-type ATPase similar to the Menkes gene*, *Nat Genet*, **1993**, 5, 327-337
- [34] A. Ramirez, A. Heimbach, J. Grpndemann, B. Stiller, D. Hampshire, L. P. Cid, I. Goebel, A. F. Mubaidin, A. Wriekat, J. Roeper, A. Al-Din, A. M. Hillmer, M. Karsak, B. Liss, C. G. Woods, M. I. Behrens, C. Kubisch, *Hereditary parkinsonism with dementia is caused by mutations in ATP13A2, encoding a lysosomal type 5 P-type ATPase*, *Nat Genet*, **2006**, 38, 1184- 1191
- [35] X. Tang, M. S. Halleck, R. A. Schlegel, P. Williamson, *A Subfamily of p-Type ATPases with Aminophospholipid Transporting Activity*, *Science*, **1996**, 272, 1495-1497
- [36] M. Solioz, C. Vulpe, *CPx-type ATPase: a class of P-type ATPases that pump heavy metals*, *Trends in Biological Sciences*, **1996**, 21, 237-241

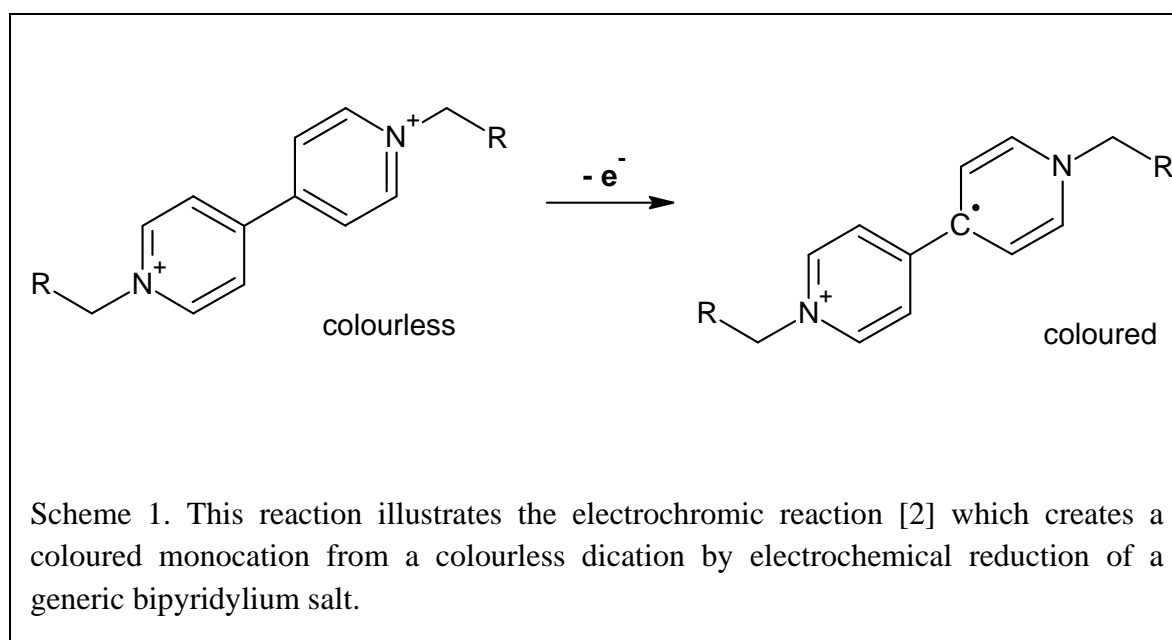
- [37] C. Rensing, Y. Sun, B. Mitra, B. Rosen, *Pb(II)-translocating P-type ATPases*, J Biol Chem, **1998**, 49, 32614-32617
- [38] D. S. Alves, G. A. Farr, P. Seo-Mayer, M. J. Caplan, *AS160 Associates with the Na⁺,K⁺-ATPase and Mediates the Adenosine Monophosphate-stimulated Protein Kinase-dependent Regulation of Sodium Pump Surface Expression*, Mol Biol Cell, **2010**, 21, 4400-4408
- [39] M. Turel, A. Dürkop, A. Yegorova, A. Karasyov, Y. Scripintes, A. Lobnik, *Microtiterplate phosphate assay based on luminescent quenching of a terbium complex amenable to decay time detection*, Anal Chim Acta, **2010**, 675, 42-48
- [40] A. Dürkop, M. Turel, A. Lobnik, O. S. Wolfbeis, *Microtiter plate assay for phosphate using a europium-tetracycline complex as a sensitive luminescent probe*, Anal Chim Acta, **2006**, 555, 292-298
- [41] H. H. Taussky, E. Shorr, *A Microcolorimetric Method For The Determination Of Inorganic Phosphorus*, J Biol Chem, **1953**, 202, 675-685
- [42] A. Riechers, F. Schmidt, S. Stadlbauer, B. König, *Detection of Protein Phosphorylation on SDS-PAGE Using Probes with a Phosphate-Sensitive Emission Response*, Bioconjugate Chem, **2009**, 20, 804-807
- [43] C. M. Spangler, C. Spangler, M. Schäferling, *Luminescent Lanthanide Complexes as Probe for the Determination of Enzyme Activities*, Ann N.Y. Acad Sci, **2008**, 1130, 138-148
- [44] C. Spangler, C. M. Spangler, M. Soerer, M. Schäferling, *Kinetic determination of the GTPase activity of Ras proteins by means of a luminescent terbium complex*, Anal Bioanal Chem, **2009**, 394, 989-996
- [45] R. Joseph, J. P. Chinta, C. P. Rao, *Calix[4]arene-Based 1,3-Diconjugate of Salicyl Imine Having Dibenzyl Amine Moiety (L): Synthesis, Characterization, Receptor Properties toward Fe²⁺, Cu²⁺, and Zn²⁺, Crystal Structure of Its Zn²⁺ and Cu²⁺ Complexes, and Selective Phosphate Sensing by the [ZnL]*, Inorg Chem, **2011**, 50, 7050-7058
- [46] S. Akar, V. Tek, A. Bange, L. Lagos, P. Gill, N. Munroe, T. G. Thundat, *Development of a Biosensor for Detection of Phosphate Species in Uranium Contaminated Ground Water and Wastewater Sediments*, WM2010 Conference, March 7-11, **2010**, Phoenix, AZ

- [47] W. Li, Z. Nie, X. Xu, Q. Shen, C. Deng, J. Chen, S. Yao, *A sensitive, label free electrochemical aptasensor for ATP detection*, *Talanta*, **2009**, 78, 954-958
- [48] C. B. Jacobs, M. J. Peairs, B. J. Venton, *Review: Carbon nanotube based electrochemical sensors for biomolecules*, *Anal Chim Acta*, **2010**, 662, 105-127
- [49] C. Li, M. Numata, M. Takeuchi, S. Shinkai, *A Sensitive Colorimetric and Fluorescent Probe Based on a Polythiophene Derivative for the Detection of ATP*, *Angew Chem Int Ed*, **2005**, 44, 6371-6374
- [50] H. Ho, M. Boissinot, M. G. Bergeron, G. Corbeil, Kim Dore, D. Boudreau, M. Leclerc, *Colorimetric and Fluorometric Detection of Nucleic Acids Using Cationic Polythiophene Derivatives*, *Angew Chem Int Ed*, **2002**, 41, 1548-1551
- [51] C. Spangler, M. Schäferling, O. S. Wolfbeis, *Fluorescent probes for microdetermination of inorganic phosphates and bisphosphates*, *Microchim Acta*, **2008**, 161, 1-39

2. Background

2.1 Viologens as New Phosphate-sensitive Fluorescent Probes

Bipyridylium salts can easily be reduced electrochemically to form radical anions (Scheme 1) of mostly blue colour. Hence they are duly referred to as viologens [1]. Owing to its electron



deficiency, the dication is found to readily form charge-transfer complexes with electron-rich donors thus creating a variety of other coloured compounds [1, 3].

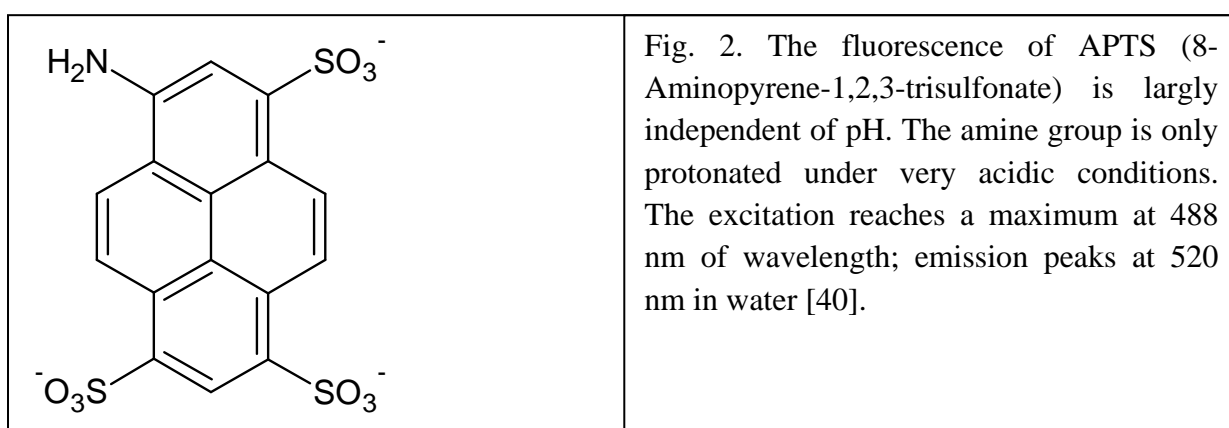
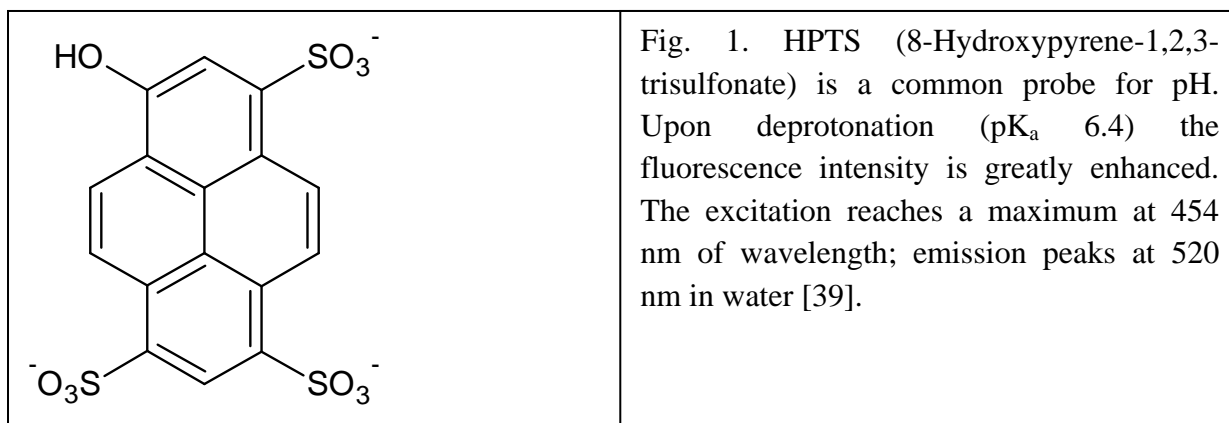
The still common herbicide paraquat consists of a mere 4,4'-bipyridine which is alkylated by chloromethane. In spite of its continued popularity it is toxic to animals and human beings coupled with serious long time effects [4]. Owing to the fact that it is easily available it has become a common substance for self-poisoning in suicides in many third world countries.

The toxicity of paraquat and its low lethal dose is partly due to the fact that viologens can coordinate biomolecules electrostatically, through π -stacking, π - π and cation- π interactions [4-6]. Yet viologens have become an integral part of many useful applications. Accordingly,

these various interactions with (bio)molecules have been utilized. Hence viologens have been extensively exploited [7-11] as potential DNA intercalating labels. Moreover, sensor schemes for nitrite [12], oxygen [13] and dopamines [14] have been developed which include a bipyridinium component. As viologens are potentially strong redox active species [15] they have attracted attention in the field of electrochemistry. Cyclic voltammetry in particular has been widely used to investigate and characterize these salts [16-18]. Furthermore, they were utilized to electrochemically switch the emission of rare earth complexes [19]. Additionally interactions with nanomaterials [20] have been examined, e.g. graphene oxide [21] and silver nanoparticles [21, 22].

Viologens are powerful quenchers of fluorescence [23, 24]. This trait was harnessed for numerous applications in (bio)chemical sensing [25, 26]. The 3-D structure of proteins, for instance, could be examined. A fluorescent ruthenium complex was linked to a viologen group via a spacer which coordinates to the protein. Quenching of the complex was observed for one tertiary structure while not for the other. This is due to the fact that upon an alteration in the folding of the involved peptide bonds quenching is induced through a closer proximity of the bipyridinium groups of the chain [27].

The worldwide prevalence of diabetes is conjectured to be 3% [28]. Hence, one of the most common sensors is for glucose. Thus, the design and production of simple, inexpensive and sensitive devices for this task is an important field of analytical chemistry, pharmacy and medicine. Accordingly glucose has remained in the focus of attention for the application of new sensing schemes. A frequent approach is utilizing boronic acid derivatives as probes [29]. They adhere to the following concept. Diols and sugars in particular coordinate on these moieties and thereby induce a transformation in the 3-D structure from a trigonal planar geometry to a tetrahedron. Thus the reactivity and characteristic features of such a probe are crucially altered enabling optical, electrochemical, or other read outs [29, 30]. Viologens have also been intensively examined as parts of sensing schemes for glucose either with [31] or without boronic acids involved [32-34]. Singaram *et al.* have contrived an approach to the detection of saccharides that utilizes the quenching effect of bipyridinium salts on HPTS [35, 36], APTS [37] and other like molecules [38]. These compounds are common aromatic dyes (Fig. 1, 2). Their fluorescence is quenched in the presence of viologens that were modified with a boronic acid moiety. When a sugar coordinates at this position, the 3-D structure is impacted and quenching can no longer be exercised. Hence an increase in fluorescence



corresponds to a rise of glucose concentration. A similar approach was contrived here. Three different viologens (Fig. 3) were synthesized which varied in the length of the alkyl spacer: TEAPB, TEABB, and TEAPeB. These will interact with APTS and HPTS by forming weak complexes with electrostatic, π - π and cation- π interactions [25, 41] thus enabling electron transfer [25] leading to decreased fluorescence intensity (Scheme 2). Nucleotides and nucleosides, however, will strongly bind to viologens in the following way. The anionic oxygen groups of the phosphoric acid will readily form salts with the quarternary ammonium cation on the side chain while the aromatic bases will prefer the aromatic bipyridin site [42-44].

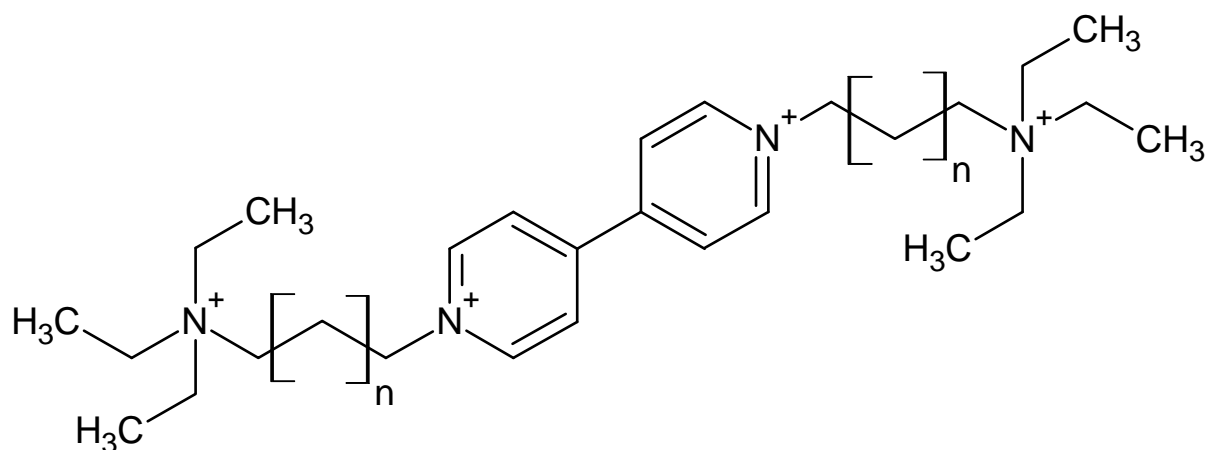
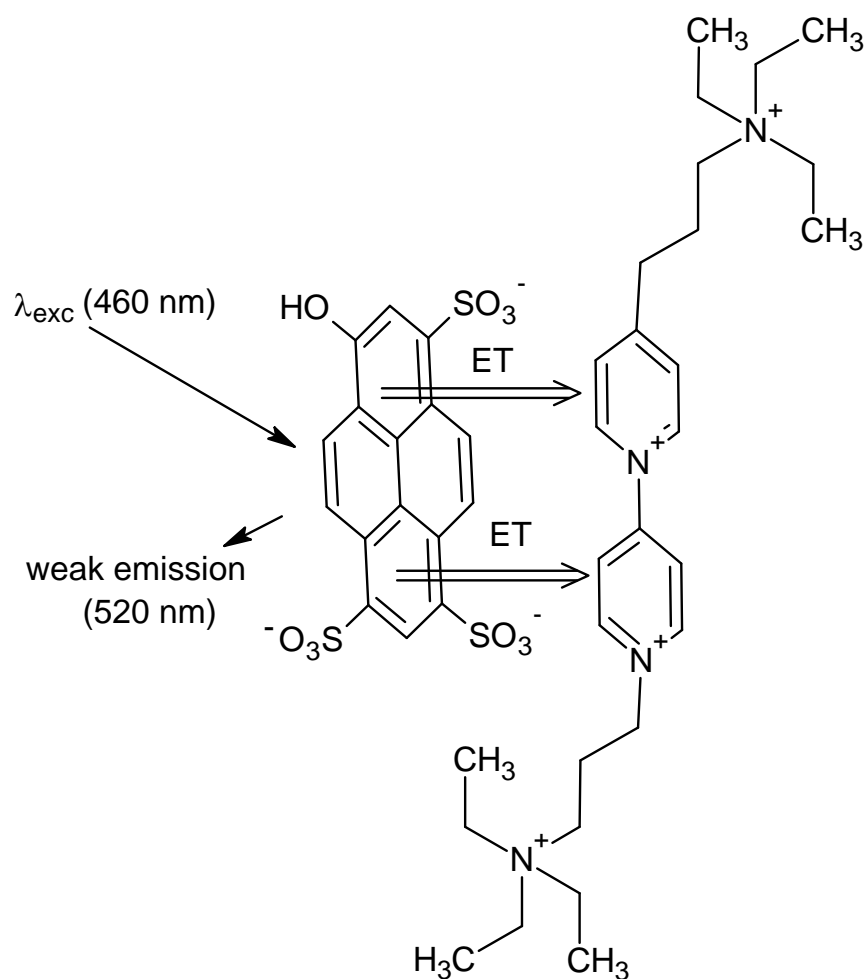


Fig. 3. Chemical structure of 1,1'-di[3-(triethylammonium)alkyl]-4,4'-bipyridylum ($n=1, 2, 3$) which has been designed as a quencher for sensing phosphate.

1,1'-di[3-(triethylammonium)propyl]-4,4'-bipyridylum (TEAPB), $n=1$

1,1'-di[3-(triethylammonium)butyl]-4,4'-bipyridylum (TEABB), $n=2$

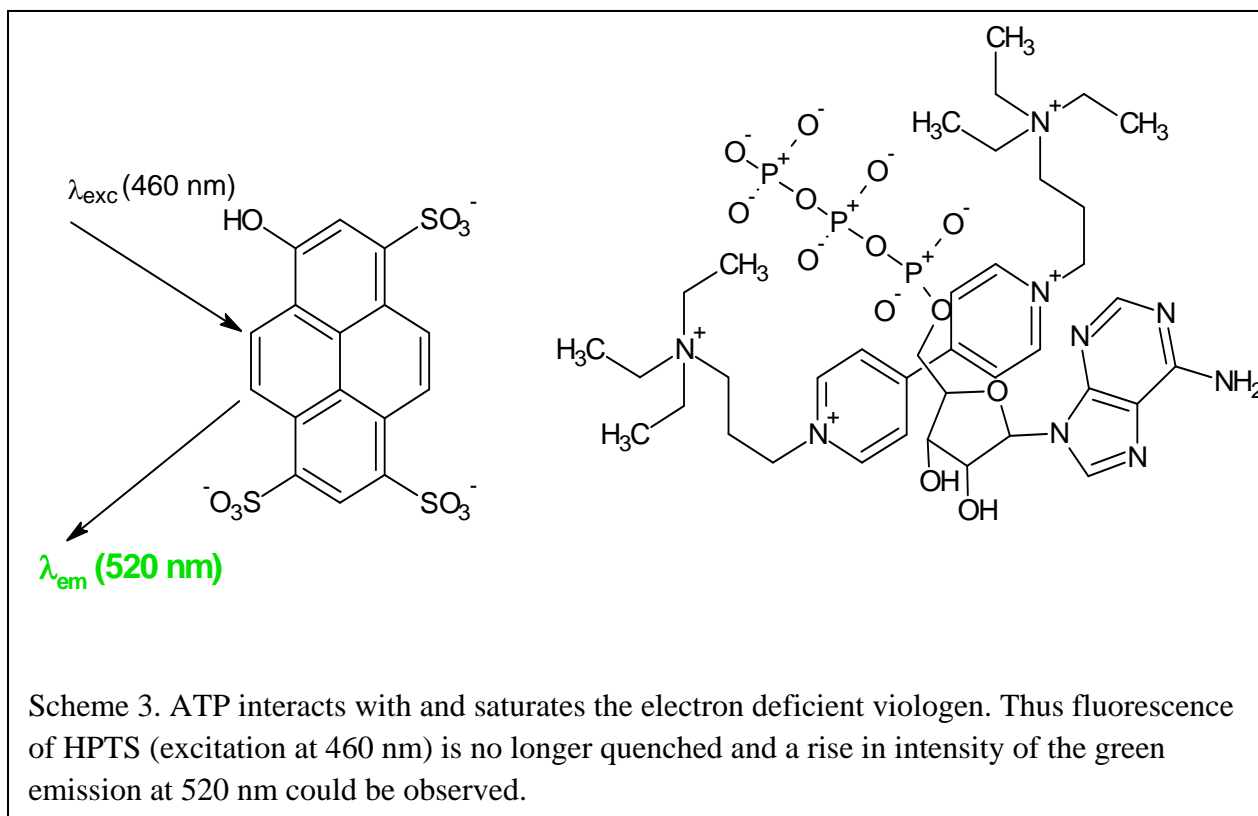
1,1'-di[3-(triethylammonium)pentyl]-4,4'-bipyridylum (TEAPeB), $n=3$



Scheme 2. Depicted here is the mechanism of fluorescence quenching of pyrenes (excitation around 450 nm) by viologens through electron transfer (ET). HPTS is coordinated by TEAPB through electrostatic, π - π and cation- π interactions. Thus electron transfer is enabled entailing to a decrease in fluorescence intensity on HPTS.

It is surmised that upon interaction with ATP, for instance, the side chains of the viologens will align and fix ATP on the phosphate groups saturating the electron deficient quencher. Thus the fluorescence of the pyrene is reinstated (Scheme 3), and the concentration of phosphate can be determined from the intensity of fluorescence.

Theoretically, different types of nucleoside phosphates can be distinguished by their nucleic base (guanine or adenine) or lack thereof, the number of phosphate groups (mono-, di, triphosphates) and structure (cAMP, cGMP). The first factor determines the extent of π - π and π -cation interactions between the nucleotide and the viologen. The number of phosphate



groups corresponds to the number of possible negative charges. The quenchers possess four cationic charges on two sites where ionic bonds can be formed, i.e. the rings and the peripheral quaternary nitrogen atoms. Additional factors to be considered are the size and the 3-D structure of the viologen. These have crucial impacts on the strength of the interaction between phosphates and viologens. It also should be taken into account that these nucleotides can affect the fluorescence of the pyrenes in a similar fashion and thus lowering fluorescence intensity though to a lesser degree.

The length of the alkyl chain carrying the quaternary ammonium function is also crucial in terms of complexation and therefore quenching potential of the bipyridinium unit. The mode of complexation determines the possible orientation of the viologens with respect to the analytes and thus the way and extent of binding to HPTS or APTS.

The objective of the following chapters is to report on the synthesis and quenching potential of three different quenchers TEAPB (chapter 4.1.1/2), TEABB (chapter 4.1.3/4), TEAPeB (chapter 4.1.5/6) as phosphate-sensitive probes, with HPTS and APTS as organic dyes with high fluorescence intensity. Their resolution, response time and capacity of quenching have been examined.

- [1] P. M. S. Monk, N. M. Hodgkinson, *Charge-transfer complexes of the viologens: effects of complexation and the rate of electron transfer to methyl viologen*, *Electrochim Acta*, **1998**, 43, 245-255
- [2] R. J. Mortimer, T. S. Varley, *Novel Color-Reinforcing Electrochromic Device Based on Surface-Confined Ruthenium Purple and Solution-Phase Methyl Viologen*, *Chem Mater*, **2011**, 23, 4077-4082
- [3] L. Pospil, J. Kuta, J. Volke, *Adsorption Coupled Electrode Kinetics Of Bipyridylum-Based Herbicides*, *Electroanal Chem Interfac Electrochem*, **1975**, 58, 217-227
- [4] M. L. Roldan, G. Corrado, O. Francioso, S. Sanchez-Cortes, *Interaction of soil humic acids with herbicide paraquat analyzed by surface-enhanced Raman scattering and fluorescence spectroscopy on silver plasmonic nanoparticles*, *Anal Chim Acta*, **2011**, 699, 87-96
- [5] A. Hori, S. Takatani, T. K. Miyamoto, M. Hasegawa, *Luminescence from π - π stacked bipyridines through arene-perfluoroarene*, *Cryst Eng Comm*, **2009**, 11, 567-569
- [6] Y. Gao, D. Wu, *4-(4-Pyridyl)pyridinium perchlorate methanol solvate*, *Acta Cryst*, **2010**, 1068
- [7] E. G. Hvastkos, D. A. Buttry, *Recent advances in electrochemical DNA hybridization sensors*, *Analyst*, **2010**, 135, 1817-1829
- [8] S. Takenaka, T. Ihara, M. Takagi, *Bis-9-acridinyl Derivative Containing a Viologen Linker Chain: Electrochemically Active Intercalator for Reversible Labelling of DNA*, *Chem Comm*, **1990**, 1585-1487
- [9] G. Bellia, E. Vittorino, Salvatore, Sortino, *A novel molecular conjugate for the simultaneous DNA oxidation and targeted delivery of nitric oxide triggered by light*, *Photochem Photobiol Sci*, **2009**, 8, 1534-1538
- [10] P. P. Neelakandam, K. S. Sanju, D. Ramaiah, *Effect of Bridging Units on Photophysical and DNA Binding Properties of a Few Cyclophanes*, *Photochem Photobiol*, **2010**, 86, 282-289
- [11] J. E. Satterwhite, A. M. Pugh, A. S. Danell, E. G. Hvastkovs, *Electrochemical Detection on ant-Benzo[a]pyrene Diol Epoxide DNA Damage on TP53 Codon 273 Oligomers*, *Anal Chem*, **2011**, 83, 3327-3335

- [12] D. Quan, W. Shin, *A Nitrite Biosensor Based on Co-immobilizaion of Nitrite Reductase and Viologen-modified Chitosan on a Glassy Carbon Electrode*, *Sensors*, **2010**, 10, 6241-6256
- [13] L. Roberts, R. Lines, S. Reddy, J. Hay, *Investigation of polyviologens as oxygen indicators in food packaging*, *Sens Actuat B*, **2011**, 152, 63-67
- [14] C. Hsu, V.S. Vasantha, P. Chen, K. Ho, *A new stable $Fe(CN)_6^{3-/4-}$ -immobilized poly(butyl viologen)-modified electrode for dopamine determination*, *Sens Actuat B*, **2009**, 137, 313-319
- [15] W. W. Porter, T. P. Vaid, A. L. Rheingold, *Synthesis and Characterization of a Highly Reducing Neutral "Extended Viologen" and the Isostructural Hydrocarbon 4,4''''-Di-n-octyl-p-quarterphenyl*, *J Am Chem Soc*, **2005**, 127, 16559-16566
- [16] S. C. Dorman, R. A. O'Brien, A. T. Lewis, E. A. Slater, A. Wierzbicki, P. W. Hixon, R. E. Sykora, A. Mirjafari, J. H. Davis, *A new block for electroactive organic materials? Synthesis, cyclic voltammetry, single crystal X-ray structure, and DFT treatment of a unique boron-based viologen*, *Chem Comm*, **2011**, 47, 9072-9074
- [17] M. Bonchio, M. Carraro, G. Casella, V. Causin, F. Rastrelli, G. Saielli, *Thermal behavior and electrochemical properties of bis(trifluoromethanesulfonyl)amide and dodecatungstosilicate viologen dimmers*, *Phys Chem Chem Phys*, **2012**, 14, 2710-2717
- [18] I. Yamaguchi, N. Mizoguchi, M. Sato, *Self-Doped Polyphenylenes Containing Electron-Accepting Viologen Side Group*, *Macromol*, **2009**, 42, 4416-4425
- [19] K. Nakamura, K. Kanazawa, N. Kobayashi, *Electrochemically controllable emission and coloration by using europium(III) complex and viologen derivatives*, *Chem Comm*, **2011**, 47, 10064-10066
- [20] N. Vlachopoulos, J. Nissfolk, M. Möller, A. Briancon, D. Corr, C. Grave, N. Leyland, R. Mesmer, F. Pichot, M. Ryan, G. Boschloo, A. Hagfeldt, *Electrochemical aspects of display technology based on nanostructured titanium dioxide with attached viologen chromophores*, *Electrochim Acta*, **2008**, 53, 4065-4071
- [21] S. Krishnamurty, I. V. Lightcap, P. V. Kamat, *Electron transfer between methyl viologen radicals and graphene oxide: Reduction, electron storage and discharge*, *J Photochem Photobiol A: Chemistry*, **2011**, 221, 214-219

- [22] L. Guerrini, J. V. Garcia-Ramos, C. Domingo, S. Sanchez-Cortes, *Nanosensors Based on Viologen Functionalized Silver Nanoparticles: Few Molecules Surface-Enhanced Raman Spectroscopy Detection of Polycyclic Aromatic Hydrocarbons in Interparticle Hot Spots*, *Anal Chem*, **2009**, 81, 1418-1425
- [23] T. Ogoshi, A. Harada, *Chemical Sensors Based on Cyclodextrin Derivatives*, *Sensors*, **2008**, 8, 4961-4982
- [24] A. L. Holt, J. P. Bearinger, C. L. Evans, S. A. Carter, *Chemically robust conjugated polymer platform for thin-film sensors*, *Sensor Actuator B*, **2010**, 143, 600-605
- [25] L. Chen, D. W. McBranch, H. Wang, R. Helgeson, F. Wudl, D. G. Whitten, *Highly sensitive biological and chemical sensors based on reversible fluorescence quenching in a conjugated polymer*, *Proc Natl Acad Sci USA*, **1999**, 96, 12287-12292
- [26] S. W. Thomas, G. D. Joly, T. M. Swager, *Chemical Sensors Based on Amplifying Fluorescent Conjugated Polymers*, *Chem Rev*, **2007**, 107, 1339-1386
- [27] K. J. Oh, K. J. Cash, K. W. Plaxco, *Beyond Molecular Beacons: Optical Sensors Based on the Binding-Induced Folding of Proteins and Polypeptides*, *Chem Eur J*, **2009**, 15, 2244-2251
- [28] S. Wild, G. Roglic, A. Green, R. Sicree, H. King, *Global Prevalence of Diabetes*, *Diabetes Care*, **2004**, 27, 1047-1053
- [29] J. S. Hansen, J. B. Christensen, J. F. Petersen, T. Hoeg-Jensen, J. C. Norrild, *Arylboronic acids: A diabetic eye on glucose sensing*, *Sens Actuat B*, **2012**, 161, 45-79
- [30] J. Yan, G. Springsteen, S. Deeter, B. Wang, *The relationship among pKa, pH, and binding constants in the interactions between boronic acids and diols – it is not as simple as it appears*, *Tetrahedron*, **2004**, 60, 11205-11209
- [31] D. Das, D. Kim, D. Park, Y. Shim, *A Glucose Sensor Based on an Aminophenyl Boronic Acid Bonded Conducting Polymer*, *Electroanal*, **2011**, 23, 2036-2041
- [32] C. P. Sousa, A. S. Polo, R. M. Torresi, S. I. Córdoba de Torresi, W. A. Alves, *Chemical modification of a nanocrystalline TiO₂ film for efficient electric connection of glucose oxidase*, *J Coll Interf Sci*, **2010**, 346, 442-447

- [33] D.B. Cordes, S. Gamsey, B. Singaram, *Fluorescent Quantum Dots with Boronic Acid Substituted Viologens To Sense Glucose in Aqueous Solution*, *Angew Chem Int Ed*, **2006**, 45, 3829-3832
- [34] N. DiCesare, M. R. Pinto, K. S. Schanze, J. R. Lakowicz, *Saccharide Detection Based on the Amplified Fluorescence Quenching of a Water-Soluble Poly(phenylene ethynylene) by a Boronic Acid Functionalized Benzyl Viologen Derivative*, *Langmuir*, **2002**, 18, 7785-7787
- [35] S. Gamsey, A. Miller, M. M. Olmstead, C. M. Beavers, L. C. Hirayama, S. Pradhan, R. A. Wessling, B. Singaram, *Boronic Acid-Based Bipyridinium Salts as Tunable Receptors for Monosaccharides and α -Hydroxycarboxylates*, *J Am Chem Soc*, **2007**, 129, 1278-1286
- [36] S. Gamsey, J. T. Suri, R. A. Wessling, B. Singaram, *Continuous Glucose Detection Using Boronic Acid-Substituted Viologens in Fluorescent Hydrogels: Linker Effects and Extension to Fiber Optics*, *Langmuir*, **2006**, 22, 9067-9074
- [37] B. Vilozny, A. Schiller, R. A. Wessling, B. Singaram, *Multiwell plates loaded with fluorescent hydrogel sensors for measuring pH and glucose concentration*, *J Mater Chem*, **2011**, 21, 7589-7595
- [38] D. B. Cordes, A. Miller, S. Gamsey, Z. Sharrett, P. Thoniyot, R. Wessling, B. Singaram, *Optical glucose detection across the visible spectrum using anionic fluorescent dyes and a viologen quencher in a two-component saccharide sensing system*, *Org Biomol Chem*, **2005**, 3, 1708-1713
- [39] O. S. Wolfbeis, E. Furlinger, H. Kroneis, H. Marsoner, *Fresenius Z., Fluorimetric Analysis*, *Fresen J Ana. Chem*, **1983**, 314, 119-124.
- [40] <http://www.sigmaaldrich.com/catalog>
- [41] K. Sato, T. Nakahodo, H. Fujihara, *Redox-active π -conjugated polymer nanotubes with viologen for encapsulation and release of fluorescent dye in the nanospace*, *Chem Commun*, **2011**, 47, 10067-10069
- [42] A. N. Swinburne, M. J. Paterson, K. H. Fischer, S. J. Dickson, E. V. B. Wallace, W. J. Belcher, A. Beeby, J. W. Steed, *Colourimetric Carboxylate Anion Sensors Derived from Viologen-Based Receptors*, *Chem Eur J*, **2010**, 16, 1480-1492

[43] S. L. Tobey, E. V. Anslyn, *Energetics of Phosphate Binding to Ammonium and Guanidinium Containing Metallo-Receptors in Water*, J Am Chem Soc, **2003**, 125, 14807-14815

[44] Y. Zhou, Z. Xu, J. Yoon, *Fluorescent and calorimetric chemosensors for detection of nucleotides, FAD and NADH: highlighted research during 2004-2010*, Chem Soc Rev, **2011**, 40, 2222-14815

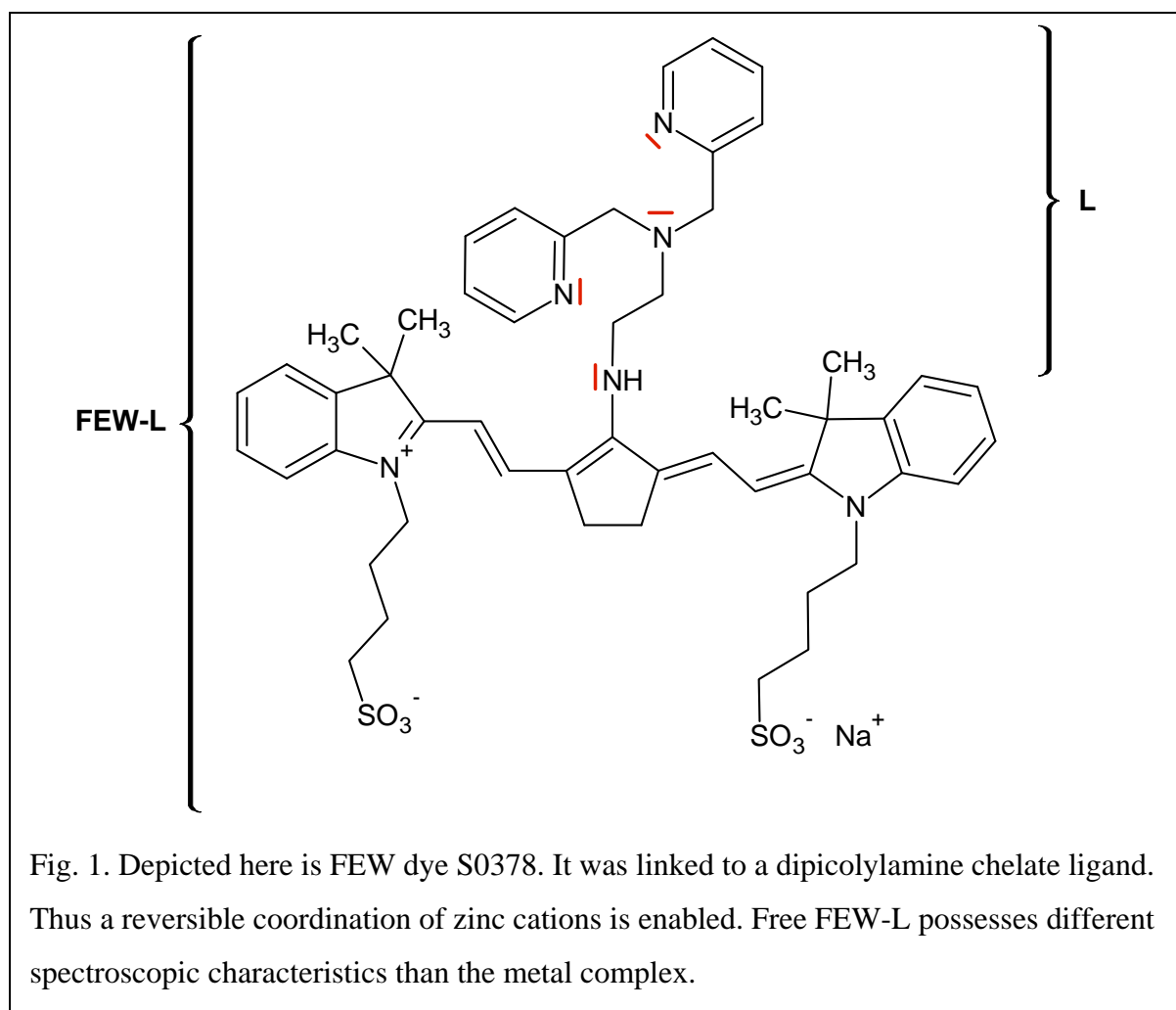
2.2 NIR Dye as New Phosphate-sensitive Fluorescent Probe

Fluorescent probes have generated a lot of interest in the last couple of decades owing to their sensitivity, low costs, and their easy and various applications [1]. One major disadvantage, however, of fluorescent probes can be identified in their excitation and emission maxima being located in the blue or even in the ultraviolet region. It would be very convenient and advantageous if these were shifted towards the near-infrared (NIR) region. Then damage of a living organism can be excluded [2]. Additionally a deeper penetration through tissue is also enabled [3]. Moreover, auto- and background fluorescence is minimized [4] rendering this approach very appealing to in vivo imaging [2, 5], especially due to the convenient operation in the “water window” (650 nm to 950 nm) [2, 6]. Furthermore, an inexpensive diodes are adequate for excitation [7].

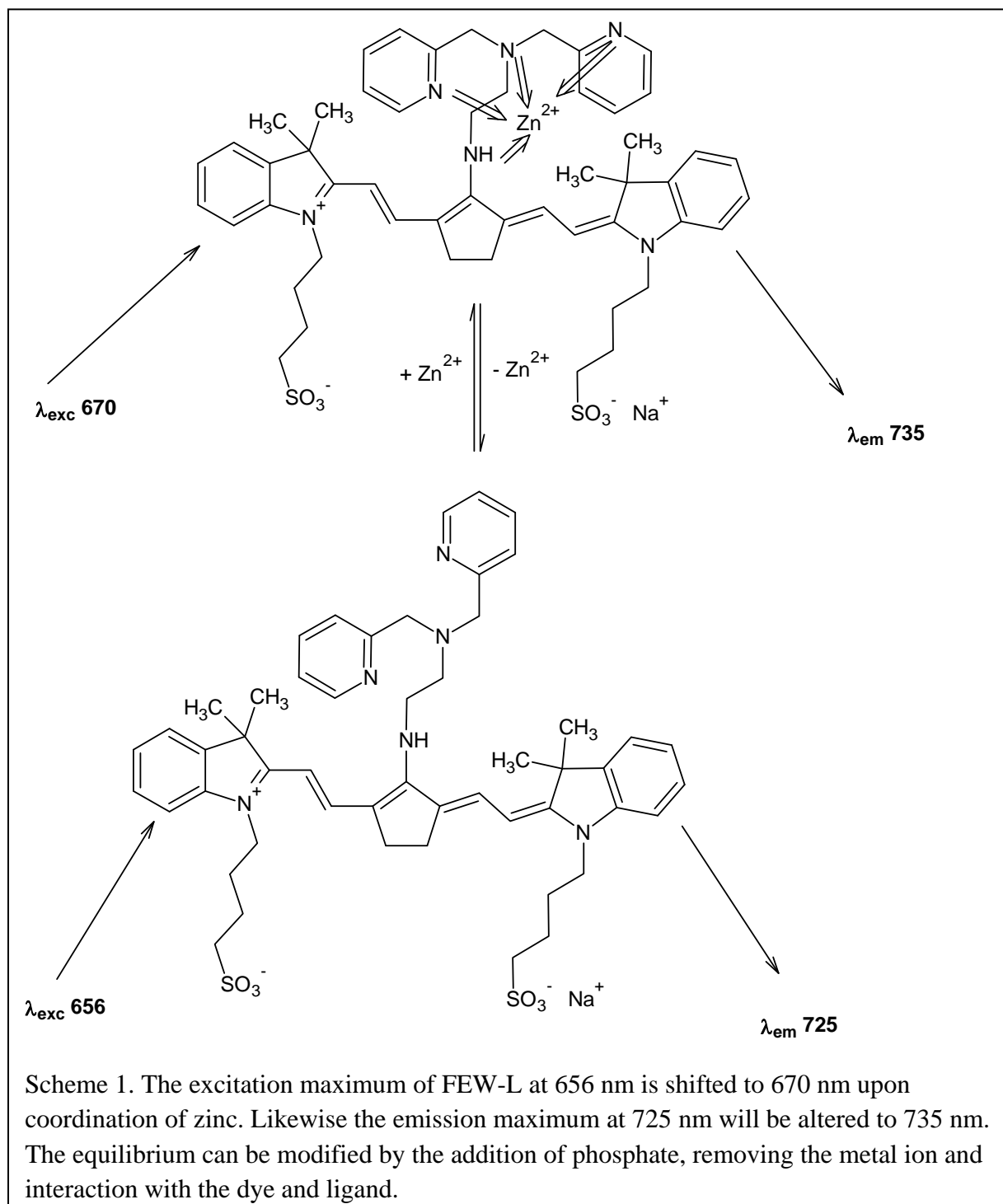
Accordingly, numerous applications and an abundance of probes have been reported. Many NIR dyes found applications in oncology [8, 9] for instance. Likewise, NIR Quantum Dots have been utilized for tumor imaging and in vivo investigations [3, 10, 11]. Upconverting nanoparticles (UCNPs) have attracted tremendous interest in recent years. Their unique capability of anti-Stokes luminescence upon excitation in the NIR region renders them promising tools for a variety of applications [12]. UCNPs have been harnessed to probe the activity of metalloproteinase [13], oxygen [14] and carbon dioxide [15]. They prospect to remain in the focus of heated research for the foreseeable future. Furthermore, phenoxazines have been used as labels for proteins and amines [16]. Cyanine dyes can serve this purpose as well [17-19]. They have become versatile molecules for a variety of applications such as in semiconductors [20], photochromic [21] and photorefractive materials [22], in photovoltaics [23], in light harvesting [24], and as smart materials [25]. Furthermore, cyanines have served in mass spectroscopy [26], in imaging pertaining to cancer studies [27, 28], in solar cells [29], in proteomics [30], as potential optical data storage [31] and in monitoring of polymerization [32]. Hence, their tailor made synthesis has duly received a lot of attention [33-36]. Sensing of cations such as potassium [37, 38], mercury [38, 39] and calcium [40] via probes based on cyanine dyes has long been established. Recently anions [41], copper [42] and especially zinc [43-45] has been added to the fold.

Nagano *et al.* [46] contrived a sensing scheme for zinc ions as follows. A cyanine dye from the FEW company [47] was linked to a ligand which carries four nitrogen atoms. The free electron pairs of these can form a tetrahedral complex with zinc. Upon coordination of the metal the spectroscopic characteristics pertaining to the free ligand/dye are altered. Hence, a shift in the excitation and emission maxima can be recorded [46]. This is due to the fact that zinc is acting as a Lewis acid, reducing electron density, and this results in a change in the 3-D structure of the molecule.

This scheme was exploited for phosphate sensing here. An identical dipicolylamine ligand (L) was synthesized in two straightforward steps (see 2.2.1 below) rendering this an easier, quicker and more inexpensive approach than described by Nagano *et al.* [46]. This particular moiety has been reported to form chelates with zinc numerous times. [33, 46, 48, 49] Then a like dye was attached to this polydentate ligand (Fig. 1).



Upon complexation with metal cations, the spectroscopic properties of this probe are crucially altered. When phosphate interacts with zinc, removing it from the equilibrium of free ion/coordinated ion, a reverse effect can be observed (Scheme 1).



Additionally to the minor shift in the maxima of excitation and emission, the fluorescence intensity is substantially decreased if metal ions are present. Different types of phosphates

exercise different impacts on the complex [Zn(FEW-L)], either by releasing zinc or by electrostatic interaction with dye or through the π -systems from the nucleic bases.

Theoretically, different types of phosphates can be distinguished by their nucleic base (guanine or adenine) or lack thereof, the number of phosphate groups (mono-, di-, triphosphates) and structure (cAMP, cGMP). The base determines if, and to what extent, π - π and π -cation interactions can be formed between the sample and FEW-L. The number of phosphate groups corresponds to the number of negative charges. The dye possesses one, while zinc ions carry two positive charges to form ionic bonds. The third factor, size and 3-D structure is very important and crucially impacts the extent to which interaction between phosphates, the metal ion, FEW-L and [Zn(FEW-L)] is possible. Thus it needs to be taken into account that these phosphates can impact the zinc complex and/or the free FEW-L in a like way and thus affecting fluorescence intensity.

The objective of chapter 5 is to report on the potential of [Zn(FEW-L)] as a phosphate-sensitive probe. Hence P_i , PP_i , GTP, GDP, GMP, cGMP and their adenine counterparts are probed by applying this particular sensing scheme in this work.

- [1] U. Resch-Genger, M. Grabolle, S. Cavaliere-Jaricot, R. Nitschke, T. Nann, *Quantum dots versus organic dyes as fluorescent labels*, Nat Methods, **2008**, 5, 763-775
- [2] M. Y. Berenzin, H. Lee, W. Akers, S. Achilefu, *Near Infrared Dyes as Lifetime Solvatochromic Probes for Micropolarity Measurements of Biological Systems*, Biophys J, **2007**, 93, 2892-2899
- [3] L. A. Bentolila, Y. Ebenstein, S. Meiss, *Quantum Dots for In Vivo Small-Animal Imaging*, J Nucl Med, **2009**, 50, 493-496
- [4] H. Lee, M. Y. Berenzin, M. Henary, L. Streckowski, S. Achilefu, *Fluorescence lifetime properties of near-infrared cyanine dyes in relation to their structures*, J Photoch Photobio A, **2008**, 200, 438-444
- [5] J. O. Escobedo, O. Rusin, S. Lim, R. M. Strongin, *NIR dyes for bioimaging applications*, Current Opinion in Chem Biol, **2010**, 14, 64-70
- [6] K. Umezawa, A. Matsui, Y. Nakamura, D. Citterio, K. Suzuki, *Bright, Color-Tunable Fluorescent Dyes in the Vis/NIR Region: Establishment of New "Tailor.Made" Multicolor Fluorophores Based on Borondipyrrromethane*, Chem Eur J, **2009**, 15, 1096-1106
- [7] G. M. Fischer, M. Isomäki-Kron Dahl, I. Göttker-Schnetmann, E. Daltrozzo, A. Zumbusch, *Pyrrlopyrrole Cyanine Dyes: A New Class of Near-Infrared Dyes and Fluorophores*, Chem Eur J, **2009**, 15, 4857-4864
- [8] S. Luo, E. Zhang, Y. Su, T. Cheng, C. Shi, *A review of NIR dyes in cancer targeting and imaging*, Biomaterials, **2011**, 7127-7138
- [9] K. Licha, B. Riefke, V. Ntziachristos, A. Becker, B. Chance, W. Semmler, *Hydrophilic Cyanine Dyes as Contrast Agents for Near-infrared Tumor Imaging: Synthesis, Photophysical Properties and Spectroscopic In vivo Characterization*, Photochem Photobiol, **2000**, 72, 392-398
- [10] P. P. Neelakandam, K. S. Sanju, D. Ramaiah, *Effect of Bridging Units on Photophysical and DNA Binding Properties of a Few Cyclophanes*, Photochem Photobiol, **2010**, 86, 282-289
- [11] K. Yong, *Mn-doped near-infrared quantum dots as multimodal targeted probes for pancreatic cancer imaging*, Nanotechnology, **2009**, 20, 1-11

- [12] F. Wang, D. Debapriya, Y. Liu, X. Chen, X. Liu, *Upconversion nanoparticles in biological labeling, imaging, and therapy*, *Analyst*, **2010**, 135, 1839-1854
- [13] D. E. Achatz, G. Mezö, P. Kele, O. S. Wolfbeis, *Probing the Activity of Matrix Metalloproteinase II with a Sequentially Click-Labelled Silica Nanoparticle FRET Probe*, *Chem Bio Chem*, **2009**, 10, 2316-2320
- [14] D. E. Achatz, R. Ali, O. S. Wolfbeis, *Luminescent Chemical Sensing, Biosensing, and Screening Using Upconverting Nanoparticles*, *Top Curr Chem*, **2011**, 300, 29-50
- [15] D. E. Achatz, R. J. Meier, L. H. Fischer, O. S. Wolfbeis, *Luminescent Sensing of Oxygen Using a Quenchable Probe and Upconverting Nanoparticles*, *Angew Chem Int Ed*, **2011**, 50, 260-263
- [16] M. Link, P. Kele, D. E. Achatz, O. S. Wolfbeis, *Brightly fluorescent purple and blue labels for amines and proteins*, *Bioorg Med Chem Lett*, **2011**, 21, 5538-5542
- [17] H. H. Gorris, Sayed M. Saleh, D. B. M. Groegel, S. Ernst, K. Reiner, H. Muströph, O. S. Wolfbeis, *Long-Wavelength Absorbing and Fluorescent Chameleon Labels for Proteins, Peptides, and Amines*, *Bioconjugate Chem*, **2011**, 22, 1433-1437
- [18] K. Saatchi, P. Soema, N. Gelder, R. Misri, K. McPhee, J. H. E. Baker, S. A. Reinsberg, D. E. Brooks, U. O. Häfeli, *Hyperbranched Polyglycerols as Trimodal Imaging Agents: Design, Biocompatibility, and Tumor Uptake*, *Bioconjugate Chem*, **2012**, published online ahead of print
- [19] B. Renard, Y. Aubert, U. Asseline, *Fluorinated squaraine as near-IR label with improved properties for the labeling of oligonucleotides*, *Tetrahedron Lett*, **2009**, 50, 1897-1901
- [20] P. Schouwink, H. von Berlepsch, L. Dähne, R. F. Mahrt, *Observation of strong exciton-photon coupling in an organic microcavity in transmission and photoluminescence*, *J Lumin*, **2001**, 94-95, 821-826
- [21] K. Yumoto, M. Irie, K. Matsuda, *Control of the Photoreactivity of Diarylethene Derivatives by Quarternarization of the Pyridylethynyl Group*, *Org Lett*, **2008**, 10, 2051-2054
- [22] F. Würthner, S. Yao, J. Schilling, R. Wortmann, M. Redi-Abshiro, E. Mecher, F. Gallego-Gomez, K. Meerholz, *ATOP Dyes. Optimization of a Multifunctional Merocyanine*

Chromophore for High Refractive Index Modulation in Photorefractive Materials, J Am Chem Soc, **2001**, 123, 2810-2824

[23] P. Bouit, D. Rauh, S. Neugebauer, J. L. Delgado, E. Di Piazza, S. Rigaut, O. Maury, C. Andraud, V. Dyakonov, N. Martin, *A "Cyanine-Cyanine" Salt Exhibiting Photovoltaic Properties*, Org Lett, **2009**, 11, 4806-4809

[24] K. R. J. Thomas, J. T. Lin, Y. Hsu, K. Ho, *Organic dyes containing thienylfluorene conjugation for solar cells*, Chem Commun, **2005**, 4098-4100

[25] P. M. Mendes, *Stimuli-responsive surfaces for bio-applications*, Chem Soc Rev, **2008**, 37, 2512-2529

[26] A. Kameyama, Y. Kaneda, H. Yamanaka, H. Yoshimine, H. Narmatsu, Y. Shinohara, *Detection of Oligosaccharides Labeled with Cyanine Dyes Using Matrix-Assisted Laser Desorption/Ionization Mass Spectroscopy*, Anal Chem, **2004**, 76, 4537-4542

[27] S. Ke, X. Wen, M. Gurfinkel, C. Charnsangavej, S. Wallace, E. M. Sevick-Muraca, C. Li, *Near-Infrared Optical Imaging of Epidermal Growth Factor Receptor in Breast Cancer Xenografts*, Cancer Res, **2003**, 63, 7870-7875

[28] L. J. Jones, V. L. Singer, *Fluorescence Microplate-Based Assay for Tumor Necrosis Factor Activity Using SYTOX Green Stain*, Anal Biochem, **2001**, 293, 8-15

[29] B. Fan, F. A. de Castro, J. Heier, R. Hany, F. Nüesch, *High performing doped cyanine bilayer solar cell*, Org Electron, **2010**, 11, 583-588

[30] N. A. Karp, K. S. Lilley, *Maximising sensitivity for detecting changes in protein expression: Experimental design using minimal CyDyes*, Proteomics, **2005**, 5, 3105-3115

[31] M. Heilemann, E. Margeat, R. Kasper, M. Sauer, P. Tinnefeld, *Carbocyanine Dyes as Efficient Reversible Single-Molecule Optical Switch*, J Am Chem Soc, **2005**, 127, 3801-3806

[32] J. Kabatc, A. Bajorek, R. Dobosz, *Bichromophoric hemicyanine dyes as fluorescence probes applied for monitoring of the photochemically initiated polymerization*, J Mol Struct, **2011**, 985, 95-104

[33] R.K. Das, A. Samanta, H. Ha, Y. Chang, *Solid phase synthesis of ultra-photostable cyanine NIR dye library*, RSC Adv, **2011**, 1, 573-575

- [34] M. Panigrahi, S. Dash, S. Patel, B. K. Mishra, *Synthesis of cyanines: a review*, *Tetrahedron*, **2012**, 68, 781-805
- [35] M. R. Mazieres, C. Duprant, J. Bellan, J. G. Wolf, *Synthesis and characterization of new phosphonate labeled cyanines*, *Dyes Pigments*, **2007**, 74, 404-409
- [36] A. V. Kulinich, N. A. Derevyanko, A. A. Ischenko, *Synthesis and spectral properties of cyanine dyes – Derivatives of 10,10-dimethyl-7,8,9,10-tetrahydro-6H-pyrido[1,2- α]indolium*, *J Photoch Photobio A: Chemistry*, **2008**, 198, 119-125
- [37] O. S. Wolfbeis, B. P. H. Schaefer, *Optical Sensors: An Ion-Selective Optrode For Potassium*, *Anal Chim Acta*, **1987**, 198, 1-12
- [38] G. J. Mohr, I. Murkovic, F. Lehmann, C. Haider, O. S. Wolfbeis, *Application of potential-sensitive fluorescent dyes in anion- and cation-sensitive polymer membranes*, *Sensor Actuator B*, **1997**, 38-39, 239-245
- [39] I. Murkovic, O. S. Wolfbeis, *Fluorescence-based sensor membrane for mercury (II) detection*, *Sensor Actuator B*, **1997**, 38-39, 246-251
- [40] B. P. H. Schaefer, O. S. Wolfbeis, *A Calcium-Selective Optrode Based On Fluorimetric Measurements Of Membrane Potential*, *Anal Chim Acta*, **1989**, 217,1-9
- [41] X. Cao, W. Lin, L. He, *A Near-Infrared Fluorescence Turn-On Sensor for Sulfide Anions*, *Chem Commun*, **2011**, 13, 4716-4719
- [42] T. Hirayama, G. C. Van de Bittner, L. W. Gray, S. Lutsenko, C. J. Chang, *Near-Infrared fluorescent sensor for in vivo copper imaging in a murine Wilson disease model*, *PNAS*, **2012**, 109, 2228-2233
- [43] K. Kiyose, H. Kojima, T. Nagano, *Functional Near-Infrared Fluorescent Probes*, *Chem Asian J*, **2008**, 3, 506-515
- [44] P. Carol, S. Sreejith, A. Ajayaghosh, *Ratiometric and Near-Infrared Molecular Probes for the Detection and Imaging of Zinc Ions*, *Chem Asian J*, **2007**, 2, 338-348
- [45] D. Oushiki, H. Kojima, T. Terai, M. Arita, K. Hanaoka, Y. Urano, T. Nagano, *Development and Application of a Near-Infrared Fluorescence Probe for Oxidative Stress Based on Differential Reactivity of Linked Cyanine Dyes*, *J Am Chem Soc*, **2010**, 132, 2795-2801

[46] <http://www.few.de/English/index.htm>

[47] K. Kiyose, H. Kojima, Y. Urano, T. Nagano, *Development of a Ratiometric Fluorescent Zinc Ion Probe in Near-Infrared Region, Based on Tricarbocyanine Chromophore*, J Am Chem Soc, **2006**, 128, 6548-6549

[48] Y. You, S. Lee, T. Kim, K. Ohkubo, W. Chae, S. Fukuzumi, G. John, W. Nam, S. J. Lippard, *Phosphorescent Sensor for Biological Mobile Zinc*, J Am Chem Soc, **2011**, 133, 18328-18342

[49] A. J. Moro, P. J. Cywinski, S. Körsten, G. J. Mohr, *An ATP fluorescent chemosensor based on a Zn(II)-complexed dipicolylamine receptor coupled with a naphthalimide chromophore*, Chem Commun, **2010**, 46, 1085-1087

3. Experimental

3.1 Materials and Methods

3.1.1 Instrumental Set Up

All NMR spectra were recorded on a 300 MHz Bruker Avance spectrometer (Bruker, www.bruker-biospin.com).

HRMS was acquired on an Agilent **Q-TOF 6540 UHD** (www.agilent.co.uk).

All measurements dealing with quenchers were carried out on a Tecan GENios Plus microtiter plate reader F129024 (www.mtxlsi.com/TECANGENIOS.htm).

Experimenta parameters: Temperature: 37 °C; Filter (emission): 535 nm; Filter (excitation): 430 nm; Gain: 84 V; Integration time: 30 µs; Shaking: 25 s; Number of flashes: 110; Duration: 1800 s

Microtiter Plate: Micro-Assay-Plate, Chimney, 96Well, 127, 8/86/15, Black, Clear Bottom by Greiner Bio-One (655096, www.gbo.com) was exclusively used.

All emission and excitation spectra were recorded on a Jasco FP-6200 (www.jasco.co.uk).

Measurement parameters: PMT Voltage: 400 V; Excitation Band Width: 5 nm; Emission Band Width: 10 nm; Speed: 100 nm/s; Data Pitch: 0.5 nm; Response: Medium; Filters (excitation): 670 nm; Filters (emission): 740 nm

3.1.2 Chemicals

All chemicals were obtained from commercial sources, e.g. Sigma Aldrich (www.sigmaaldrich.com) in the highest purity available or from Deutero GmbH (www.deutero.de) (Table 1). The FEW dye S0378 was obtained from FEW Chemicals GmbH (Bitterfeld) (<http://www.few.de>).

All measurements were carried out in TRIS buffer of the following composition:

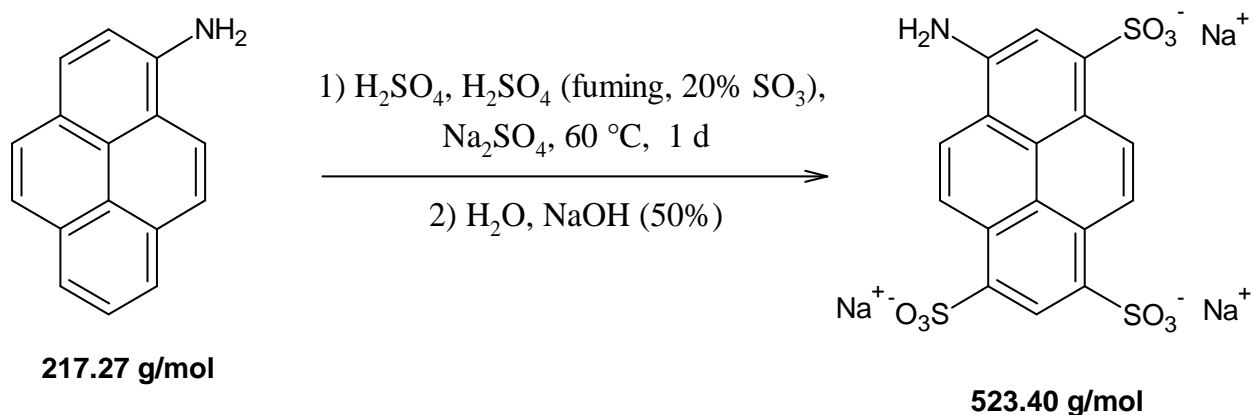
24 mM*L⁻¹ Tris(hydroxymethyl)aminomethan (TRIS), 160 mM*L⁻¹ NaCl, 3.60 mM*L⁻¹ KCl, 0.50 mM*L⁻¹ MgCl₂.

pH was adjusted to 7.4 by addition of 1 M*L⁻¹ HCl. It was monitored using a CG 842 pH meter (Schott, www.schott.com). The following stock conc. Were adjusted. Phosphates: 17.5 μM*L⁻¹, FEW-L: 1 μM*L⁻¹, zinc perchlorate: 5.00 μM*L⁻¹, pyrenes: 0.50 μM*L⁻¹, and viologens: 5 μM*L⁻¹

All chemicals were added in the following order: Quencher, buffer, pyrene, and sample phosphate.

3.1.2 Syntheses

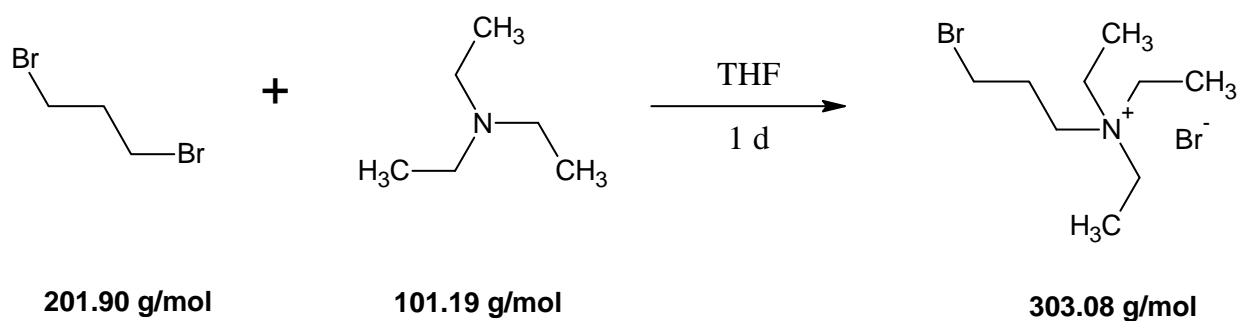
Synthesis of Trisodium 8-Aminopyrene-1,2,3-trisulfonate (APTS) [1]



The synthesis of APTS was carried out according to the protocol by Singaram *et al.* [1]. First, sodium sulfate (1.13g, 8.00 mmol), conc. sulphuric acid (5 ml), and aminopyrene (434 mg, 2.00 mmol) were placed into a dry round-bottom flask equipped with a drying tube. Next 6 ml of fuming sulphuric acid (20% SO_3) was added, and the reaction mixture was stirred at 60 °C. After 24 hours the solution was carefully poured into 50 ml of water. The aqueous mixture was neutralized using 50 % m/m sodium hydroxide solution. Water was removed on a rotary evaporator then methanol was added to the crude product. The mixture was sonicated in an ultrasonic bath for 30 minutes then insolubles were removed by filtration. Volatiles were removed by evaporation. The crude product was kept in the fridge over-night to solidify. Ethanol was added, and after filtration the solvents were removed by evaporation. The product did not require further purification. A brown solid was obtained in 3% yield (30.00 mg, 0.05 mmol). ESI-MS: $[\text{M}-\text{H}]^-$ (calculated): 456.4, $[\text{M}-\text{H}]^-$ (found): 456.0; ^1H NMR (CD_3OD , 300 MHz) δ 8.19 (s, 1H), δ 8.41 (d, $J = 9.88$ Hz, 1H), δ 8.91(d, $J = 9.88$ Hz, 1H), δ 9.03 (d, $J = 9.88$ Hz, 1H), δ 9.15 (d, $J = 9.88$ Hz, 1H), δ 9.30 (s, 1 H); ^{13}C NMR (CD_3OD , 75 MHz) δ 114.92, δ 117.74, δ 119.52, δ 122.20, δ 124.18, δ 124.99, δ 126.20, δ 127.76, δ 128.00, δ 128.94, δ 131.51, δ 131.93, δ 136.07, δ 136.54, δ 142.35, δ 145.83.

[1] Z. Sharrett, S. Gamsey, L. Hirayama, B. Vilozny, J. T. Suri, R. A. Wessling, B. Singaram, *Exploring the use of APTS as a fluorescent reporter dye for continuous glucose sensing*, *Org Biomol Chem*, **2009**, 7, 1461-1470

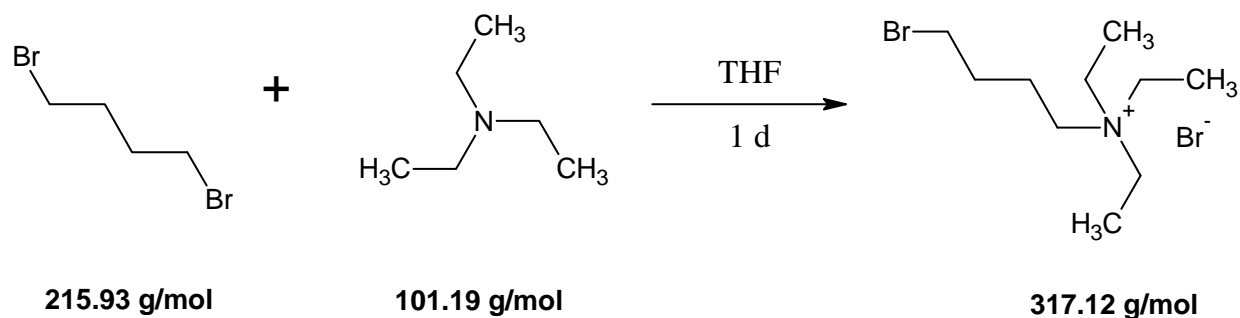
Synthesis of 3-bromo-N,N,N-triethylpropane-1-ammonium-bromide



The synthesis of the 3-Bromo-N,N,N-triethylalkyl-1-ammonium-bromides was carried out using a modified protocol of Kim *et al.* [2]. A round-bottom flask was charged with dibromopropane (24 ml, 47.52 g, 235.36 mmol), 1.64 ml triethylamine (1.20 g, 11.86 mmol) and 5 ml THF and the resulting mixture was stirred at room temperature over-night. Ethanol was added and product was collected by filtration, yielding 1.16 g (3.83 mmol, 32.04%) of a white solid. HR-ESI-MS: [M^{*+}] (calculated): 208.0695, [M^{*+}] (found): 208.0700; ¹H NMR (D₂O, 300 MHz) δ 1.21 (t, *J* = 6.59, 9H), δ 2.21 (m, 2H), δ 3.25 (m, 8H), δ 3.47 (t, *J* = 6.04 Hz, 2H); ¹³C NMR (D₂O, 75 MHz) δ 6.72, δ 24.25, δ 29.32, δ 52.87, δ 55.36.

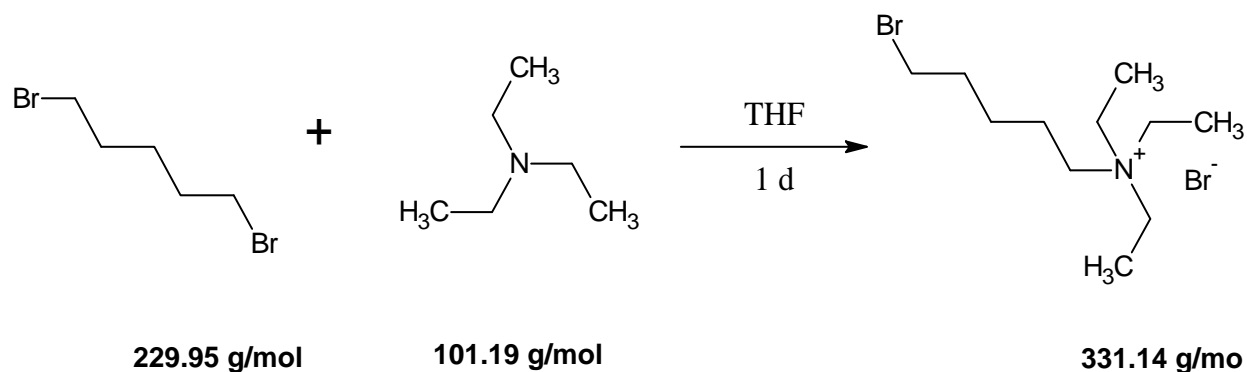
[2] W. S. Jeon, E. Kim, Y. H. Ko, I. Hwang, J. W. Lee, S. Kim, H. Kim, K. Kim, *Molecular Loop Loc: A Redox-Driven Molecular Machine Based on a Host-Stabilized Charge-Transfer Complex*, *Angew Chem Int Ed*, **2005**, 44, 87-91

Synthesis of 3-Bromo-N,N,N-triethylbutyl-1-ammonium bromide



Dibromobutane (64.37 ml, 117.41 g, 543.75 mmol), 3.8 ml triethylamine (2.763 g, 27.30 mmol) and 5 ml THF were placed into a round-bottom flask and stirred at room temperature over-night. Ethanol was added and the product was filtered off, yielding 6.66 g (21.00 mmol, 76.91%) of a white solid. HR-ESI-MS: $[M^{*+}]$ (calculated): 236.1008, $[M^{*+}]$ (found): 236.1007; ^1H NMR (D_2O , 300 MHz) δ 1.17 (t, $J = 7.14$, 9H), δ 1.80 (m, 4H), δ 3.17 (t, $J = 6.66$ Hz, 2H), δ 3.20 (q, $J = 7.14$, 6H), δ 3.47 (t, $J = 6.66$ Hz, 2H); ^{13}C NMR (D_2O , 75 MHz) δ 6.79, δ 19.89, δ 28.67, δ 33.37, δ 52.62, δ 55.63.

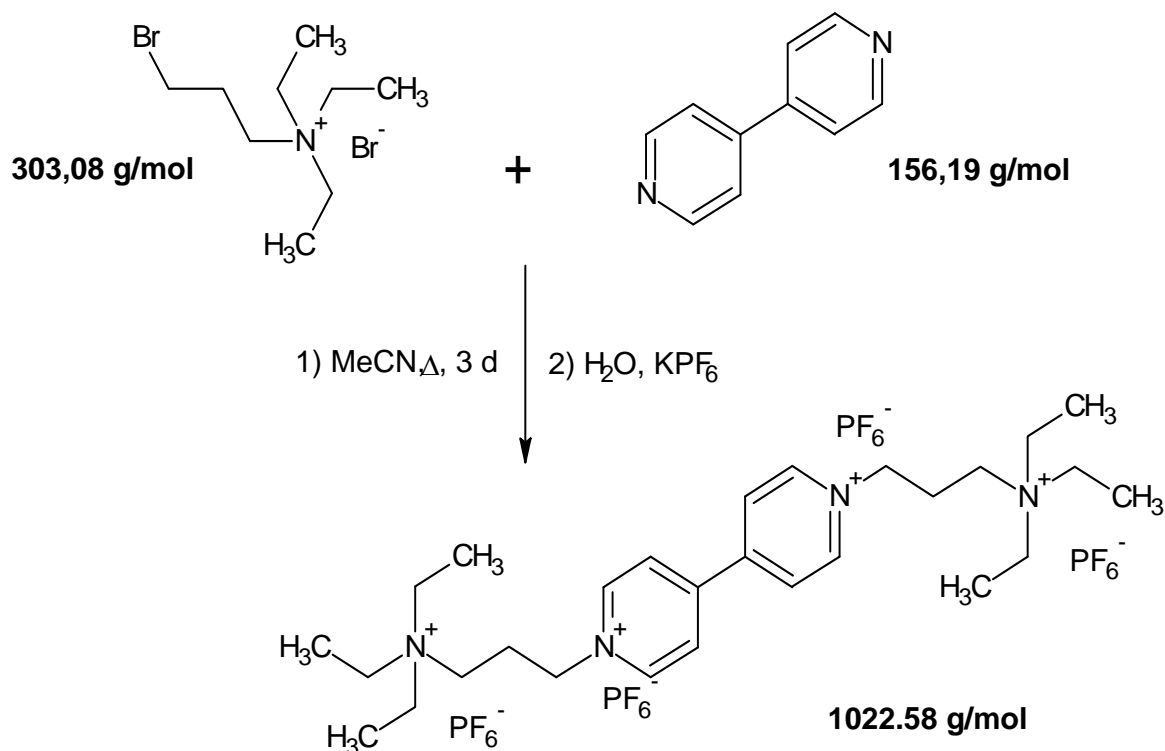
Synthesis of 3-Bromo-N,N,N-triethylpentyl-1-ammonium-bromide



Dibromopentane (74.37 ml, 125.09 g, 543.75 mmol), 3.8 ml triethylamine (2.763 g, 27.30 mmol) and 5 ml THF were placed into a round-bottom flask and stirred at room temperature over-night. Ethanol was added and the product was filtered off, yielding 6.26 g (18.90 mmol, 69.23%) of a white solid. HR-ESI-MS: $[M^{*+}]$ (calculated): 252.1144, $[M^{*+}]$ (found): 252.1149; ^1H NMR (D_2O , 300 MHz) δ 1.18 (t, $J = 7.14$, 9H), δ 1.43 (m, 2H), δ 1.63 (m, 2H),

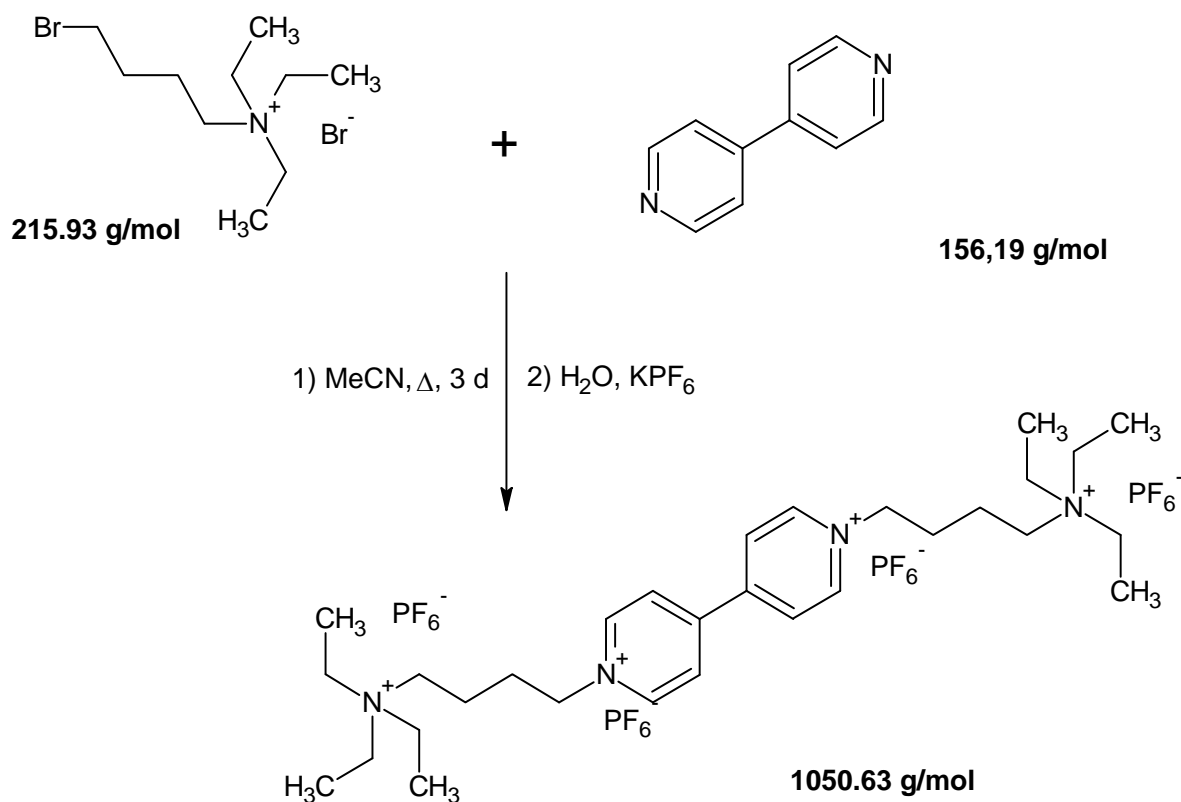
δ 1.85 (m, 2H), δ 3.10 (t, $J = 6.54$ Hz, 2H), δ 3.20 (q, $J = 7.14$, 6H), δ 3.45 (t, $J = 6.54$ Hz, 2H); ^{13}C NMR (D_2O , 75 MHz) δ 6.84, δ 20.34, δ 24.42, δ 31.48, δ 34.49, δ 52.64, δ 56.53.

Synthesis of 1,1'-di[3-(triethylammonium)propyl]-4,4'-bipyridilium (TEAPB)



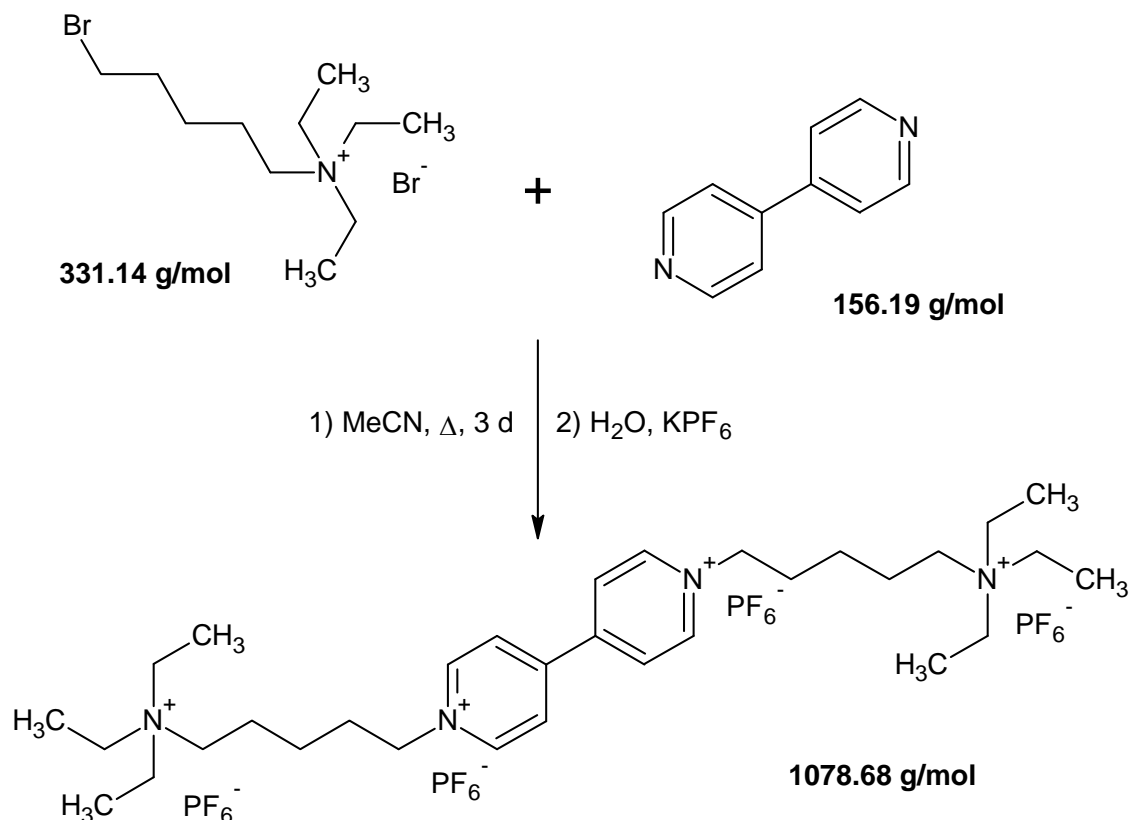
3-Bromo-N,N,N-triethylpropyl-1-ammonium bromide (1.16 g, 3.82 mmol) and 4,4'-bipyridin (74.60 mg, 0.48 mmol) were dissolved in acetonitrile and the reaction mixture was refluxed for three days. The resulting mixture was allowed to cool to room temperature then crude product was collected by filtration and dissolved in water. Addition of excessive amount of potassium hexafluorophosphate induced crystallization of the product as its hexafluorophosphate salt. An off white solid was obtained in a yield of 288.00 mg (0.28 mmol, 58.33%). HR-ESI-MS: $[\text{M}^{*+}]$ (calculated): 372.4, $[\text{M}^{*+}]$ (found): 372.9; ^1H NMR (DMSO, 300 MHz) δ 1.20 (t, $J = 7.28$, 18H), δ 2.40 (m, 4H), δ 3.22 (m, 16H), δ 4.70 (t, $J = 7.14$ Hz, 4H), δ 8.81 (d, $J = 8.23$ Hz, 4H), δ 9.40 (d, $J = 8.23$ Hz, 4H); ^{13}C NMR (DMSO, 75 MHz) δ 7.00, δ 23.19, δ 52.26, δ 52.40, δ 126.32, δ 146.07, δ 148.59.

Synthesis of **1,1'-di[3-(triethylammonium)butyl]-4,4'-bipyridylium** (TEABB)



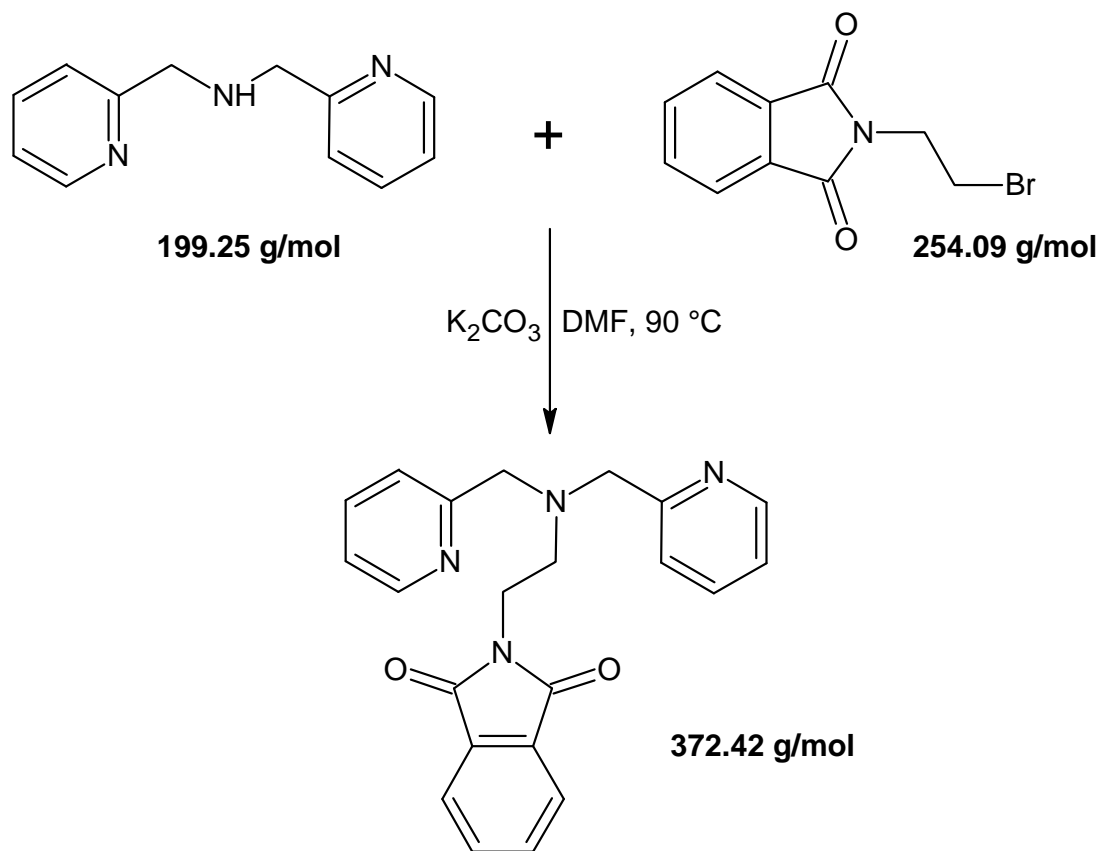
3-Bromo-N,N,N-triethylbutyl-1-ammonium-bromide (4.00 g, 12.62 mmol) and 4,4'-bipyridine (200.00 mg, 1.28 mmol) were dissolved in acetonitrile and refluxed for three days. The crude product was filtered off, dissolved in water and precipitated by addition of potassium hexafluorophosphate. An off white solid was obtained in a yield of 956.50 mg (0.93 mmol, 72.66%). HR-ESI-MS: [M^{*+}] (calculated): 560.4296, [M^{*+}] (found): 560.4294; ¹H NMR (DMSO, 300 MHz) δ 1.24 (m, 22H), δ 1.70 (m, 4H), δ 3.24 (m, 16H), δ 4.76 (t, J = 7.14 Hz, 4H), δ 8.82 (d, J = 8.23 Hz, 2H), δ 9.41 (d, J = 8.23 Hz, 2H); ¹³C NMR (DMSO, 75 MHz) δ 7.06, δ 18.05, δ 27.55, δ 51.93, δ 52.02, δ 126.48, δ 145.77, δ 148.51.

Synthesis of **1,1'-di[3-(triethylammonium)pentyl]-4,4'-bipyridylium** (TEAPeB)



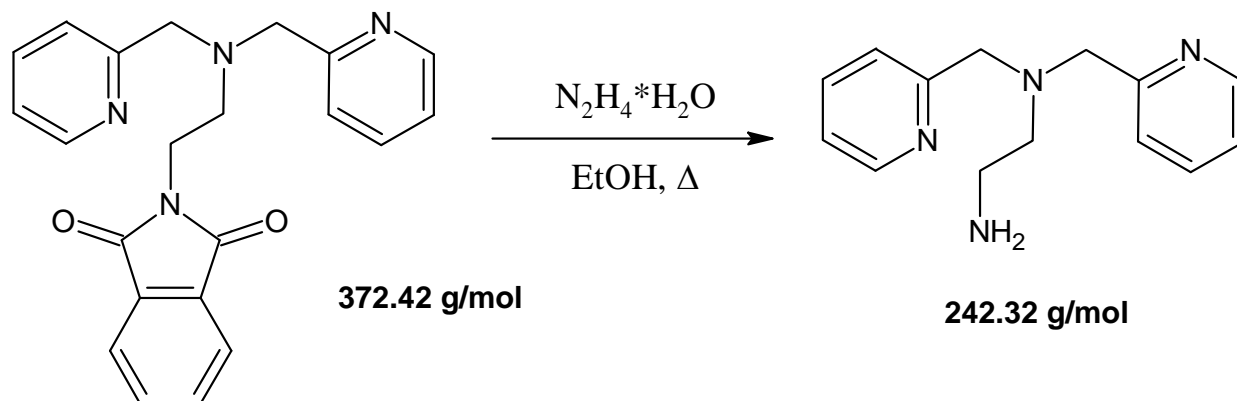
3-Bromo-N,N,N-triethylpentyl-1-ammonium-bromide (4.58 g, 13.83 mmol) and 4,4'-bipyridin (255.00 mg, 1.63 mmol) were dissolved in acetonitrile and refluxed for three days. The crude product was filtered off, dissolved in water and precipitated by addition of potassium hexafluorophosphate. An off white solid was obtained in a yield of 331.20 mg (0.31 mmol, 19.02%). HR-ESI-MS: [M^{*+}] (calculated): 588.4609, [M^{*+}] (found): 588.4611; ¹H NMR (DMSO, 300 MHz) δ 1.20 (t, J = 7.28, 18H), δ 1.40 (m, 4H), δ 1.64 (m, 4H), δ 3.22 (m, 16H), δ 4.70 (t, J = 7.14 Hz, 4H), δ 8.81 (d, J = 8.23 Hz, 2H), δ 9.40 (d, J = 8.23 Hz, 2H); ¹³C NMR (DMSO, 75 MHz) δ 6.96, δ 29.99, δ 31.43, δ 34.60, δ 51.91, δ 126.49, δ 145.65, δ 148.56.

Synthesis of N-(2-[di(2-picoly)amino]ethyl)phthalimide



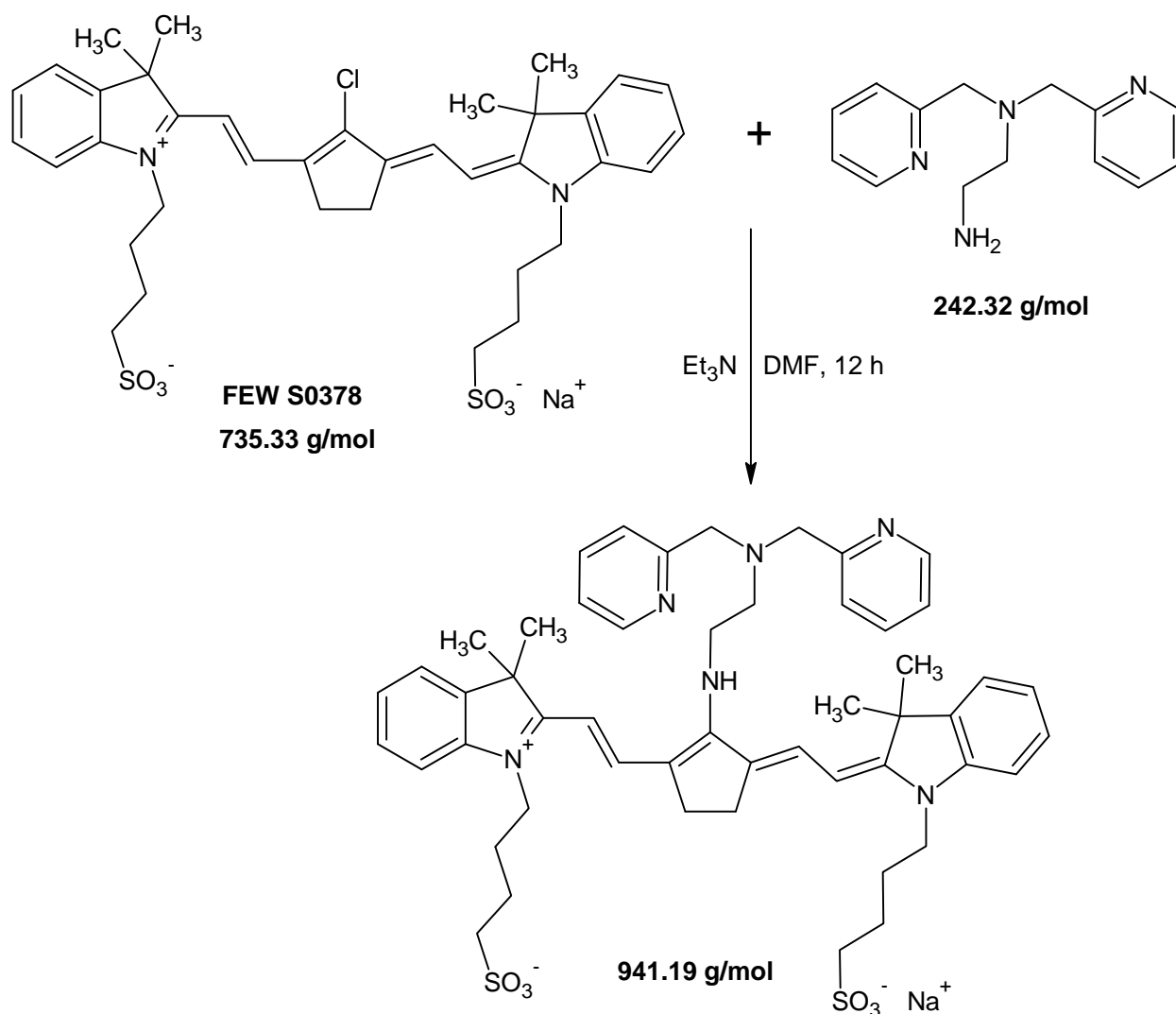
Di(2-picoly)amine (2.70 ml, 15.00 mmol), N-(2-bromoethyl)phthalimide (4.17 g, 16.42 mmol) and potassium carbonate (3.30 g, 23.88 mmol) were heated at 90 °C in DMF overnight. After cooling to room temperature the reaction mixture was poured onto ice-water. Two hours later the crude product was filtered off and washed with cold water and was dried over calcium chloride *in vacuo*. An off white solid was obtained in a yield of 2.45 mg (6.58 mmol, 43.87%). ESI-MS: $[MH^+]$ (calculated): 472.4, $[MH^+]$ (found): 472.9; 1H NMR ($CDCl_3$, 300 MHz) δ 2.79 (t, $J = 6.86$, 2H), δ 3.79 (m, 6H), δ 6.99 (t, $J = 7.69$ Hz, 2H), δ 7.31 (m, 4H), δ 7.71 (m, 4H), δ 8.34 (d, $J = 7.69$ Hz, 2H); ^{13}C NMR ($CDCl_3$, 75 MHz) δ 36.04, δ 51.60, δ 60.20, δ 121.92, δ 122.98, δ 123.06, δ 132.20, δ 133.79, δ 136.18, δ 148.85, δ 159.6, δ 168.06.

Synthesis of [di(2-picolyl)amine]ethane-1,2-diamine (L)



N-(2-[di(2-picolyl)amino]ethyl)phthalimide (2.35 g, 6.31 mmol) was dissolved in boiling ethanol (40.00 ml) and hydrazine monohydrate (0.43 ml, 8.25 mmol) was added to it. After refluxing for four hours a white solid had precipitated. The reaction mixture was cooled to ambient temperature and conc. hydrochloric acid (10.00 ml) was added. The precipitate was filtered off after one hour and the filtrate adjusted to pH 10 with aqueous sodium hydroxide ($1 \text{ mol} \cdot \text{L}^{-1}$). The solution was extracted 5 times with diethyl ether, and the combined organic phases were dried over magnesium sulfate. The solvent was removed *in vacuo* and the oily crude product was kept in the fridge over night to crystallize. A yellow solid was obtained in a yield of 650.00 mg (2.68 mmol, 42.47%), which was found to be satisfactorily pure and was used in the next step. ESI-MS: $[\text{M}^+]$ (calculated): 242.3, $[\text{MH}^+]$ (found): 243.0; ^1H NMR (CDCl_3 , 300 MHz) δ 2.69 (t, $J = 6.86$, 2H), δ 2.81 (t, $J = 6.86$, 2H), δ 3.84 (s, 4H), δ 7.14 (m, 2H), δ 7.46 (d, $J = 7.69$ Hz, 2H), δ 7.64 (m, 2H), δ 8.52 (d, $J = 7.69$ Hz, 2H); ^{13}C NMR (CDCl_3 , 75 MHz) δ 39.47, δ 57.06, δ 60.66, δ 122.10, δ 123.03, δ 136.48, δ 149.09, δ 159.55.

Synthesis of 2-[2-[2-[di(2-Picolyl)amine]ethane-1,2-diamine]-3-[2-[1,3-dihydro-3,3-dimethyl-1-(4-sulfobutyl)-2H-indol-2-ylidene]-ethylidene]-1-cyclopenten-1-yl]-ethenyl]-3,3-dimethyl-1-(4-sulfobutyl)-3H-indolium sodium salt (FEW-L)



[di(2-Picolyl)amine]ethane-1,2-diamine (650.00 mg, 2.68 mmol), FEW S0378 (1.58 g, 2.15 mmol), and triethylamine (0.36 ml, 2.60 mmol) were stirred in DMF at room temperature over-night while a change of colour from green to blue could be observed. The reaction mixture was poured into methyl *tert*-butyl ether. The product precipitated and was collected by filtration. The crude product was washed with methyl *tert*-butyl ether and dried *in vacuo*. A blue solid was obtained in a yield of 2.00 g (2.12 mmol, 79.10%). HR-ESI-MS: $[\text{M}-2\text{H}^{2+}]$ (calculated): 460.2159, $[\text{M}-2\text{H}^{2+}]$ (found): 460.2164; ^1H NMR (DMSO, 600 MHz) δ 1.52 (s,

12H), δ 1.69 (m, 4H), δ 1.75 (m, 4H), δ 2.52 (t, $J = 7.14$ Hz, 4H), δ 2.62 (m, 4H), δ 2.68 (m, 4H), δ 3.01 (t, $J = 6.00$ Hz, 2H), δ 3.87 (t, $J = 6.00$ Hz, 2H), δ 3.91 (m, 4H), δ 4.16 (t, $J = 7.14$ Hz, 1H), δ 5.61 (d, $J = 12.00$ Hz, 2H), δ 7.04 (t, $J = 8.00$ Hz, 2H), δ 7.13 (d, $J = 8.00$ Hz, 2H), δ 7.27 (m, 2H), δ 7.46 (d, $J = 8.00$ Hz, 2H), δ 7.49 (d, $J = 8.00$ Hz, 2H), δ 7.73 (d, $J = 8.00$ Hz, 2H), δ 7.73 (d, $J = 12.00$ Hz, 2H), δ 7.74 (d, $J = 8.00$ Hz, 2H), δ 8.46 (d, $J = 4.00$ Hz, 2H); ^{13}C NMR (DMSO, 600 MHz) δ 22.57, δ 22.70, δ 25.55, δ 25.96, δ 26.13, δ 26.21, δ 27.55, δ 36.00, δ 42.44, δ 43.85, δ 44.18, δ 45.83, δ 47.15, δ 49.00, δ 50.80, δ 51.08, δ 52.35, δ 58.89, δ 59.44, δ 96.45, δ 102.72, δ 109.29, δ 111.63, δ 122.16, δ 122.54, δ 122.69, δ 123.28, δ 126.40, δ 128.35, δ 135.72, δ 136.90, δ 137.12, δ 139.81, δ 141.44, δ 142.33, δ 143.10, δ 148.78, δ 149.37, δ 158.44, δ 162.63, δ 164.52, δ 166.33, δ 170.85.

4. Viologen-Type Probes for Phosphates

4.11 Results and Discussion

This chapter deals with the luminescence of various probe designs (see Table1) of HPTS and APTS with the quenchers TEAPB, TEABB, and TEAPeB in the presence of numerous phosphates.

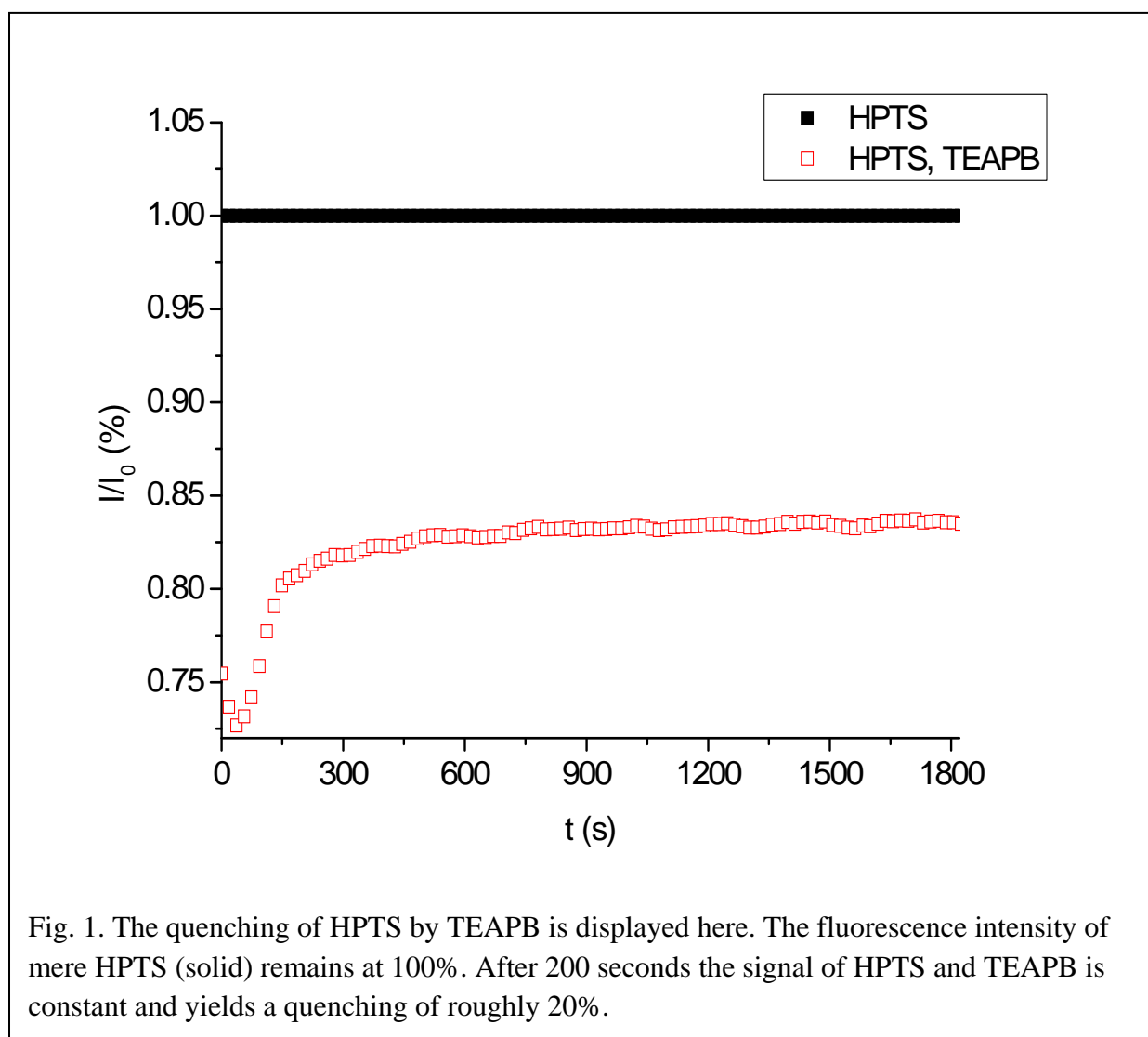
A large number of phosphates was investigated. Hence it is convenient to group these analyte phosphates. ATP, ADP and P_i are involved in the ATPase reaction (see Introduction, scheme 1). Thus the first group includes these phosphate species. Moreover, guanosines were investigated. AMP, cAMP, and PP_i were also studied. Finally all adenines are displayed in one plot. Fluorescence intensity was recorded in a microtiter plate. All experiments were repeated at least eight times for each phosphate sample and subjected to statistical evaluation, mostly standard deviation by Excel. The concentrations were $5 \mu\text{M}\cdot\text{L}^{-1}$ for the quenchers, $17.5 \mu\text{M}\cdot\text{L}^{-1}$ for the samples and $0.5 \mu\text{M}\cdot\text{L}^{-1}$ for the pyrenes according to chapter 3.1.2. Each measurement was referenced to the emission of HPTS or APTS (I_0) without quencher and sample. The fluorescence intensity was recorded in 24 mM TRIS buffer solution (see 1.2) at pH 7.8.

Table 1. Overview of the sensing schemes for phosphate that were investigated in this chapter. The notation PQI refers to HPTS serving as fluorescent pyrene and TEAPB as quencher. PQI to PQVI were subsequently studied and exposed to phosphates in order to determine whether or not a viable sensing scheme could be achieved.

<i>Pyrene</i>	<i>Quencher</i>	<i>Notation</i>
HPTS	TEAPB	PQI
	TEABB	PQIII
	TEAPeB	PQV
APTS	TEAPB	PQII
	TEABB	PQIV
	TEAPeB	PQVI

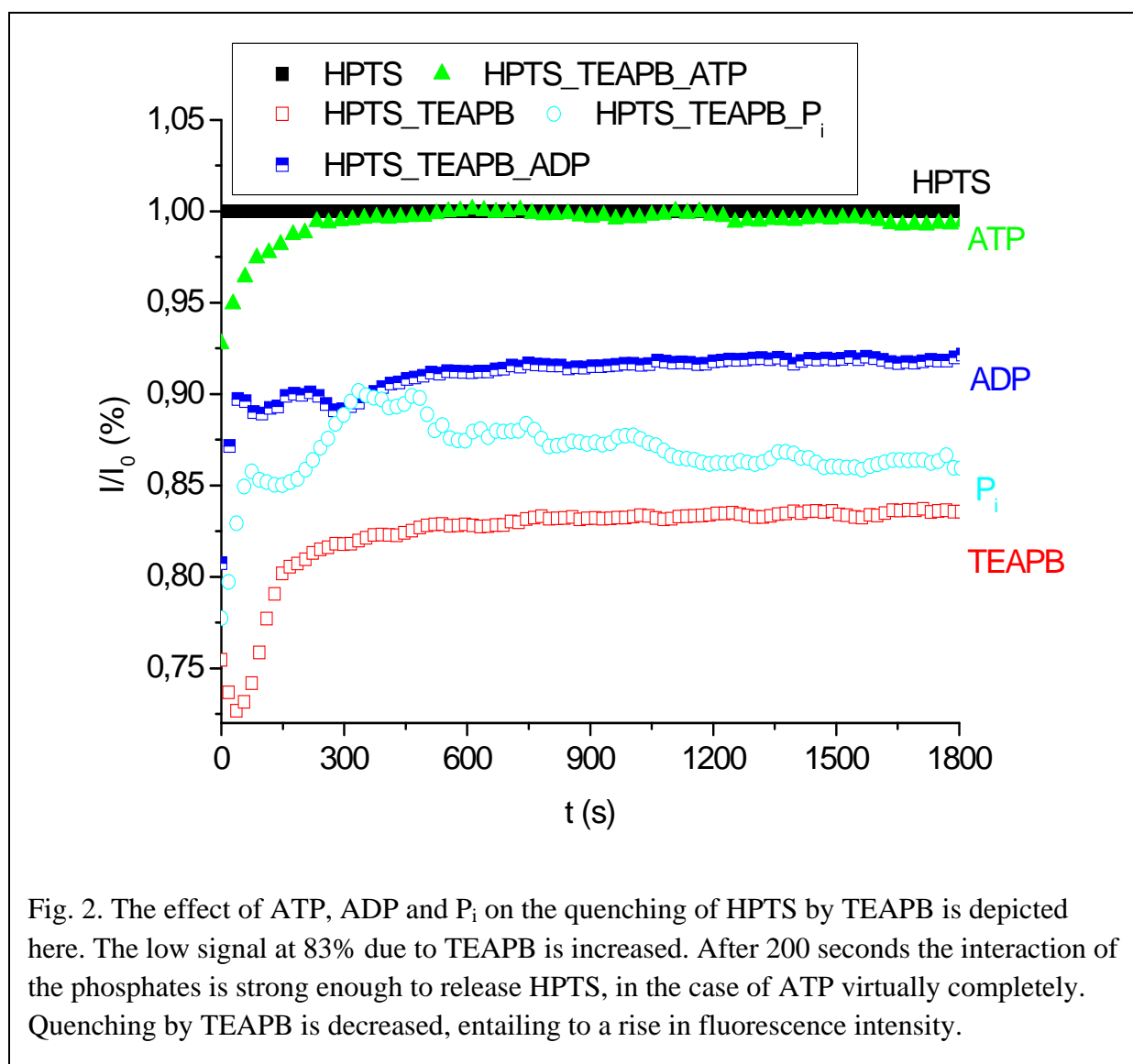
4.1.1 HPTS with TEAPB as fluorescent probe for the detection of ATP and other phosphates

Fig. 1 displays the quenching of HPTS by TEAPB. The signal became stable after 200 seconds and yielded a drop to 83%.



Upon addition of phosphates a reverse effect, i.e. a partial recovery of the fluorescence signal, is expected due to interaction of the negative charges and the aromatic nucleic bases with the viologens (see 1.1).

The intensity plots upon the addition of ATP, ADP and P_i are displayed in Fig. 2.



It was found that there is a sufficiently strong interaction between ATP and TEAPB entailing to a release of virtually all HPTS. Hence the fluorescence intensity recovers to the level I_0 of the reference. A substantially weaker interaction takes place between ADP and TEAPB. This can be explained on the basis of remaining electron transfer from HPTS to the quencher not being completely disabled and thus fluorescence intensity is of intermediate magnitude. Contrary to this, P_i carries no sugar and aromatic base moieties. As a consequence there is no possibility for π - π or similar interactions, only electrostatic interaction between phosphate and the quaternary nitrogen groups of TEAPB can be accounted for any effect. Accordingly, the

weakest fluorescence recovery can be observed in the case of P_i . Due to the difference in the interacting forces a clear distinction between the three phosphates involved can be drawn.

Guanosine Phosphates

Guanine carrying nucleotides constitute the next group of phosphates. Their response is depicted in Fig. 3. GTP is analogous to ATP and the strongest interaction with TEAPB is recorded in this case. The signal is recovered to 95% of the reference. A slightly lower signal was recorded for GMP. This is surprising as the molecule is substantially smaller and it possesses fewer phosphate groups as opposed to GTP. Hence the possibility for interaction with the quaternary nitrogen moiety of TEAPB is limited. A substantial gap is observed

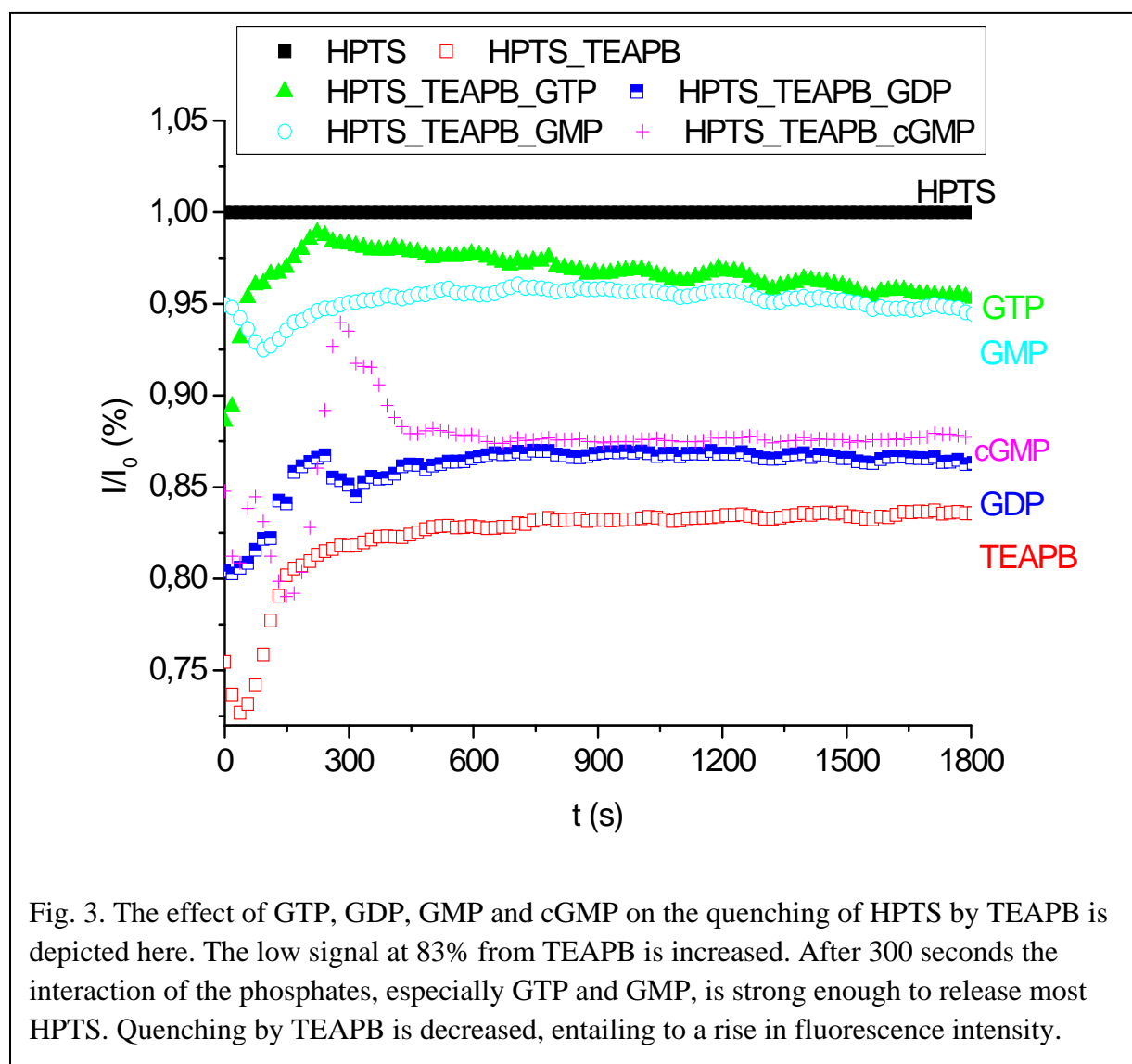
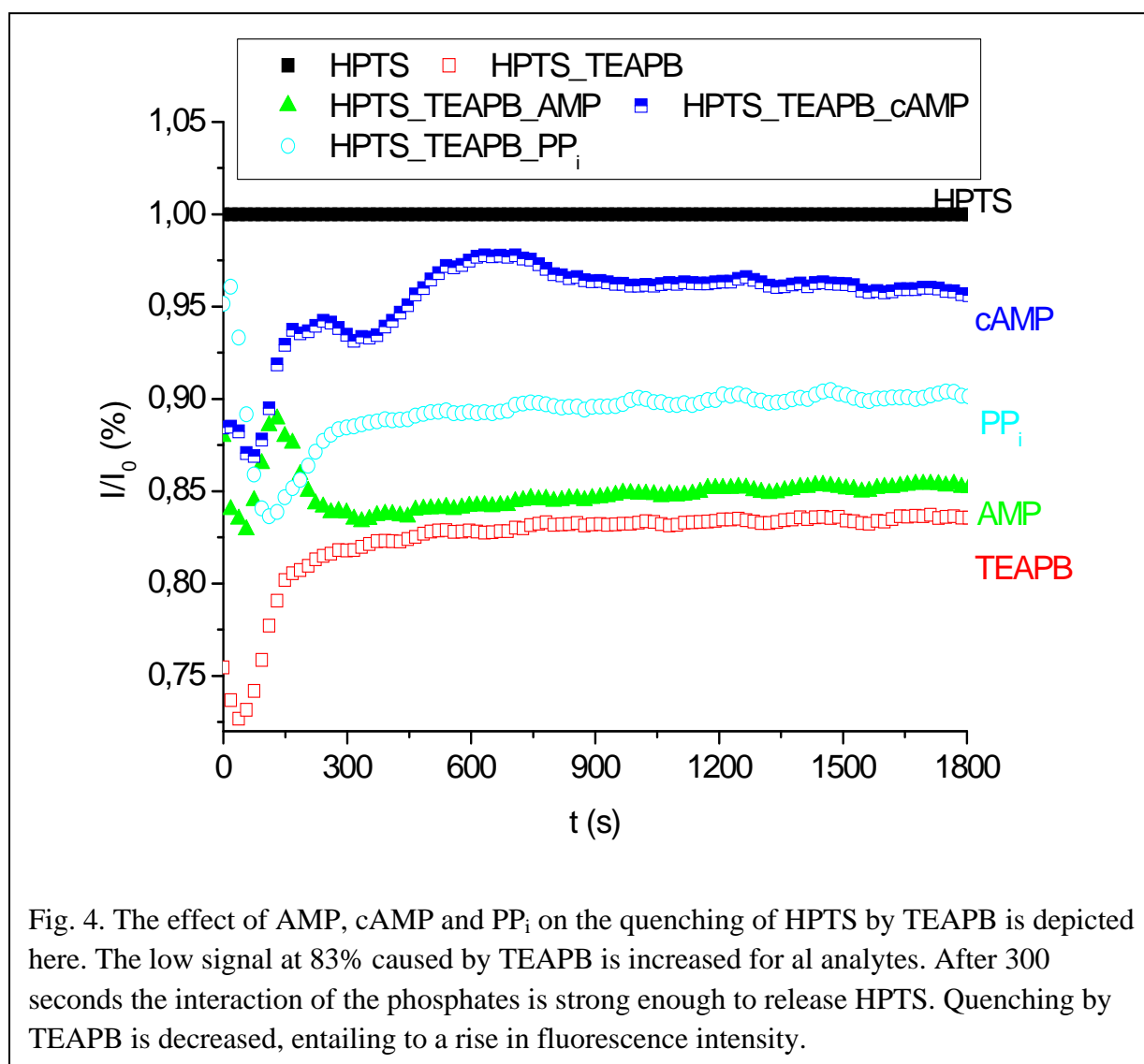


Fig. 3. The effect of GTP, GDP, GMP and cGMP on the quenching of HPTS by TEAPB is depicted here. The low signal at 83% from TEAPB is increased. After 300 seconds the interaction of the phosphates, especially GTP and GMP, is strong enough to release most HPTS. Quenching by TEAPB is decreased, entailing to a rise in fluorescence intensity.

between the signal of GTP/GMP and that of cGMP. The response of GDP is similar to that of the latter. Again, this is surprising as the diphosphate group and the bulky cyclic phosphate groups are clearly distinct. The fluorescence intensity is recovered to a level of roughly 87% in both cases.

AMP, cAMP and PP_i

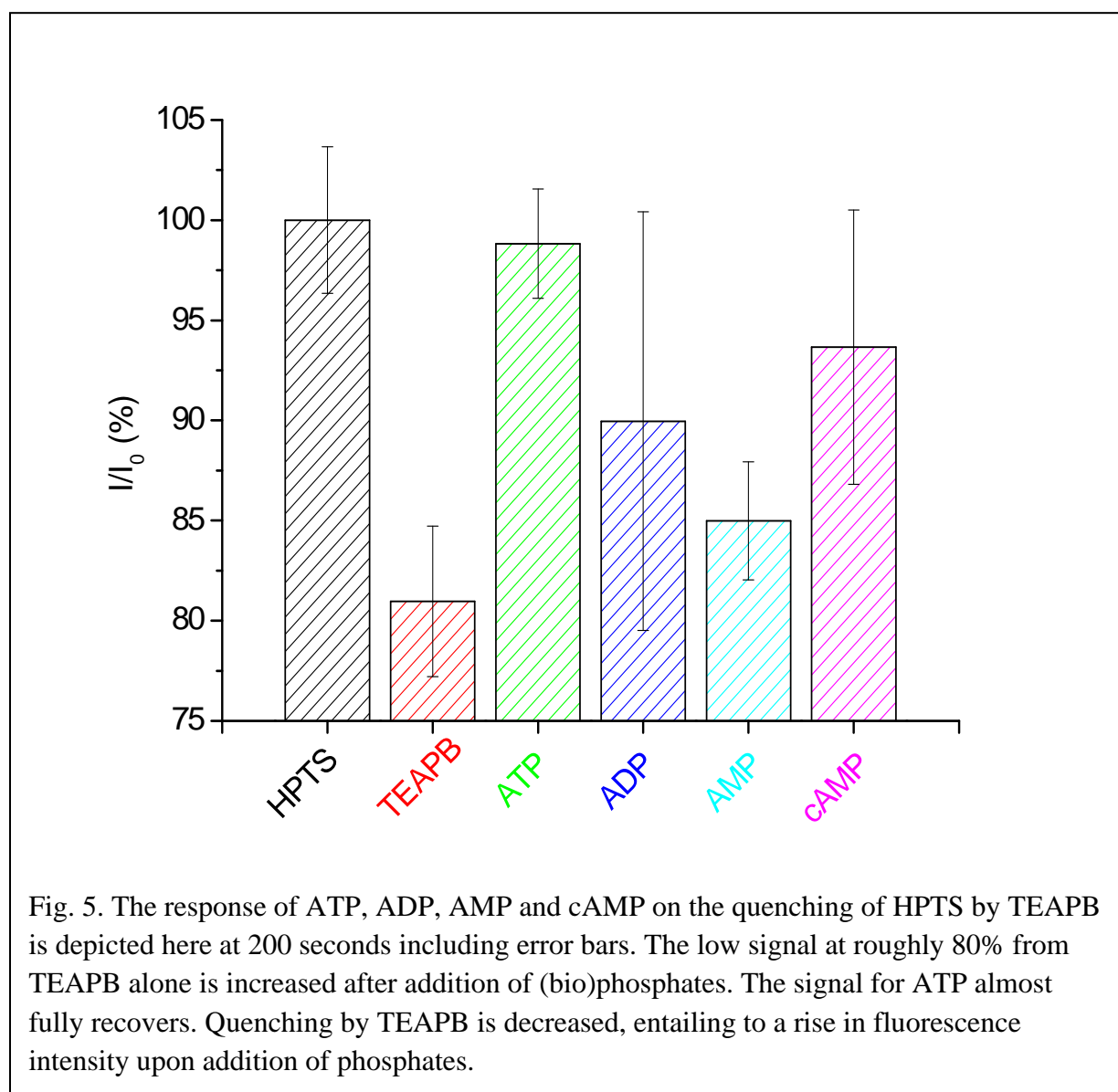
The response of AMP, cAMP and PP_i is depicted in Fig. 4. A clear distinction between the three phosphates involved can be drawn. Fluorescence intensity recovers to a level of 95% when cAMP is present. The signal for PP_i is of intermediate magnitude at 90%. cAMP has the least impact on TEAPB, hence the signal only rises to 85% of the original level. This



confirms the assumption that due to their distinct structure, distinct signals are to be expected from different modes and intensity of interaction with the fluorescent quencher TEAPB. The signal requires a considerably longer time to become stable. This might be due to the presence of the bulky phosphate ester. The equilibrium requires longer time to be set in such a case.

Adenosine Phosphates

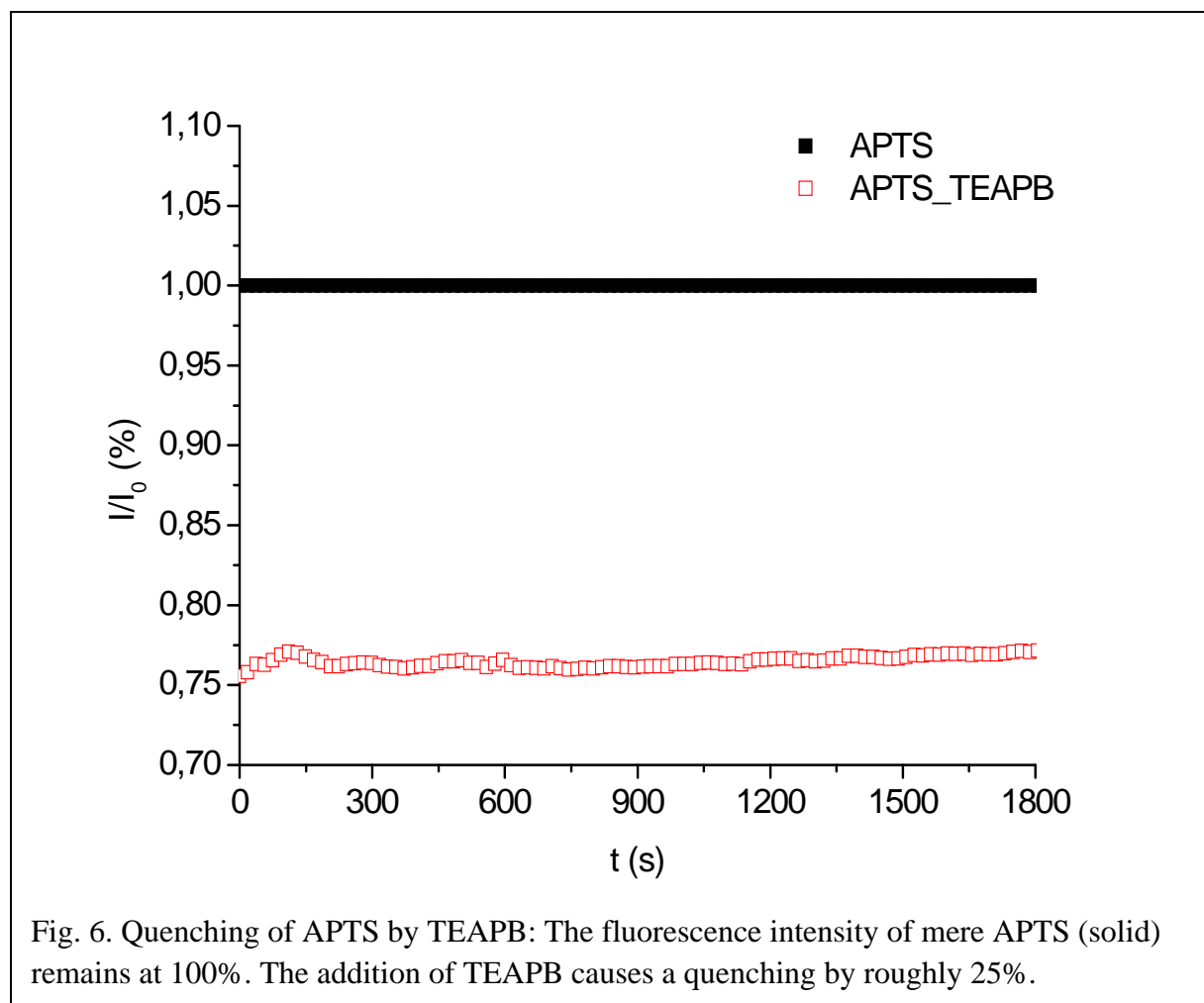
Fig. 5 summarizes the response of all adenosine derivatives. Again, a clear distinction can be drawn between the four species. The phosphate species that were investigated here all possess the same base. They only differ in size and number of phosphate groups and thus their potential to participate in electrostatic interactions. Yet that point of discrimination suffices in



order to obtain results in good resolution. Yet a sometimes high standard deviation needs to be taken into account.

4.1.2 APTS with TEAPB as fluorescent probe for the detection of ATP and other phosphates

The potential of TEAPB as a quencher is depicted in Fig. 6. The fluorescence intensity



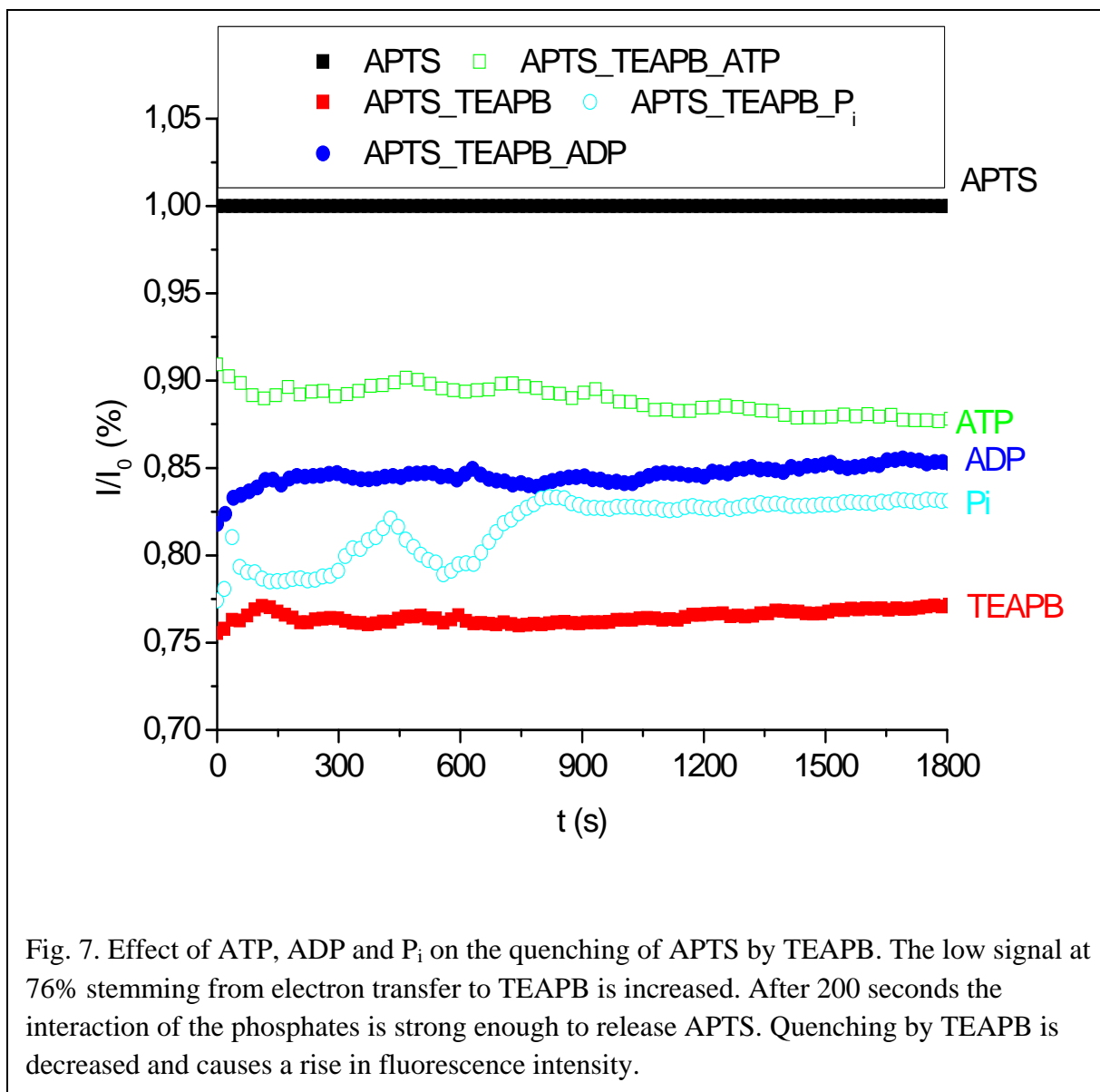
became immediately stable and dropped to 76%. For comparison, when HPTS was used, a time delay of 200 seconds was required. The only distinction between these two pyrenes lies in the side group. APTS possesses an uncharged amino group while HPTS has a negatively charged hydroxyl group at the applied pH. While relatively weak π -interactions offer the only mode

of coordination in the former case much stronger electrostatic forces are involved in the latter case. Hence, equilibration is much faster. Moreover, TEAPB quenches the fluorescence by roughly 5%. The more efficient quenching is probably due to the more compact complex as a result of the presence of stronger interacting forces.

The quenched signal is expected to recover to its original level upon addition of phosphates.

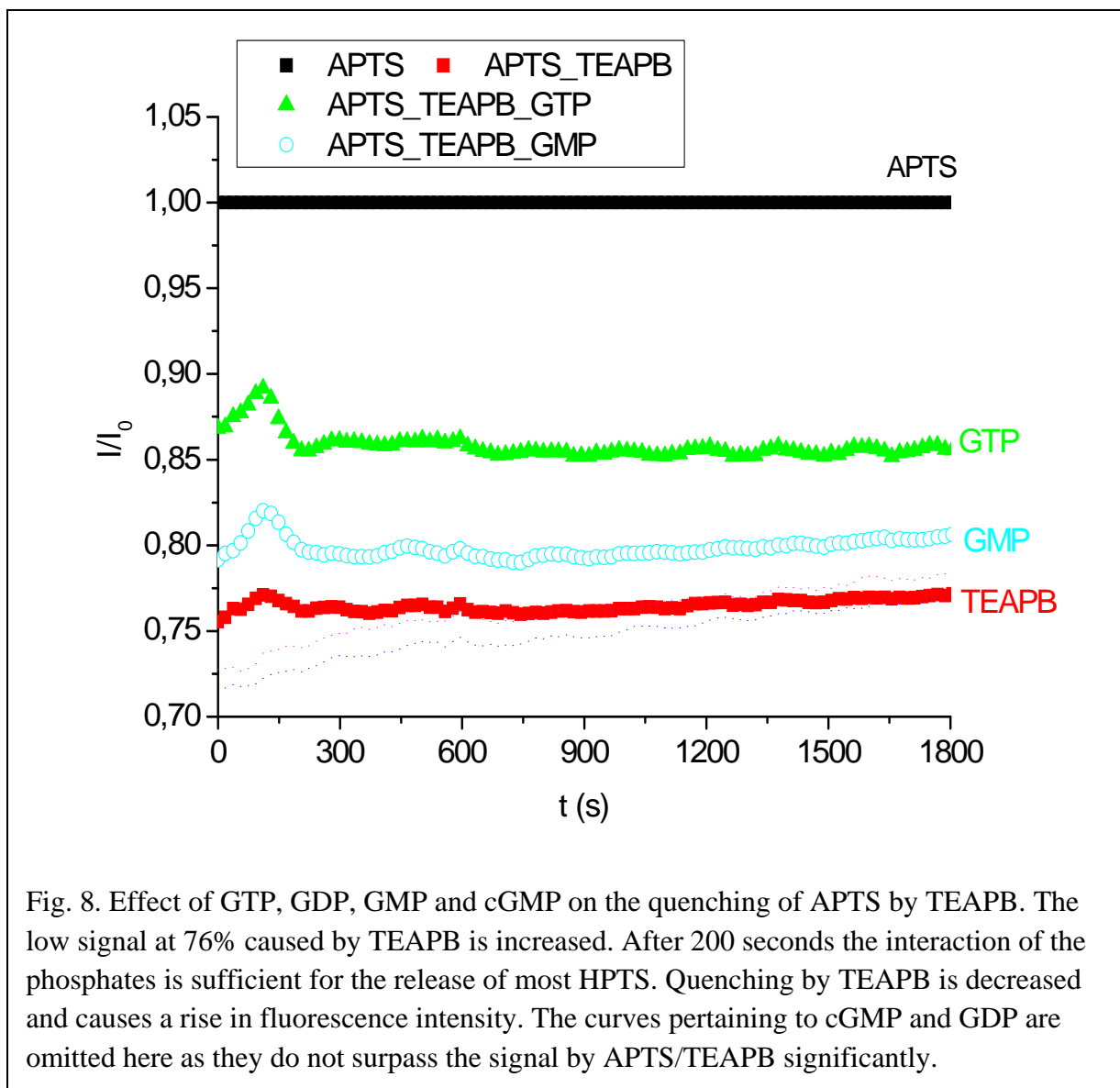
Phosphates in ATPase Reaction

The responses of ATP, ADP and P_i are displayed in Fig. 7. Contrary to HPTS, APTS does not retrieve the level of fluorescence intensity without TEAPB as quencher when phosphate is added. While it causes the strongest reverse effect, only about 90% of the fluorescence intensity of the original signal is reached upon addition of ATP. The stronger quenching of the fluorescence intensity of APTS by TEAPB would be an explanation. Thus an equal concentration of ATP entails to the signal recovering less effectively. Apparently, a weaker interaction is present between ADP and TEAPB and fluorescence intensity is of intermediate magnitude. P_i carries no sugar and aromatic base. Owing to this fact π - π or similar interactions are obviously no factor here. Phosphate and the quaternary nitrogen groups of TEAPB are only subjected to electrostatic attraction. Yet P_i raises fluorescence intensity to nearly the level of ADP. A distinction between the three phosphates investigated can be drawn. However, the resolution is less advantageous than for HPTS.



Guanosine Phosphates

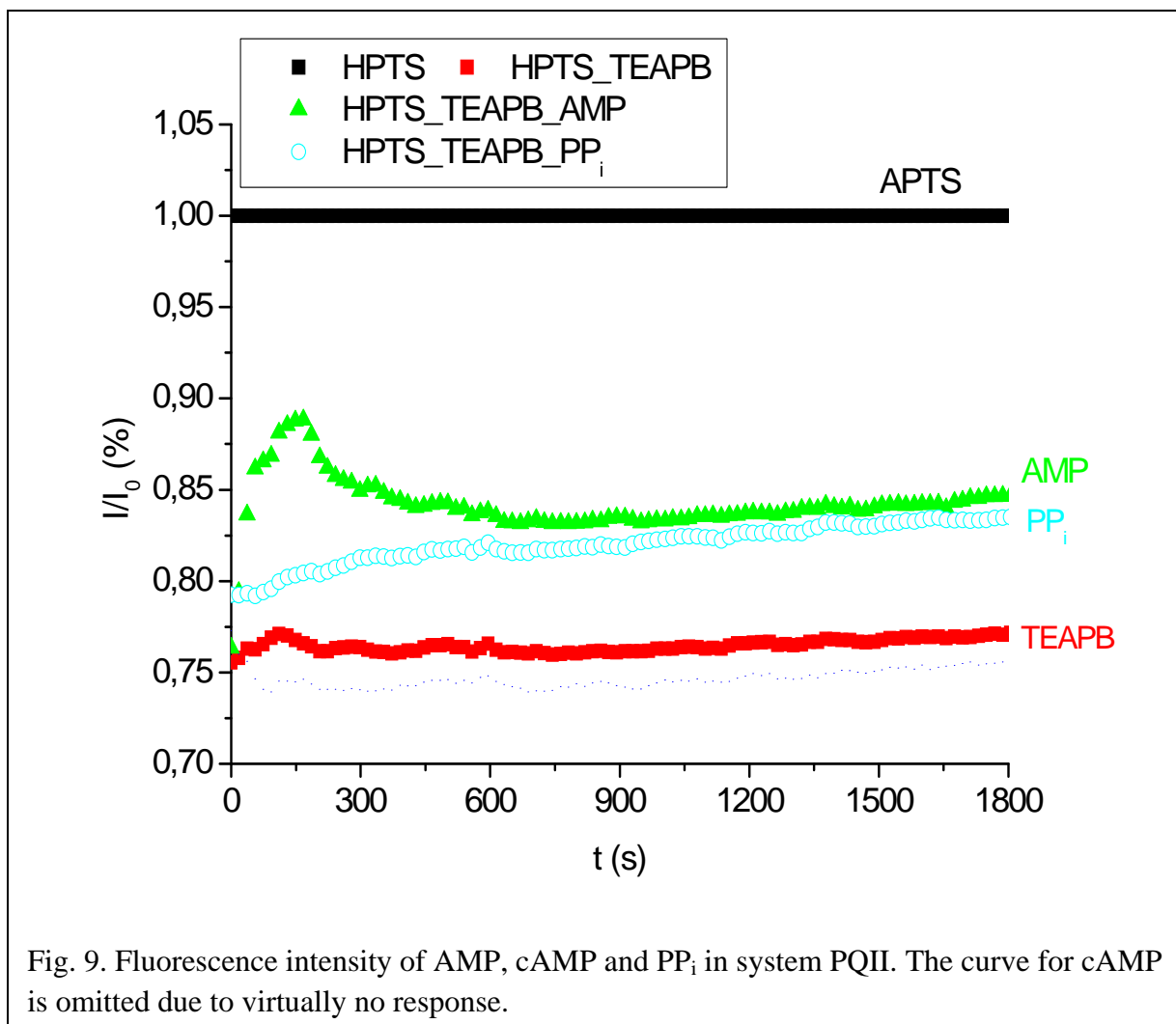
Fig. 8 yields the response of the guanine phosphates. The fluorescence intensity of cGMP and GDP is not recovered at all. A rise of 5% to 80% of the signal I_0 can be observed for GMP. GTP, in analogy to ATP, yields the highest signal recovery. This was also the case for HPTS. Yet the resolution is much poorer in this case. A possible explanation may lie behind the strong interaction between TEAPB and APTS as could be seen in a more efficient quenching and an immediate drop in fluorescence (Fig. 6). Accordingly phosphates cannot pry the quencher off the pyrene quick and sufficiently enough. cGMP might require more time for the equilibrium to become set as was the case for PQI. It can also be concluded that GMP and



GTP seem to be a better match for TEAPB regarding size and number of charges.

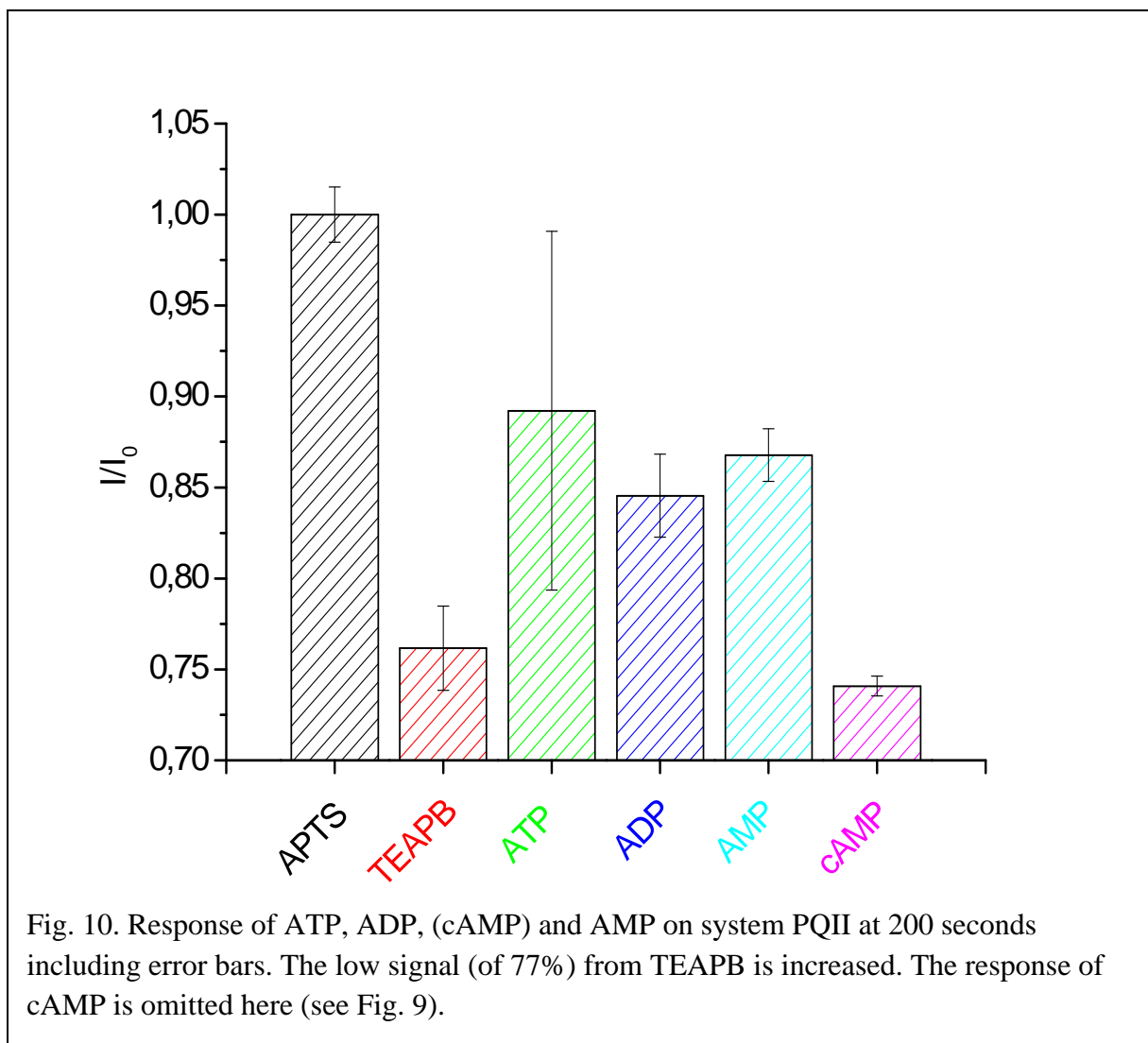
AMP, cAMP and PP_i

Fig. 9 exhibits the behaviour of cAMP, AMP and diphosphate in the sensing scheme PQII. The signal of cAMP does not surpass the response from TEAPB, i.e. no reduction of quenching occurs. Once more, resolution is poor. AMP and PP_i are of virtually the same level at slightly below 80% of the fluorescence intensity of the reference. Both molecules feature distinct building blocks and were not expected to prompt a like response. This observation is contrary to PQI. A very good resolution could be achieved there for all adenosine phosphates.



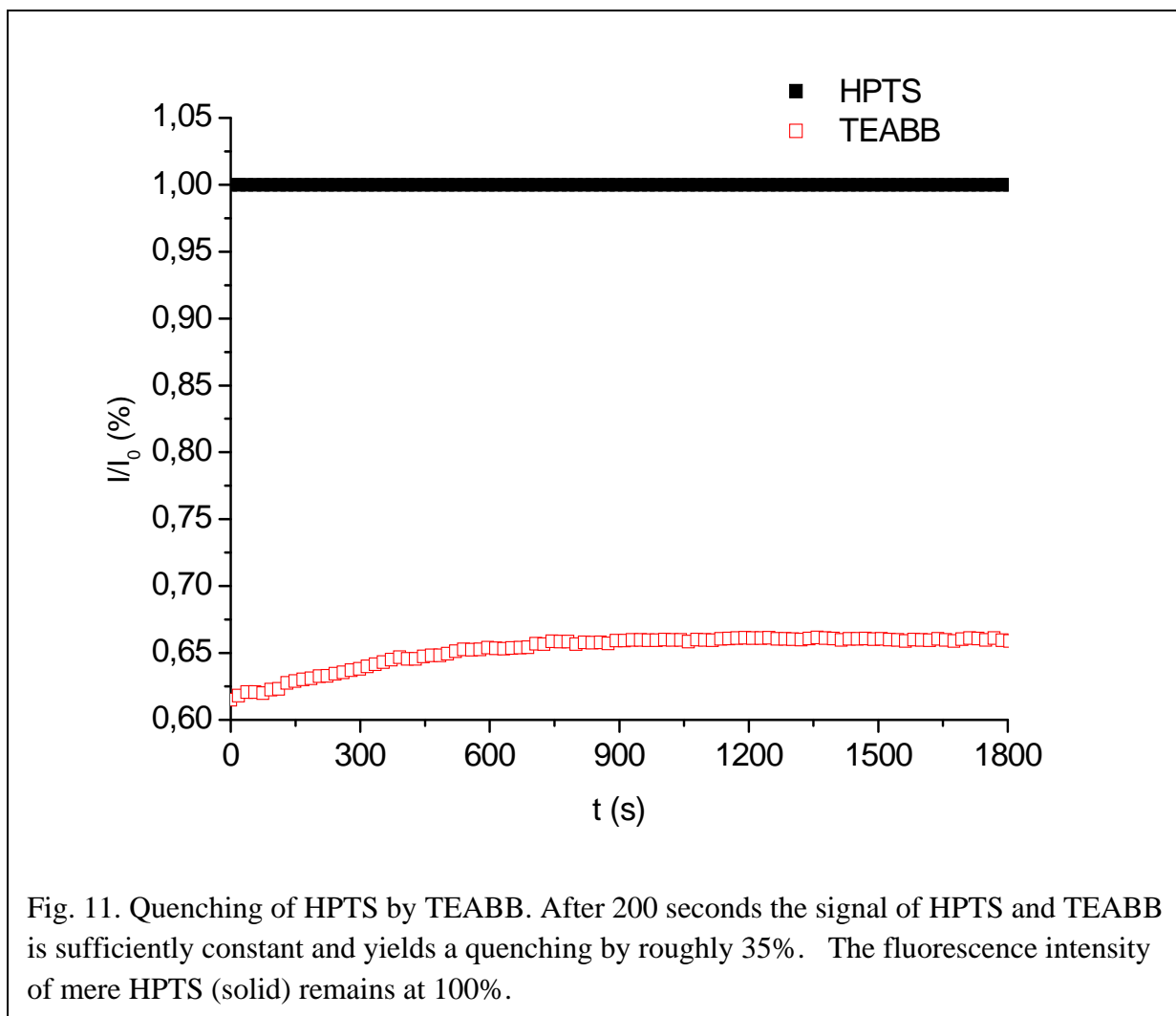
Adenosine Phosphates

The response of ATP, ADP, AMP and cAMP is on display in Fig. 10. The signal of ADP and AMP is of virtually the same magnitude. That of ATP reaches only a slightly higher level. The signal of cAMP does not surpass that of the quencher TEAPB. This renders resolution rather poor once more. Hence a stronger interaction of the viologen with APTS is conjectured while a weaker interaction with the phosphates takes place. The response seems to be largely independent of size and charge. It may be assumed, however, that cyclic phosphates require a substantially longer time to coordinate TEAPB and thus no change of signal could be recorded within the time-frame of the experiment. In any case, PQII makes up a rather inconvenient sensing scheme due to its poor resolution and sensitivity. Although standard deviation is mostly on a satisfying level, poor reproducibility is indicated in the case of ATP.



4.1.3 HPTS with TEABB as sensing design for the detection of ATP and other phosphates

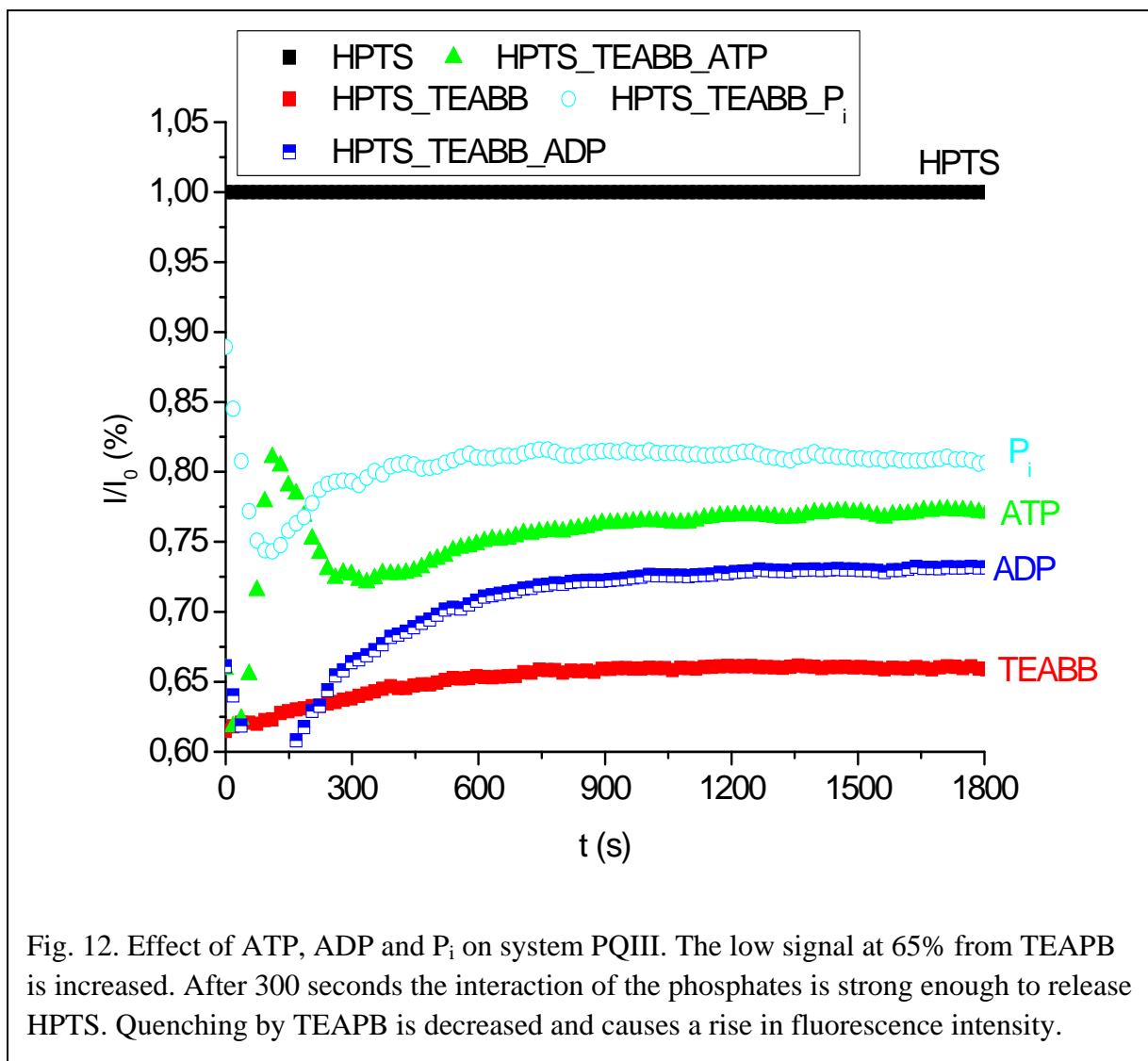
The potential of TEAPB as a fluorescent quencher of HPTS is depicted in Fig. 11. The fluorescence intensity became stable after approximately 200 seconds and yielded a drop to 65%. PQI required the same period of time. The TEABB probe entails to stronger quenching than TEAPB on HPTS. Both viologens differ in length of the alkyl chain only. Apparently a longer spacer enables a better “embrace”, i.e. a stronger mode of binding is able to fix the



quencher/pyrene complex, to render it more stable and more efficient. Upon exposure to phosphates, PQIII is expected to yield a rise in fluorescent intensity.

Phosphates in ATPase Reaction

ATP, ADP and P_i are displayed in Fig. 12. Contrary to PQI, ATP is not capable of releasing most HPTS by interaction with the quencher. P_i impacts TEABB the most while it had no substantial effect on TEAPB. Apparently electrostatic interaction was sufficient for reversing quenching. Fluorescence intensity recovers to 80% of the level of the reference. A weaker interaction takes place between ATP and TEABB. At 75% of the reference value, fluorescence intensity is of intermediate magnitude. The signal for ADP rose to 70% of the reference. Thus a clear distinction between the three phosphates involved can be drawn. Yet resolution was poorer than in the case of TEAPB.



Guanosine Phosphates

Guanine carrying nucleotides constitute the next group of phosphates investigated. Their response is depicted in Fig. 13. The signal is recovered to over 90% of the reference in the case of GDP. Hence, the strongest interaction with TEABBB takes place here. A notably lower signal at 85% was recorded for cGMP. GTP and GMP slightly raise the fluorescence intensity by 5% to a level of 70% of the reference. This is unexpected as both molecules are clearly distinct. GMP is considerably smaller and it possesses fewer phosphate groups as opposed to GTP. Hence a difference in size and charge needs to be taken into account. Yet their response, and thus their capability of impacting TEABBB, is of similar order. Despite the fact that GMP and GTP cannot be clearly distinguished, the response of PQIII to the guanine carrying phosphates offers good resolution. Thus this sensing scheme is well suited for probing

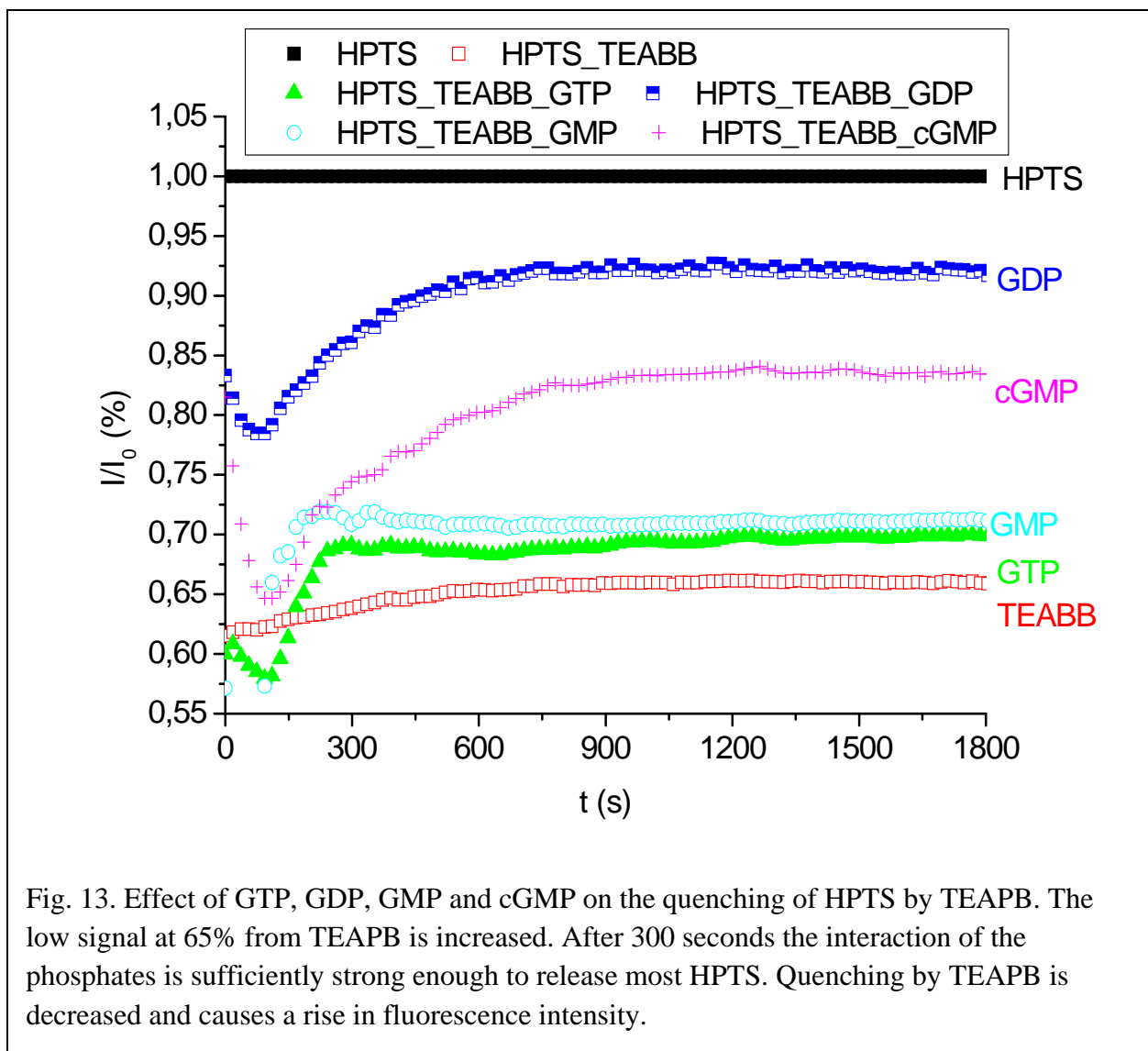
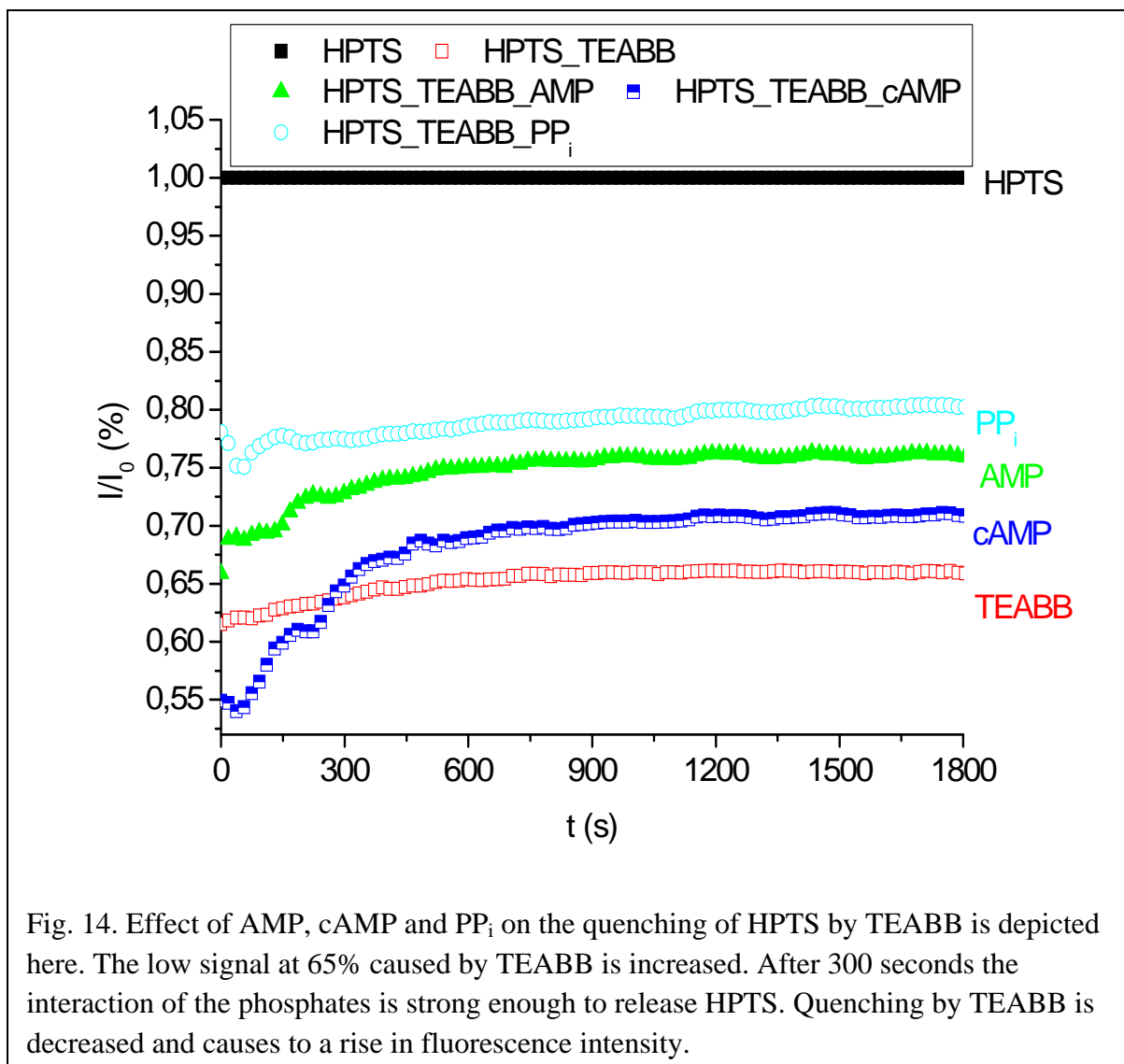


Fig. 13. Effect of GTP, GDP, GMP and cGMP on the quenching of HPTS by TEAPB. The low signal at 65% from TEAPB is increased. After 300 seconds the interaction of the phosphates is sufficiently strong enough to release most HPTS. Quenching by TEAPB is decreased and causes a rise in fluorescence intensity.

guanosine phosphates and the investigation of enzymes that produce and/or consume such species.

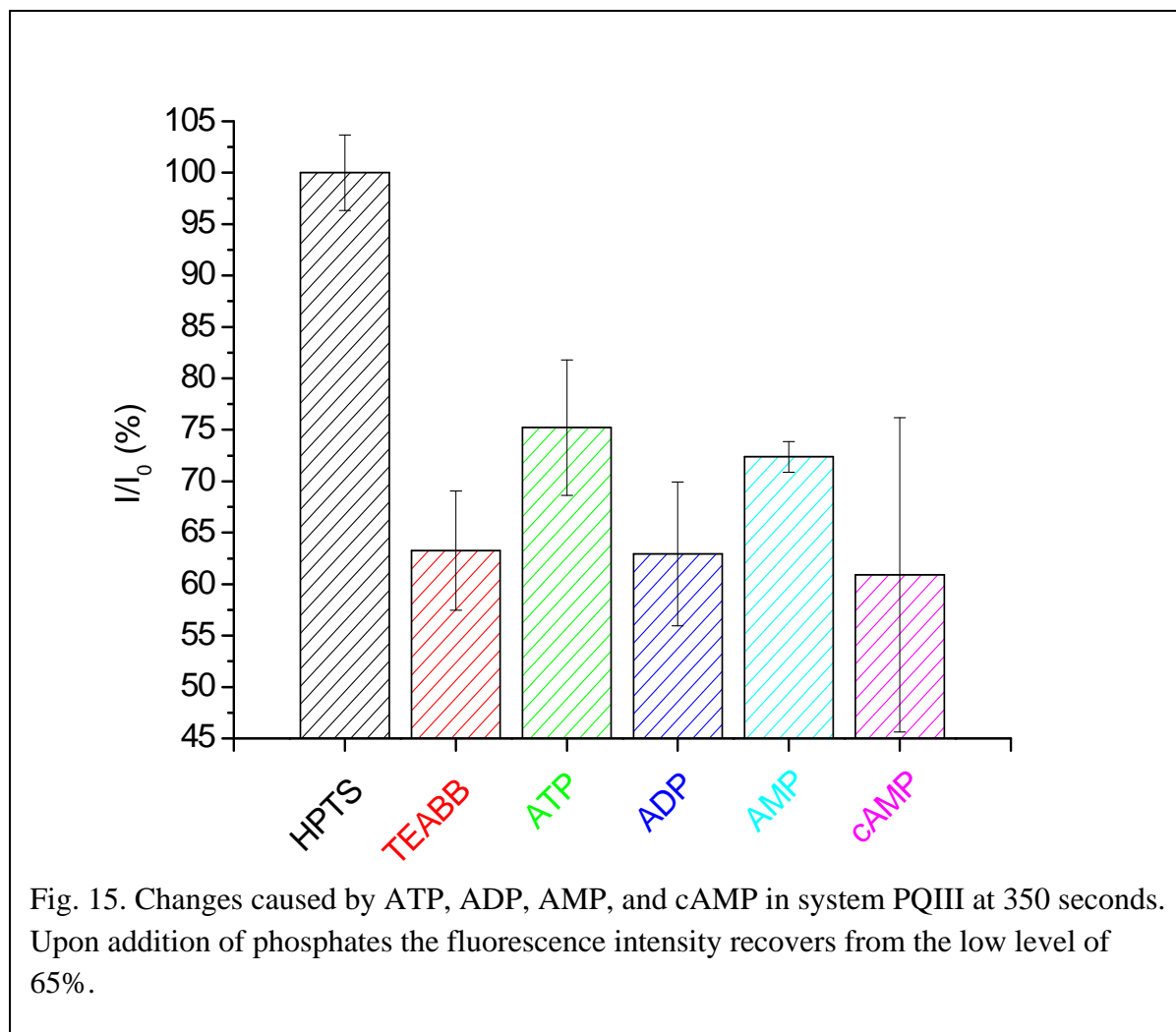
AMP, cAMP and PP_i

The response of AMP, cAMP and PP_i is depicted in Fig. 14. A clear distinction between the three phosphates involved can be drawn. Fluorescence intensity recovers to a level of nearly 80% when PP_i is present. The signal for AMP is of intermediate magnitude at 75%. cAMP has the least impact on TEABB, hence the signal only rises to 85% of the reference.



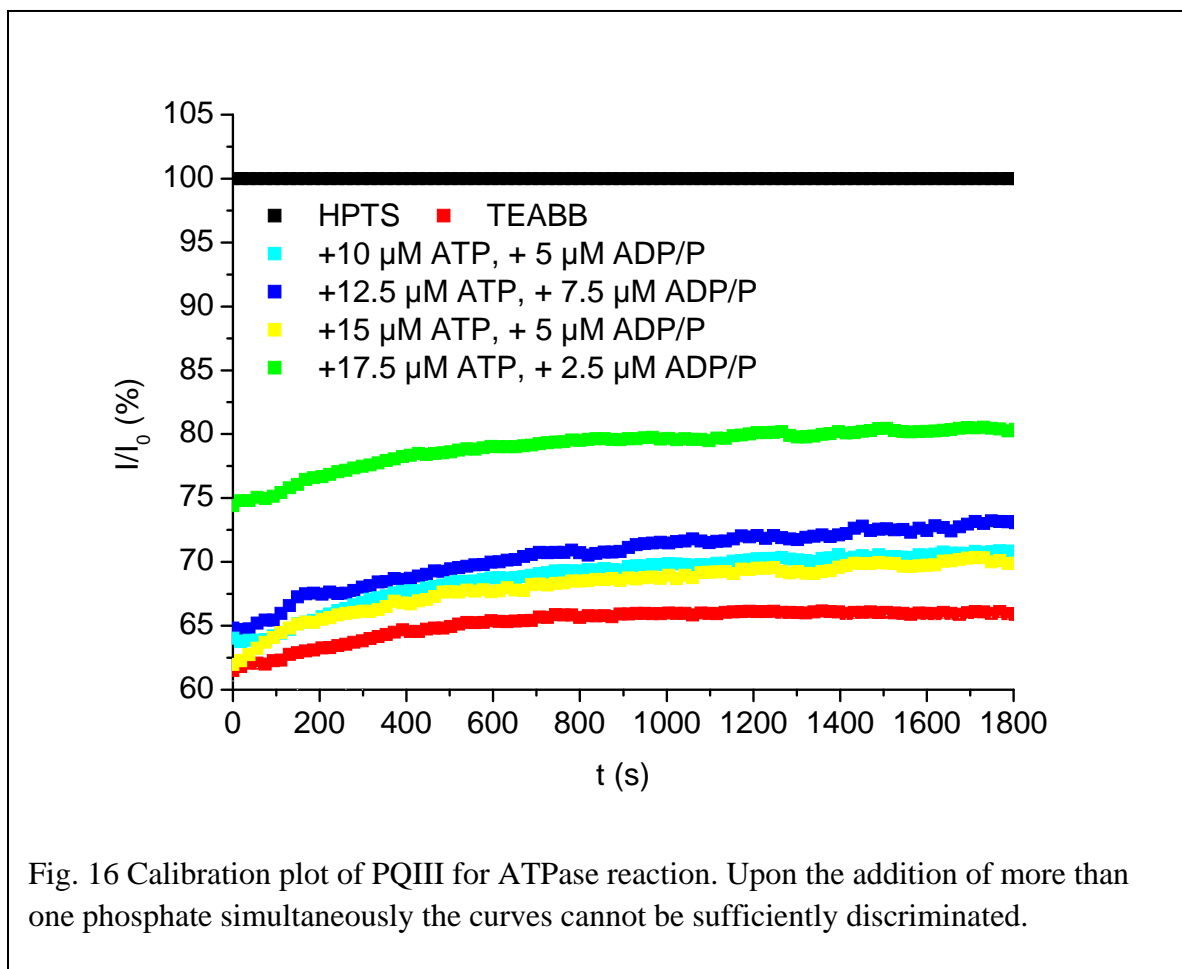
Adenosine Phosphates

Curves for all adenosine phosphates are plotted in Fig. 15 after exposure to PQIII. A distinction can be drawn albeit to a lesser degree. The response of ATP and AMP converges to virtually the same level though. Resolution and reproducibility (see error bars) are poorer than in PQI. This observation confirms the initial observation that TEABB and HPTS are more inclined to form complexes than TEAPB and HPTS. Thus phosphates can only free a smaller amount of pyrene. Poor resolution and a slower response can be explained on the same basis as well.



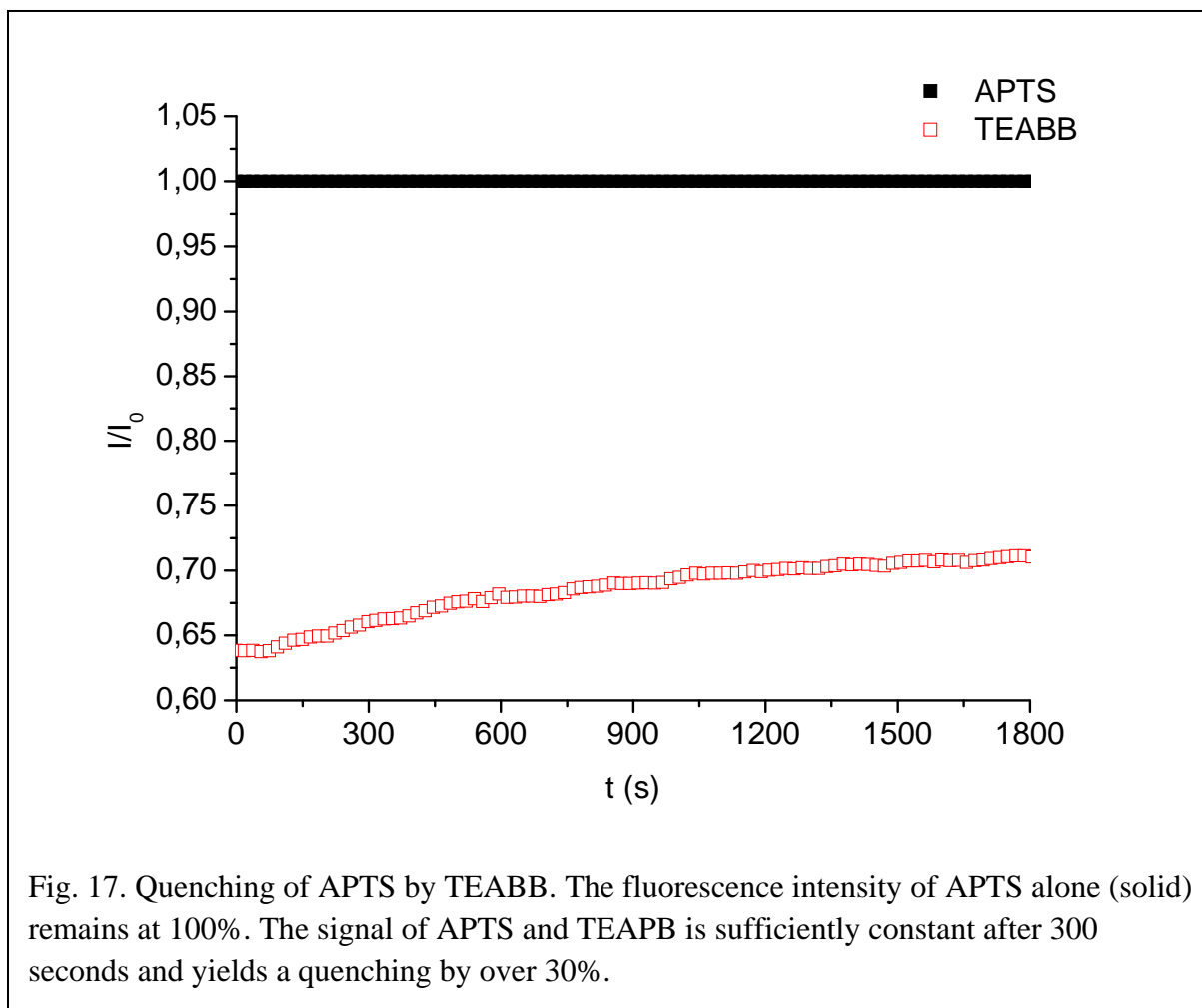
Calibration for ATPase reaction

ATPase decomposes ATP to ADP and P_i releasing energy (see Introduction, Scheme 1). Accordingly, calibration curves were recorded (Fig. 16). The concentration of ADP equalled that of P_i as for one consumed molecule of ATP one molecule of ADP and one of P_i is generated. The concentration of ATP was determined by subtraction of the ADP concentration from 20 μM . Poor resolution was achieved and no clear distinction of the curves was possible at a concentration of ATP below 17.5 μM . Accordingly, this sensing scheme cannot be applied to monitoring ATPase activity.



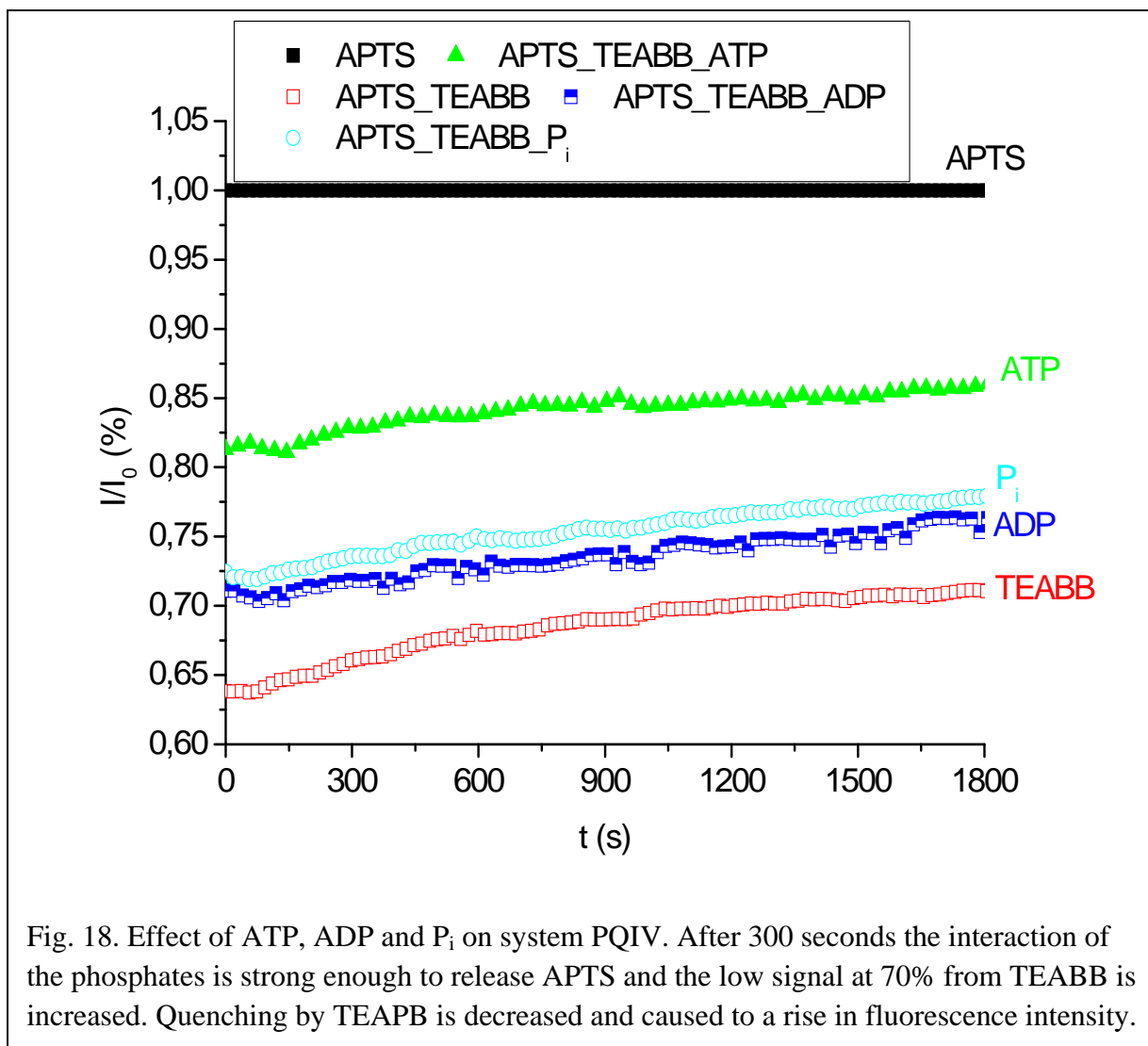
4.1.4 APTS with TEABB as sensing design for the detection of ATP and other phosphates

Fig. 17 yields the potential of TEABB on APTS as a quencher. The fluorescence intensity became stable after 300 seconds and dropped to 70%. Upon the addition of phosphates a reverse effect, i.e. a recovery of fluorescence was expected and subsequently studied.



Phosphates in ATPase Reaction

The response of ATP, ADP and P_i in PQIV are displayed in Fig. 18. Fluorescence of APTS does not retrieve the level without TEABB for any adenosine. A like observation could be made in the case of HPTS. ATP exercises the strongest influence on the viologen in PQ III and PQIV. Contrary to HPTS, a great deal of fluorescence intensity is recovered here as a rise to 85% of the reference is recorded. This confirms the behaviour observed in PQI and PQII that ATP yields the highest signal in this sensing scheme. Thus a better match between TEABB and ATP is presumed, both electrostatically and through π - π interactions, as fluorescence intensity rises to a relatively higher level compared to the previous quencher.



Apparently a weaker interaction takes place between ADP and TEABB and fluorescence intensity is of a low magnitude at below 75%. The signal for P_i lies at 75% of the reference. A better resolution and clearer discrimination was expected as phosphate and ADP are distinct due to the lack of a sugar and aromatic base of the former. A considerable difference in size needs to be taken into account as well.

Therefore this system is not suitable for monitoring the decomposition of ATP into ADP and phosphate by ATPase owing to poor discrimination of these three phosphates.

Guanosine Phosphates

The response of guanine carrying nucleotides in PQIV is depicted in Fig. 19. The strongest interaction with TEABB is recorded in the case of GMP. The signal is recovered to over almost 85% of the reference. A notably lower signal at 80% was recorded for cGMP. GTP and GDP slightly raise the fluorescence intensity by 5% to a level of above 70% of the reference. Although resolution is not sufficient, discrimination of the species is possible. This is reasonable as both molecules differ only slightly in terms of the number of the phosphate groups. Despite the fact that GDP and GTP can only be somewhat distinguished, the response of the guanine carrying phosphates features good resolution.

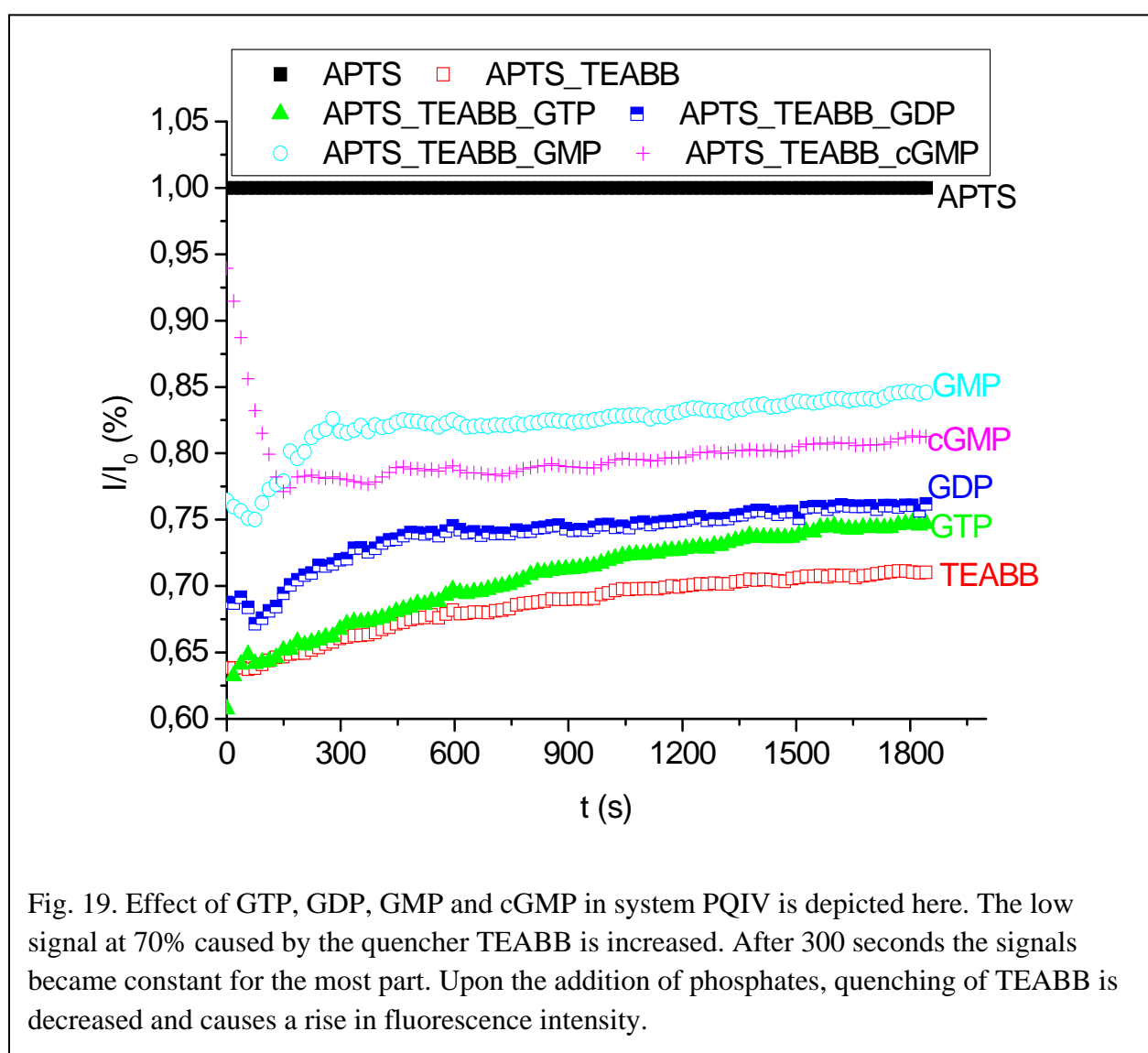


Fig. 19. Effect of GTP, GDP, GMP and cGMP in system PQIV is depicted here. The low signal at 70% caused by the quencher TEABB is increased. After 300 seconds the signals became constant for the most part. Upon the addition of phosphates, quenching of TEABB is decreased and causes a rise in fluorescence intensity.

AMP, cAMP and PP_i

The response of AMP, cAMP and PP_i is depicted in Fig. 20. A clear distinction cannot be drawn between the three phosphates involved. Fluorescence intensity recovers to a level of 80% when PP_i and cAMP are present. The signal for AMP is of intermediate magnitude at 72%. A similar behaviour was observed in PQII (see above).

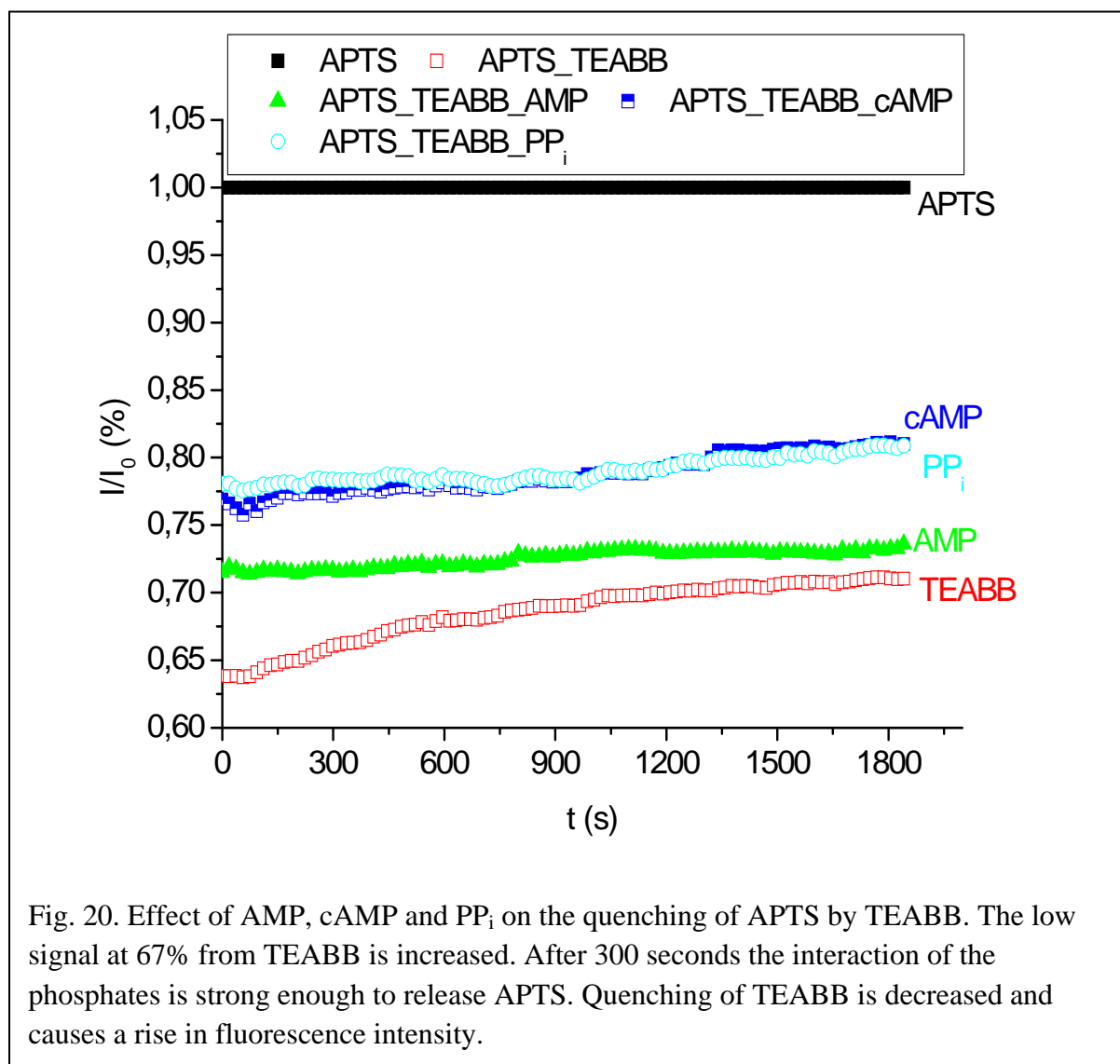
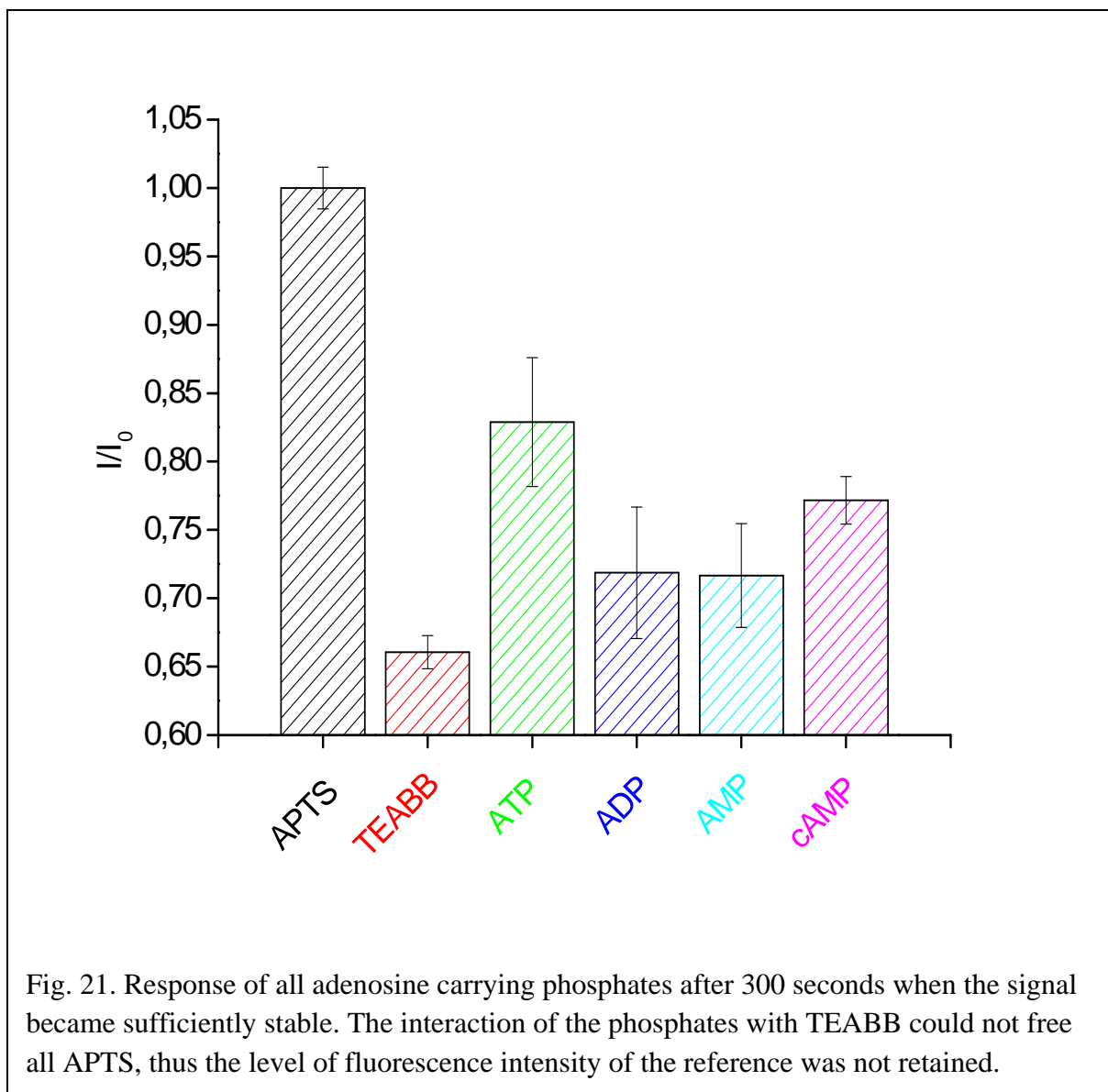


Fig. 20. Effect of AMP, cAMP and PP_i on the quenching of APTS by TEABB. The low signal at 67% from TEABB is increased. After 300 seconds the interaction of the phosphates is strong enough to release APTS. Quenching of TEABB is decreased and causes a rise in fluorescence intensity.

Adenosine Phosphates

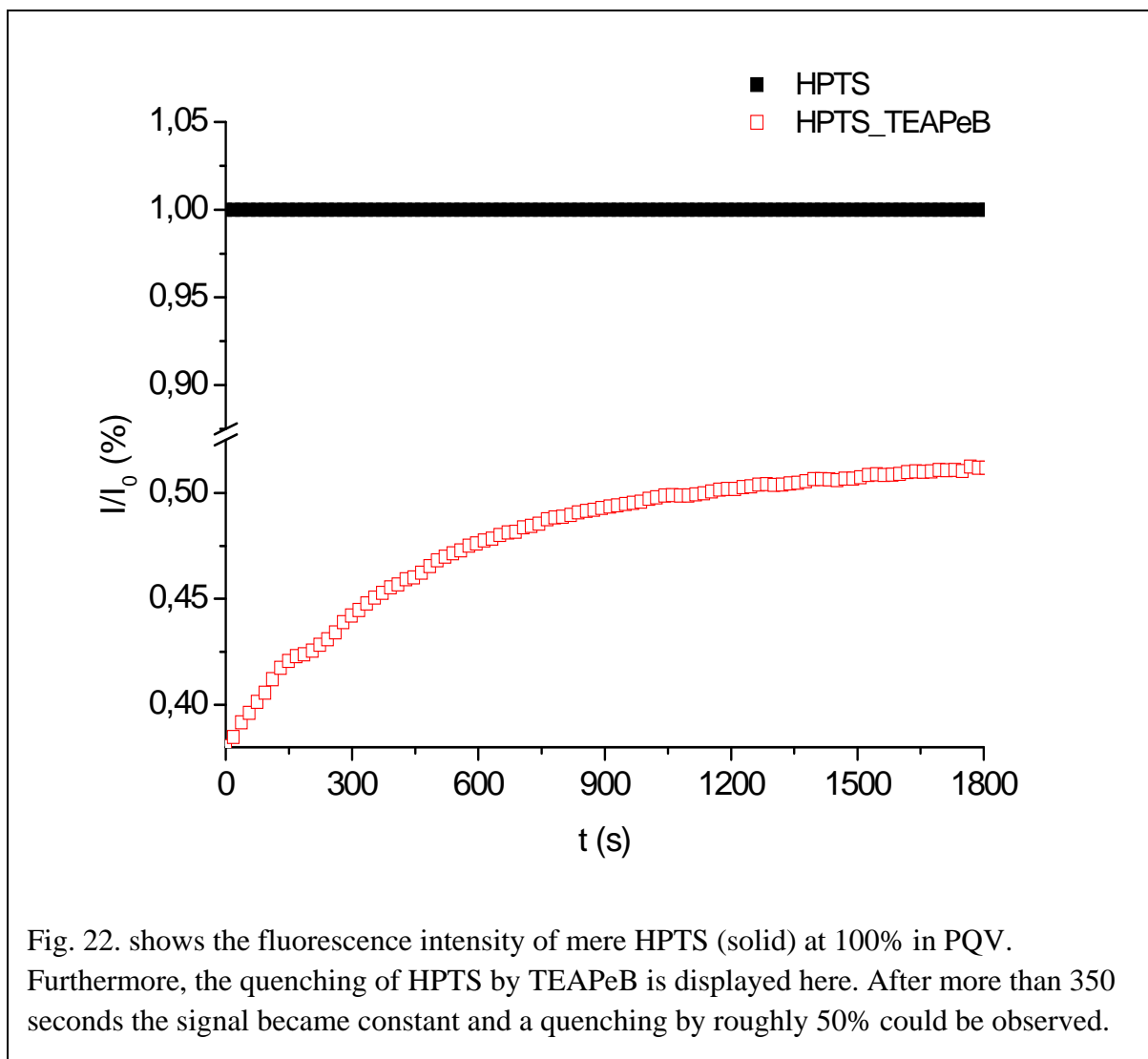
Fig. 21 puts on display the effects of all adenine phosphates on the fluorescence intensity of PQIV. Resolution surpasses that of PQIII. Yet the signals of ADP, AMP and TEABB are close albeit on a tolerable level, i.e. a distinction can be drawn between all species, yet



reproducibility can be a problem (see error bars). This might be in part due to a better recovery of fluorescence intensity. A possible explanation can be sought in a stronger interaction between the viologen and the phosphates as hinted at above.

4.1.5 HPTS with TEAPeB as sensing design for the detection of ATP and other phosphates

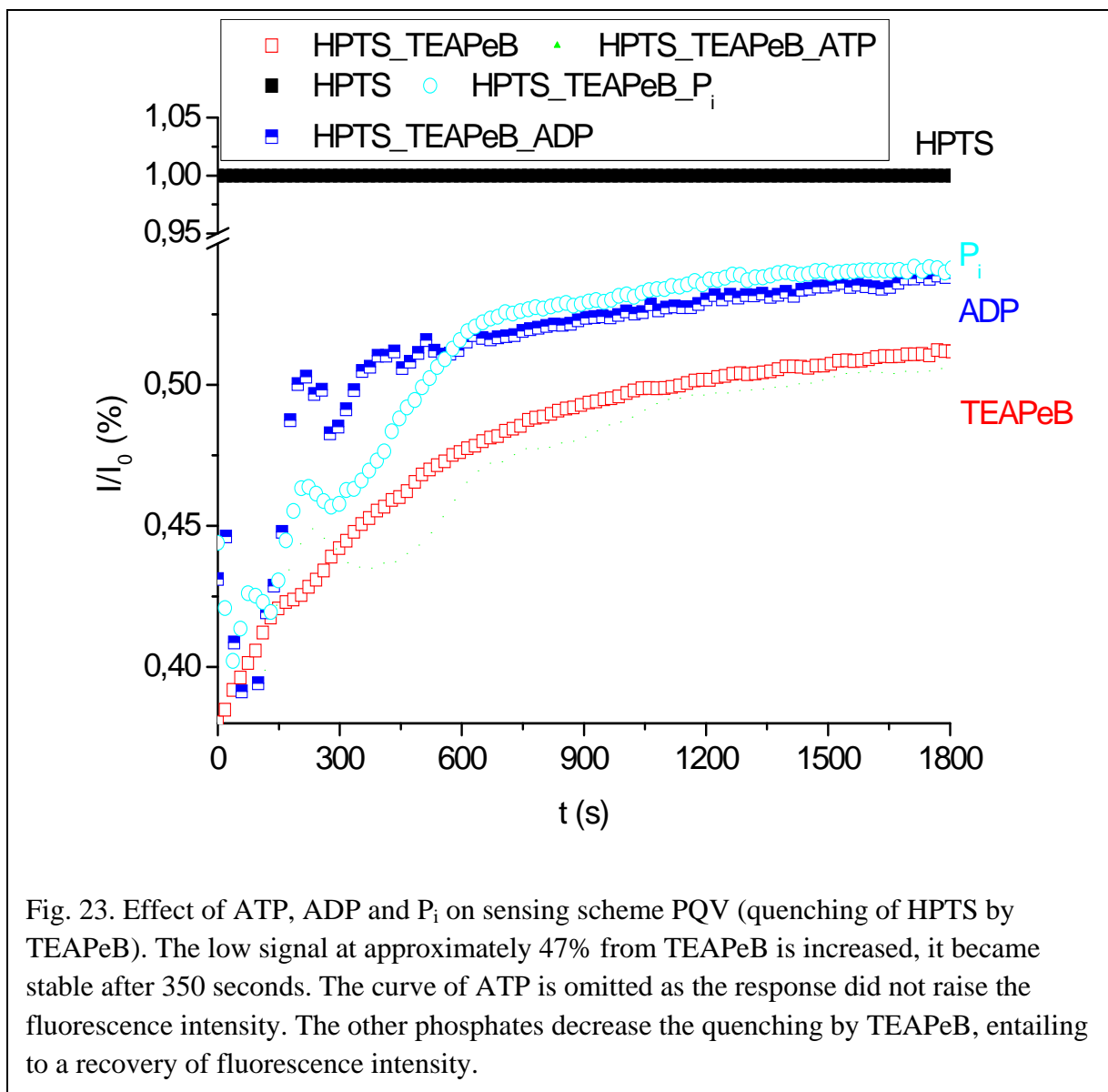
The potential of TEAPeB in PQV as a quencher for HPTS is depicted in Fig. 22.



The signal needed over 350 seconds to become stable yielding a drop to 50%. This constitutes the longest time frame required to conduct measurements, easily surpassing PQI-IV. Among the viologens studied, TEAPeB possesses the longest (pentyl) spacer. Apparently this enables a broader variety in orientation and 3 D structures that demand more time to align and interact with HPTS and for the complex to reach equilibrium.

Phosphates in ATPase Reaction

Fluorescence intensity of PQV upon exposure to ATP, ADP and P_i is displayed in Fig. 23. There is virtually no interaction between ATP and TEAPeB entailing to apparently no release of HPTS. Hence the fluorescence intensity remains at the low level caused by the quenching of TEAPeB. A substantially stronger interaction takes place between ADP/ P_i and TEAPeB



thus only some electron transfer from HPTS to the quencher is enabled. Hence fluorescence intensity recovers to a level of 53% relatively quickly in the case of ADP while for P_i a longer time is required. The fact that both of these phosphates had similar affect on TEAPeB is rather surprising as both molecules are clearly distinct regarding the number of negative charges and the fact that one carries a base and a sugar entailing to a big difference in size. This observation, a rather inconvenient resolution with a relatively long response time renders this system not suitable for application in monitoring ATPase activity for instance.

Guanosine Phosphates

The response of the guanine carrying nucleotides in PQV is depicted in Fig. 24. Results yield that GTP behaves analogously to ATP. Yet, an intermediate signal was recorded in this instance instead of the hardly detectable signal observed in the former case. The fact that GTP does not occupy the top spot is in line with PQIII-IV. A recovery to 55% of the level of the reference could be observed. GDP impacted PQV the most, with signal recovery to 67%. A slightly lower signal was recorded for GMP. Furthermore, cGMP increases the response of TEAPeB to 50%. As previously noted, it requires the longest time to free HPTS presumably due to its bulky 3 D structure. A clear distinction between all phosphates can be drawn here, resolution is at a good level. Yet the slow response time constitutes a big obstacle in utilizing this approach for monitoring enzyme activity.

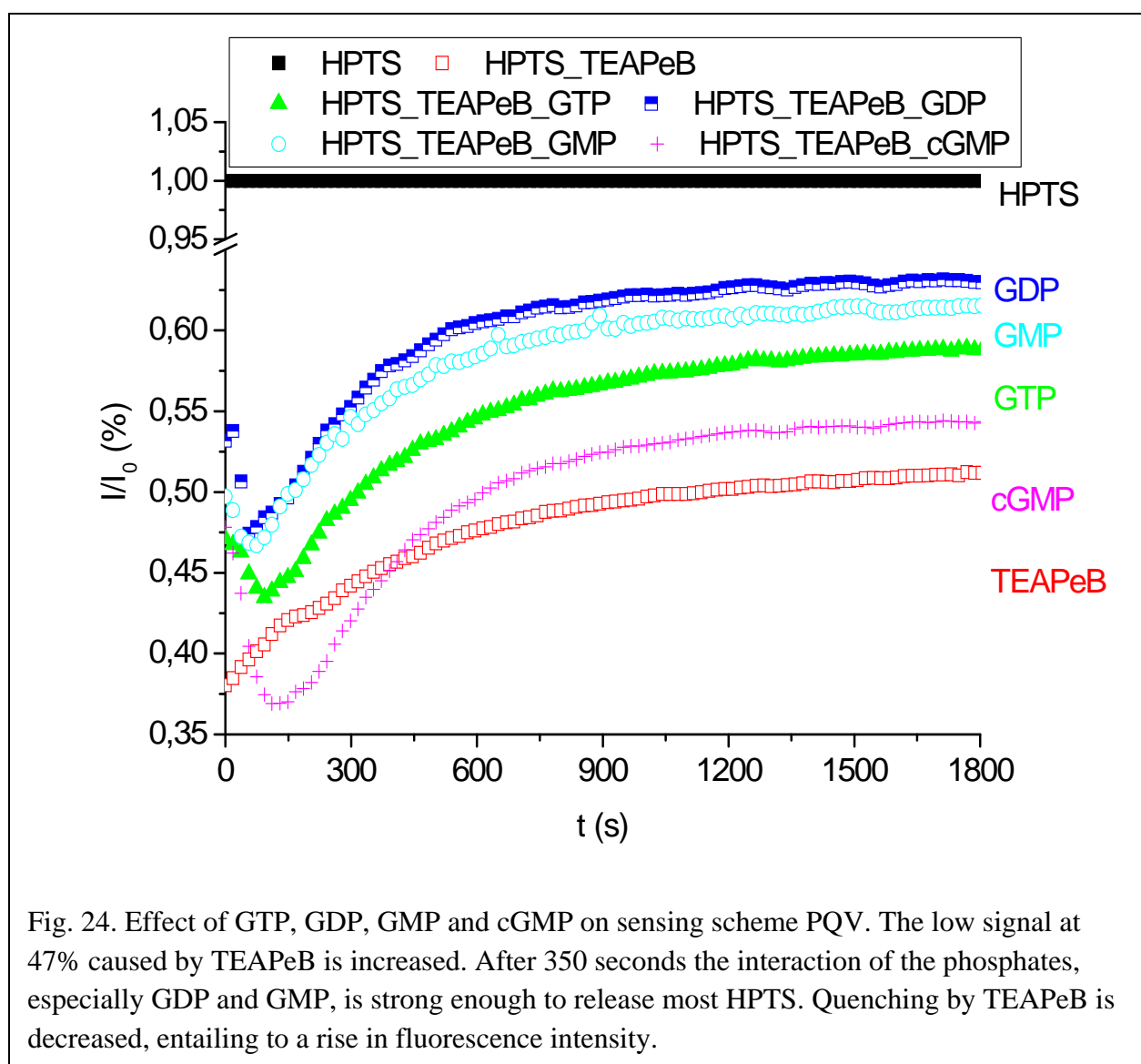


Fig. 24. Effect of GTP, GDP, GMP and cGMP on sensing scheme PQV. The low signal at 47% caused by TEAPeB is increased. After 350 seconds the interaction of the phosphates, especially GDP and GMP, is strong enough to release most HPTS. Quenching by TEAPeB is decreased, entailing to a rise in fluorescence intensity.

AMP, cAMP and PP_i

The response of AMP, cAMP and PP_i is depicted in Fig. 25. Fluorescence intensity recovers to a level of 58% when AMP is present. The signal for cAMP is of intermediate magnitude at 54%. PP_i impacts TEAPeB the least, hence the signal only rises to 51% of the reference. A clear distinction between the three phosphates involved can be drawn. This corresponds to the results obtained in PQI and PQIII. A slow response time for all species, however, needs to be taken into account. Hence, PQV is disadvantageous for possible application in sensing.

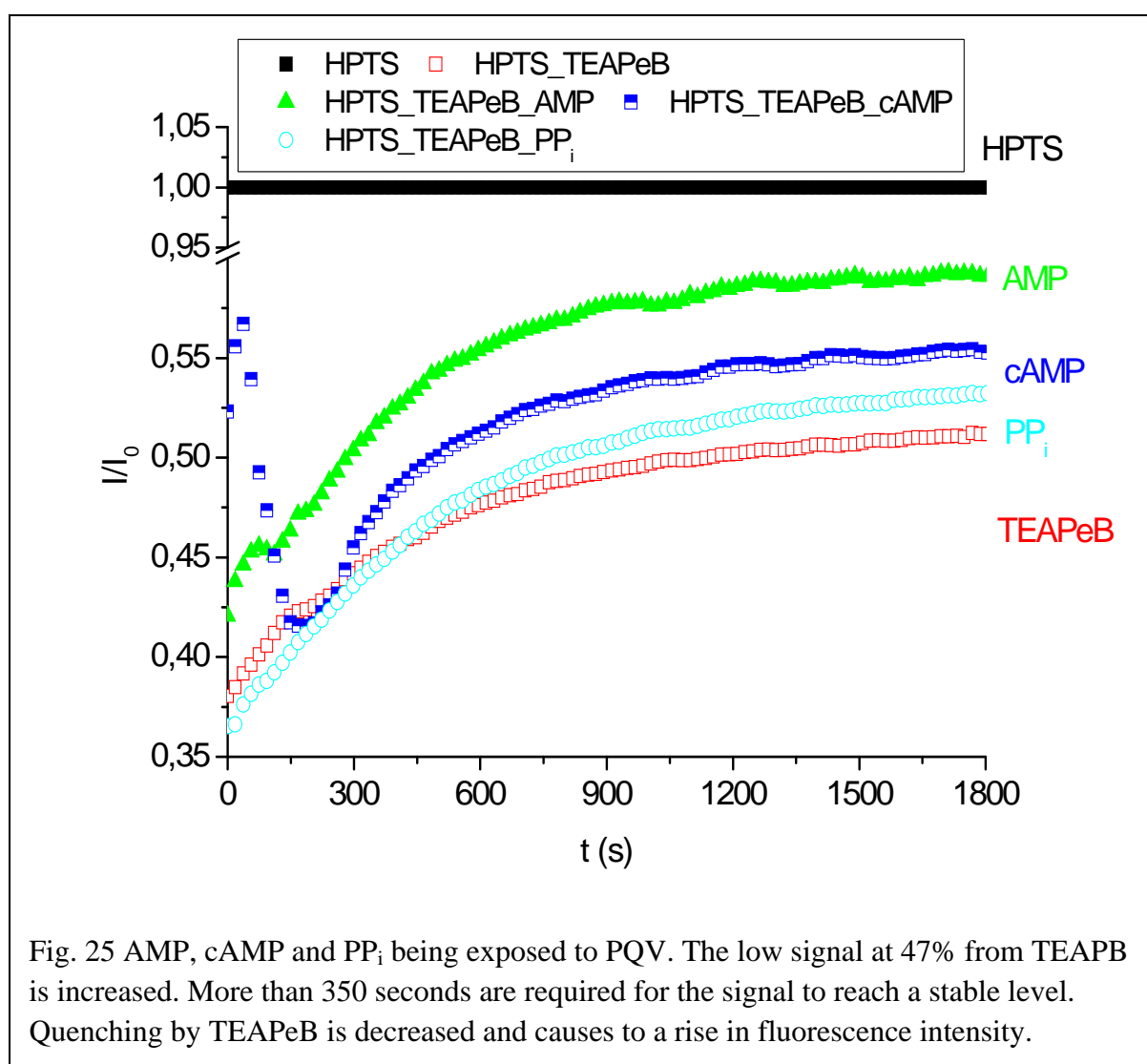
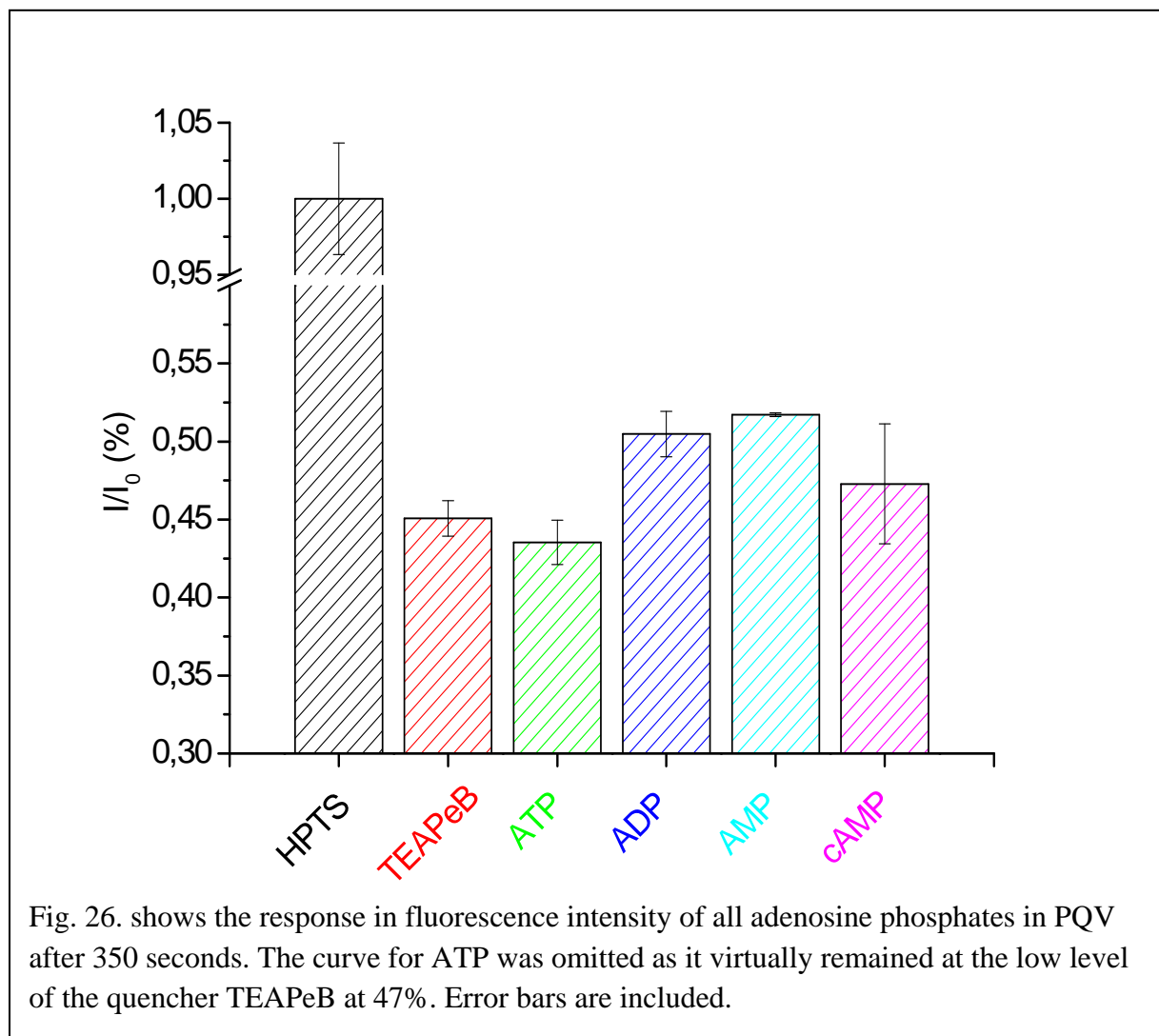


Fig. 25 AMP, cAMP and PP_i being exposed to PQV. The low signal at 47% from TEAPB is increased. More than 350 seconds are required for the signal to reach a stable level. Quenching by TEAPeB is decreased and causes to a rise in fluorescence intensity.

Adenosine Phosphates

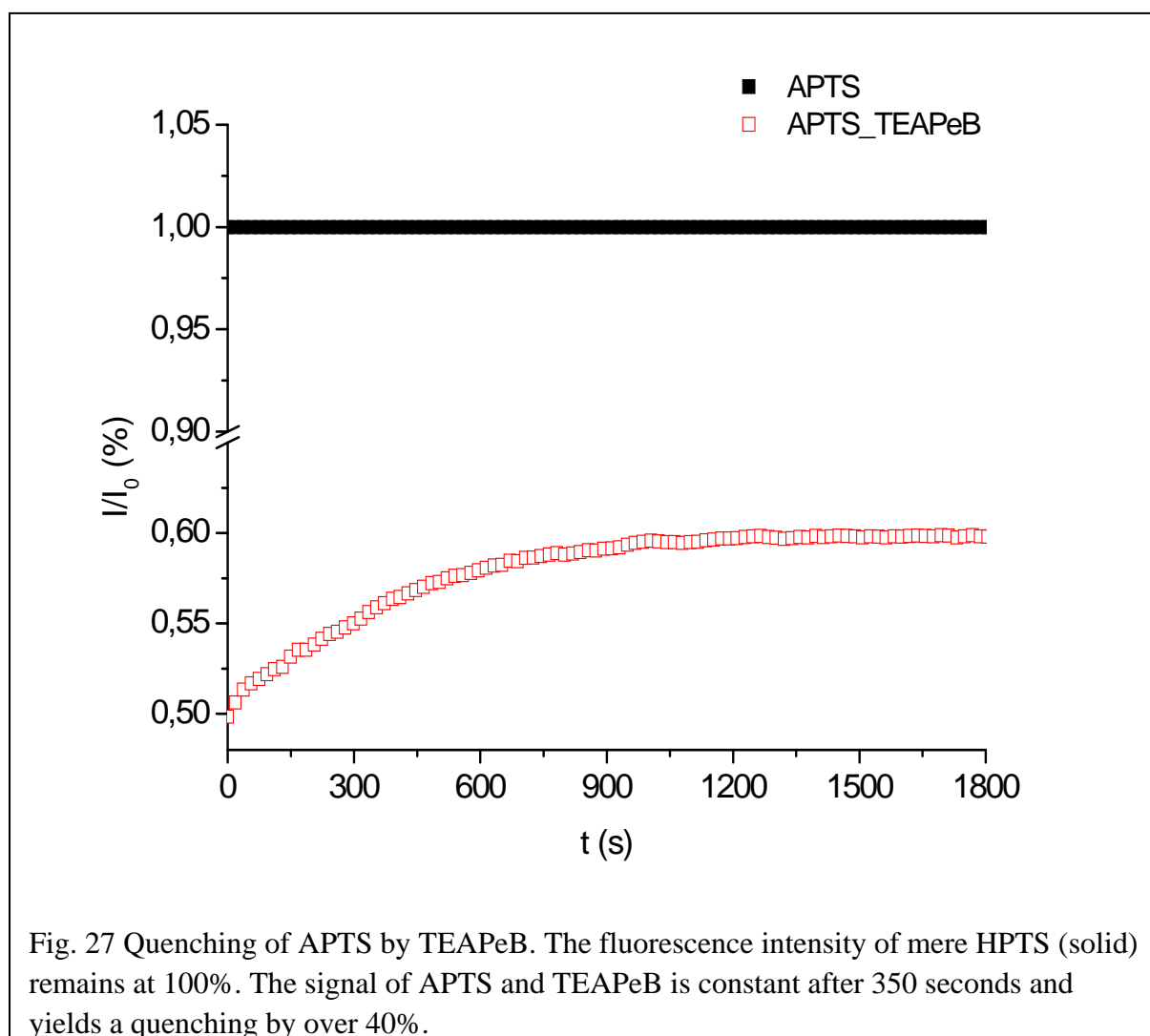
Fig. 26 reveals the response of all adenosine carrying phosphates. ATP seems not to be capable of releasing any HPTS from TEAPeB as no rise in fluorescence intensity is

recorded. This finding is quite surprising as all other adenosine species recover the signal at least partially. The only difference lies in the phosphate chain. Sufficient interaction between the pyrene and the aromatic adenosine base, as well as the cations, should take place. Resolution seems satisfying but the signals of cAMP and PP_i suffer from close proximity and cannot be discriminated with confidence (error bars).



4.1.6 APTS combined with TEAPeB as sensing design for the detection of ATP and other phosphates

The potential of TEAPeB in PQVI as a quencher is depicted in Fig. 27. The fluorescence intensity became stable after 300 seconds and yielded a drop to 60%.



Phosphates in ATPase Reaction

ATPase catalyzes the decomposition of ATP into ADP and P_i . Upon the addition of these phosphates, being subjected to PQVI, again a rise in fluorescence intensity from the low level of the quencher is expected (Fig. 28) ATP retains the level of fluorescence intensity to just

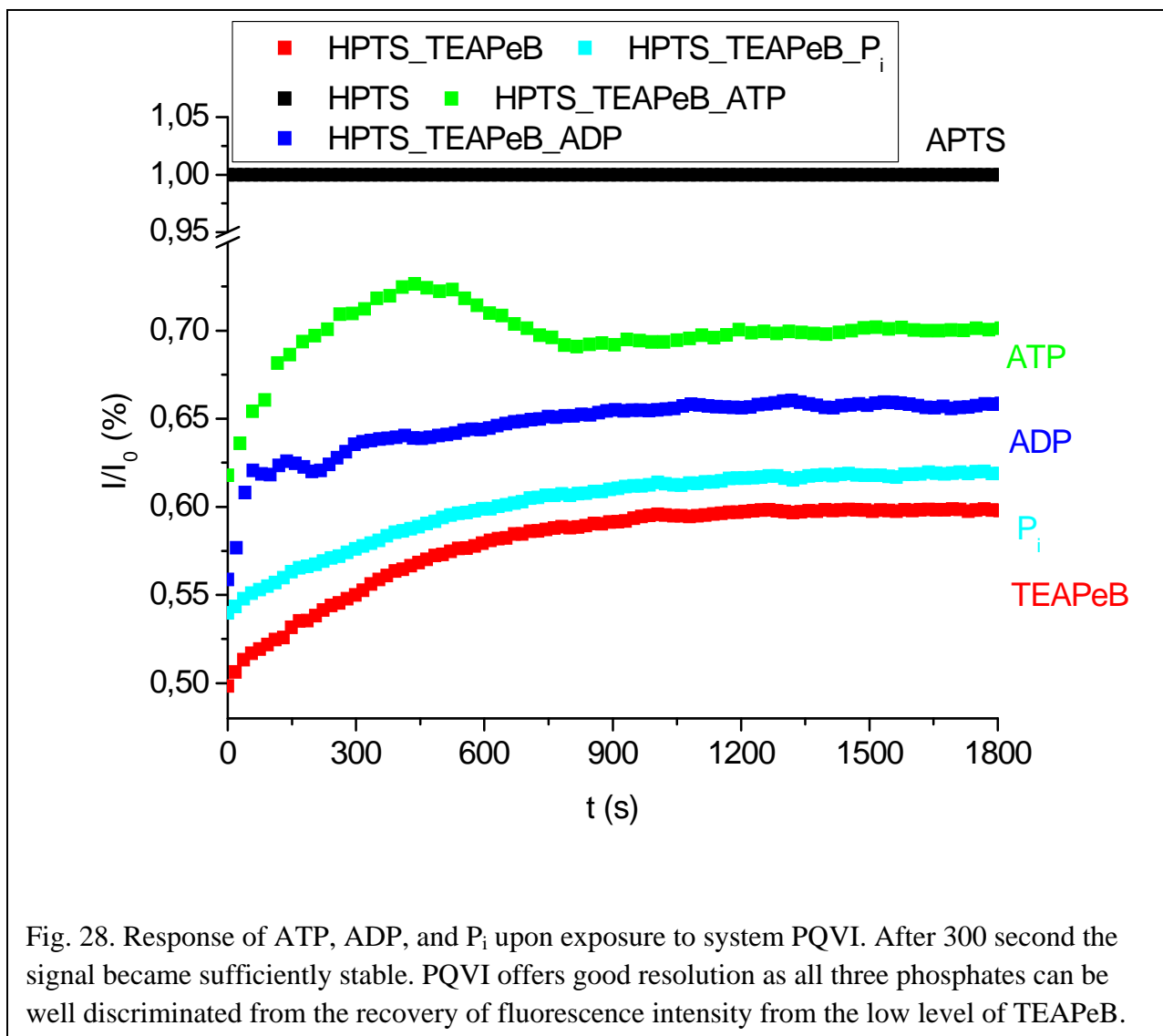
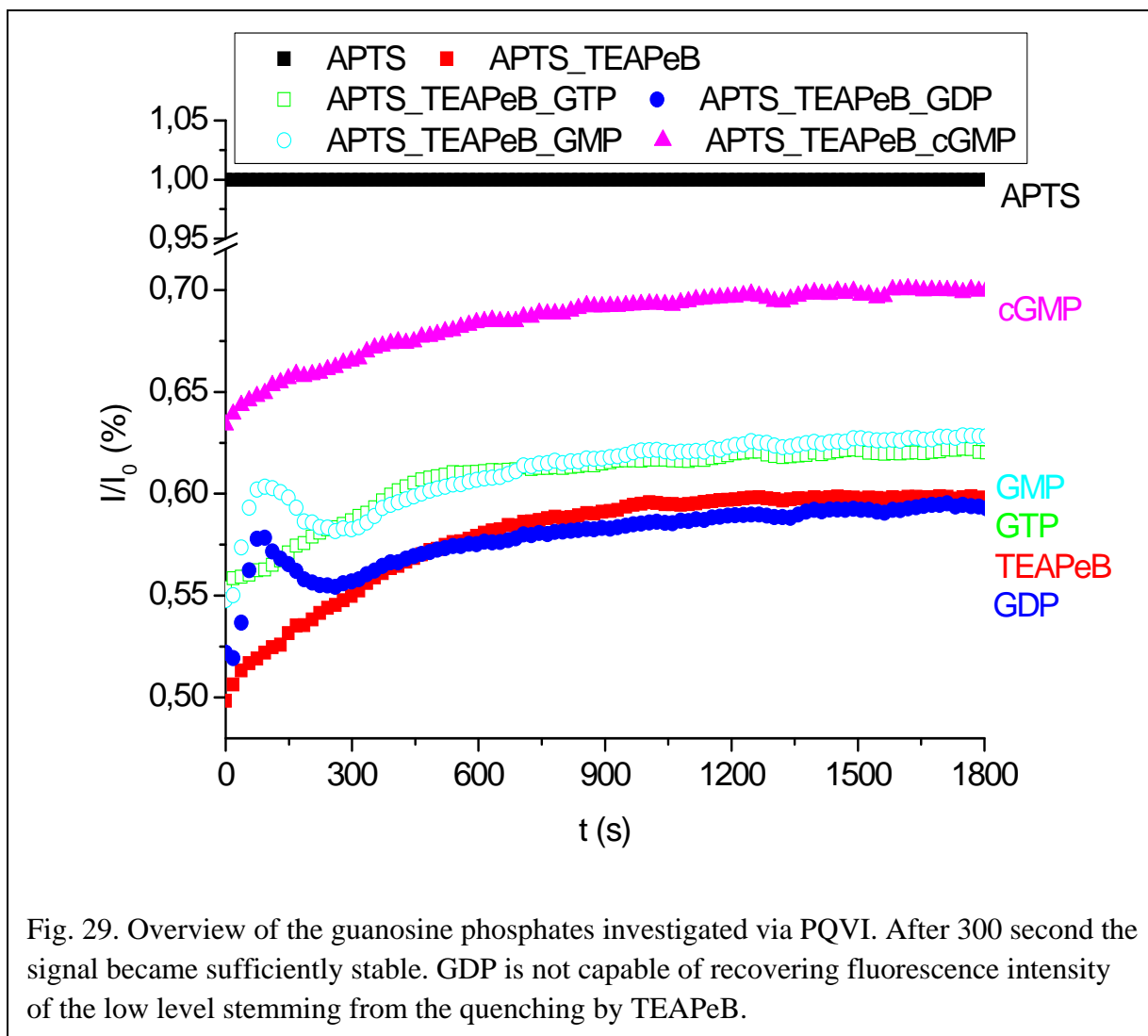


Fig. 28. Response of ATP, ADP, and P_i upon exposure to system PQVI. After 300 second the signal became sufficiently stable. PQVI offers good resolution as all three phosphates can be well discriminated from the recovery of fluorescence intensity from the low level of TEAPeB.

below 70% of the reference. This is parallel to the results obtained through PQI. The signal for ADP is of intermediate magnitude at 65% while P_i only reaches 60%. This order of reactivity is not only in line with PQI but also with the assumption that molecules with an aromatic compound (adenine) offer a broader variety of interactions (π - π , cation- π) aside from the electrostatic interactions that can be exercised by all phosphates. Contrary to PQI (HPTS), the level of APTS could not be retained though. A clear distinction between all three phosphates can be drawn. PQVI surpasses PQ III and PQV in that matter.

Guanosine Phosphates

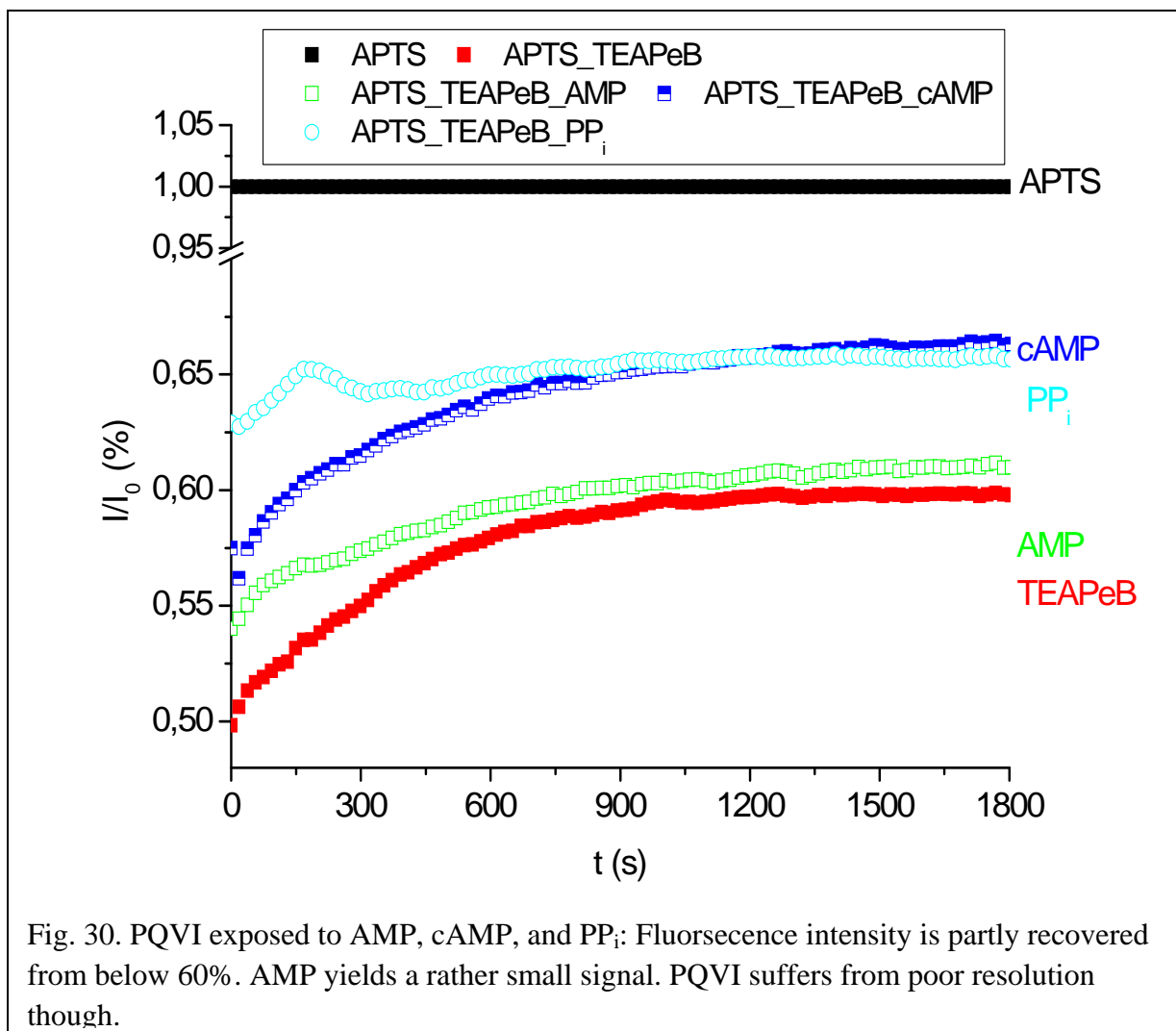
Fig. 29 yields the response of the guanosine phosphates in PQVI. The fluorescence



intensity obtained for GMP and GTP stands at 63% of the level of the reference (APTS) each. Thus discrimination is difficult, even more so considering the marginal rise in the signal as well. GDP causes no substantial effect on TEAPeB as no recovery in fluorescence intensity was recorded. cGMP, however, increases the signal to 70% of the reference. The number of the phosphate groups constitutes the only feature by which GTP, GDP, and GMP are distinct. Thus it can be argued that they should exercise a lesser impact on the viologen than cGMP. Additionally to a difference in distribution and nature of charge, the latter possesses a very bulky structure compared to the other phosphates.

AMP, cAMP, and PP_i

Fig. 30 depicts the response of AMP, cAMP, and PP_i in PQVI. Despite the different structure,



charge and the fact that PP_i carries no base, resolution of the three species is rather poor. The signal for AMP barely exceeds that of PQVI without phosphates. PP_i and cAMP settle at roughly 65% each.

Adenosine Phosphates

Fig. 31 depicts the response of all adenosine phosphates being exposed to PQVI. A distinction between all phosphates involved can be drawn to some extent. Standard deviation (error bars) is somewhat acceptable but needs to be taken into account as well. Only cAMP and ADP yield like signals. This fact is again surprising considering the difference in size, structure and charge of these species.

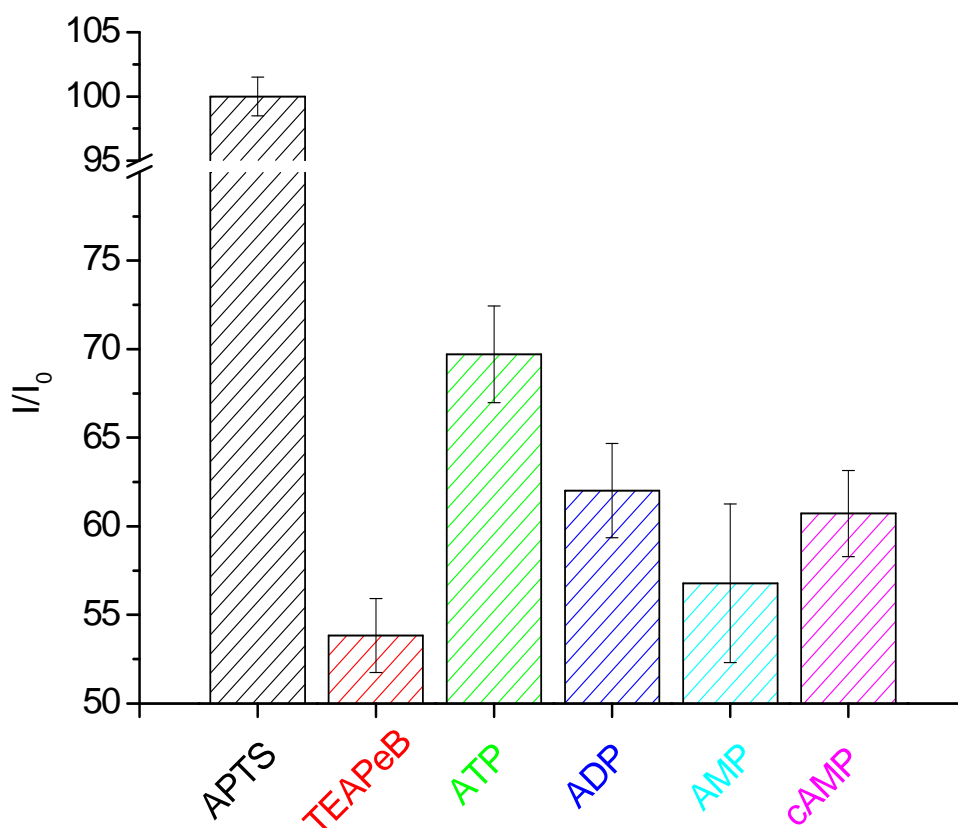


Fig. 31. Fluorescence intensity of ATP, ADP, AMP, and cAMP is put on display here. Despite similar response curves of ADP and cAMP, resolution is somewhat acceptable. AMP barely recovers the low signal at 60%.

4.1.1 Summary

In this chapter, the results from the investigations of the sensing designs PQI-VI upon treatment with various phosphates are summarized and compared regarding selectivity, resolution, and response time. In all experiments, the pyrenes were combined with the viologens first, thus forming PQI-VI according to Table 1 in section 1.3. The quenching efficiency of the diverse viologens varied from 20% to 50%. It is summarized in Table 1.

Table 1 Sensing designs PQI-VI, their response time and quenching of the luminescence of HPTS and APTS (I_0) is listed here. Response time ranges between 0 and more than 350 seconds while quenching can be achieved from a minimum of 20% to a maximum of 50%.

Pyrene	Viologen	Notation	Response time	Quenching 100- (I/I_0 *100)
HPTS	TEAPB	PQI	200 s	20%
HPTS	TEABB	PQIII	200 s	35%
HPTS	TEAPeB	PQV	>350 s	50%
APTS	TEAPB	PQII	0 s	25%
APTS	TEABB	PQIV	300 s	30%
APTS	TEAPeB	PQVI	300 s	40%

All experiments were carried out in TRIS buffer at pH 7.8 (see 1.2.3). This entails to an almost complete deprotonation of the hydroxyl group of HPTS. Hence the viologens TEAPB, TEABB, and TEAPeB can interact in two ways with it. Their positive charges are subjected to electrostatic attraction and cation- π interactions. Additionally, the aromatic part of the viologen can form π -stacks with the pyrene group (see 2.1, 2.2). While pH impacts HPTS considerably, no change in the spectroscopic properties of APTS could be recorded, safe for harsh acidic conditions. This limits the scope of possible modes of binding with the viologens

to cation- π interactions and π -stacks with the pyrene group (see section 1.1). This corresponds to the observation that TEAPB exercises a stronger quenching effect in PQI than in PQII and so forth for all quenchers in PQIII-IV.

Apparently a longer alkyl chain causes to a more efficient quenching, especially in PQV and PQVI. This is most probably due to more intimate interactions between the pyrenes and the viologens. Hence it can be conjectured that a longer spacer (e.g. TEAPeB) enables more effective binding. This is most probably due to a more effective separation - therefore a longer distance - between the positive charges on the quaternary nitrogen atoms on the periphery and those being situated on the rings. Thus the orientation of the 3 D structure of the quencher is less restricted (see section 1.3). Moreover, response time increases with the length of the alkyl chain. It can be surmised in this case as well, that a longer chain enables more possible orientations (i.e. higher degree of freedom of mobility) of the viologens. Thus a longer time is required for the equilibrium to become set.

The sensing designs PQI-VI strongly vary in their capabilities of discriminating between the different phosphate species that were examined in this work. Tables 2-4 give an overview of the results.

There are two cases that need to be taken into account in order to explain and assess the deviations and differences between the three quenchers: first, the ability of the viologens to interact with the pyrenes. That has been discussed above. Second, the different kinds of phosphates can impact the quenchers in various ways. As has been hinted at previously (1.3), there are three criteria for distinction of the phosphates investigated above: charge (and number thereof), size and 3 D structure, type of base. Moreover, the pyrenes might not only be quenched by the viologens. Nucleic bases can also form π - π interactions with pyrene as well and thus decrease fluorescence intensity.

Table 2 lists the response of PQI and PQII upon the addition of numerous phosphates. Despite the sometimes relatively long response time, a delay time of 200 seconds was sufficient to distinguish the phosphates involved. P_i and cyclic phosphates have been identified as species that require a substantially longer time periods in order for their response to become stable. An explanation can be sought in the form of the bulky structure of for instance cAMP. Phosphate on the other hand is less steric demanding. Yet it can undergo a series of acid base reaction. Due to its basic nature it will deprotonate all species with an acidic group.

An equilibrium will be eventually formed of $\text{H}_3\text{PO}_4/\text{H}_2\text{PO}_4^-/\text{HPO}_4^{2-}/\text{PO}_4^{3-}$. Thus many reactions are possible that will delay the binding of phosphate with the viologens.

Most observations show the same trend for PQI and PQII. Differences in intensity and other deviations have been discussed above. PQI offers a better sensitivity, resolution, and all phosphates yield a signal above the level of PQI without analyte. Thus it is well suited for the sensing of phosphates. PQII on the other hand is less expedient to apply.

Table 2 Response of PQI and PQII regarding different phosphate groups according to section 1.3

Notation	Phosphate Group	Phosphate	Recovery Rate	Response time
PQI	ATPase reaction	ATP	100%	200 s
		ADP	92%	200 s
		P _i	86%	600 s
	Guanines	GTP	96%	200 s
		GDP	86%	200 s
		GMP	95%	200 s
		cGMP	88%	450 s
	AMP, cAMP, PP _i	AMP	85%	200 s
		cAMP	96%	700 s
		PP _i	90%	200 s
	Adenines	ATP	100%	200 s
		ADP	92%	200 s
AMP		85%	200 s	
cAMP		96%	700 s	
PQII	ATPase reaction	ATP	88%	200 s
		ADP	85%	200 s
		P _i	83%	700 s
	Guanines	GTP	86%	200 s
		GDP	-	-
		GMP	81%	200 s
		cGMP	-	-
	AMP, cAMP, PP _i	AMP	85%	450 s
		cAMP	-	-
		PP _i	83%	200 s
	Adenines	ATP	88%	200 s
		ADP	85%	200 s
AMP		85%	450 s	
cAMP		-	-	

Table 3 Response of PQI and PQII regarding different phosphate groups according to section 1.3

Notation	Phosphate Group	Phosphate	Recovery Rate	Response time
PQIII	ATPase reaction	ATP	77%	450 s
		ADP	73%	500 s
		P _i	81%	200 s
	Guanines	GTP	70%	200 s
		GDP	92%	700 s
		GMP	71%	200 s
		cGMP	83%	700 s
	AMP, cAMP, PP _i	AMP	76%	200 s
		cAMP	71%	450 s
		PP _i	80%	200 s
	Adenines	ATP	77%	450 s
		ADP	73%	500 s
AMP		76%	200 s	
cAMP		71%	450 s	
PQIV	ATPase reaction	ATP	86%	300 s
		ADP	78%	300 s
		P _i	76%	300 s
	Guanines	GTP	75%	750 s
		GDP	76%	300 s
		GMP	84%	300 s
		cGMP	81%	300 s
	AMP, cAMP, PP _i	AMP	74%	300 s
		cAMP	81%	300 s
		PP _i	81%	300 s
	Adenines	ATP	86%	300 s
		ADP	78%	300 s
AMP		74%	300 s	
cAMP		81%	300 s	

Table 3 puts on display the response of PQIII and PQIV. In the former case, 200 seconds were required in order to differentiate between all phosphate species that were investigated here, while 300 seconds sufficed in the latter case. In PQIII, not only the bulky cAMP did require longer time frames to become stable but also a number of other phosphates. PQIV yielded only few such deviations.

As opposed to PQII, a response for all phosphates could be recorded in PQIV. Resolution was at virtually the same level for both sensing designs. They are equally suited to be harnessed for sensing phosphates. Yet PQI is much superior to them regarding resolution, sensitivity, etc.

Table 4 depicts the response of PQV and PQVI upon being exposed to phosphates. Again, phosphate and bulkier species required more time to yield a constant signal. Yet evaluation could take place after 300 seconds in PQVI, while PQV demanded 350 seconds. These long time frames are disadvantageous for the following reason. If such a sensing design was to be applied to monitoring of enzyme activity a time of five minutes elapses before detection can commence rendering this a rather inexpedient approach. Resolution for the guanines is acceptable but rather poor for adenosines.

PQI and PQIII offer a fair resolution, relatively quick response time, and good sensitivity. Thus they are well suited for monitoring enzyme activity, for instance, while the other sensing designs suffer from drawbacks that disqualify them for such applications. PQI is suitable for adenosines, while PQII is more convenient for guanosines. Cross-sensitivity might be a problem. Hence reactions where only one phosphate species is present can ideally be monitored. Further improvements are desirable in the field of reproducibility though. Furthermore, LOD and dynamic range need to be validated. Thus far signals could be obtained for concentrations of 1 μM or higher. Yet more experiments are required to confirm these results, and to distinguish several different concentrations of the same phosphate species.

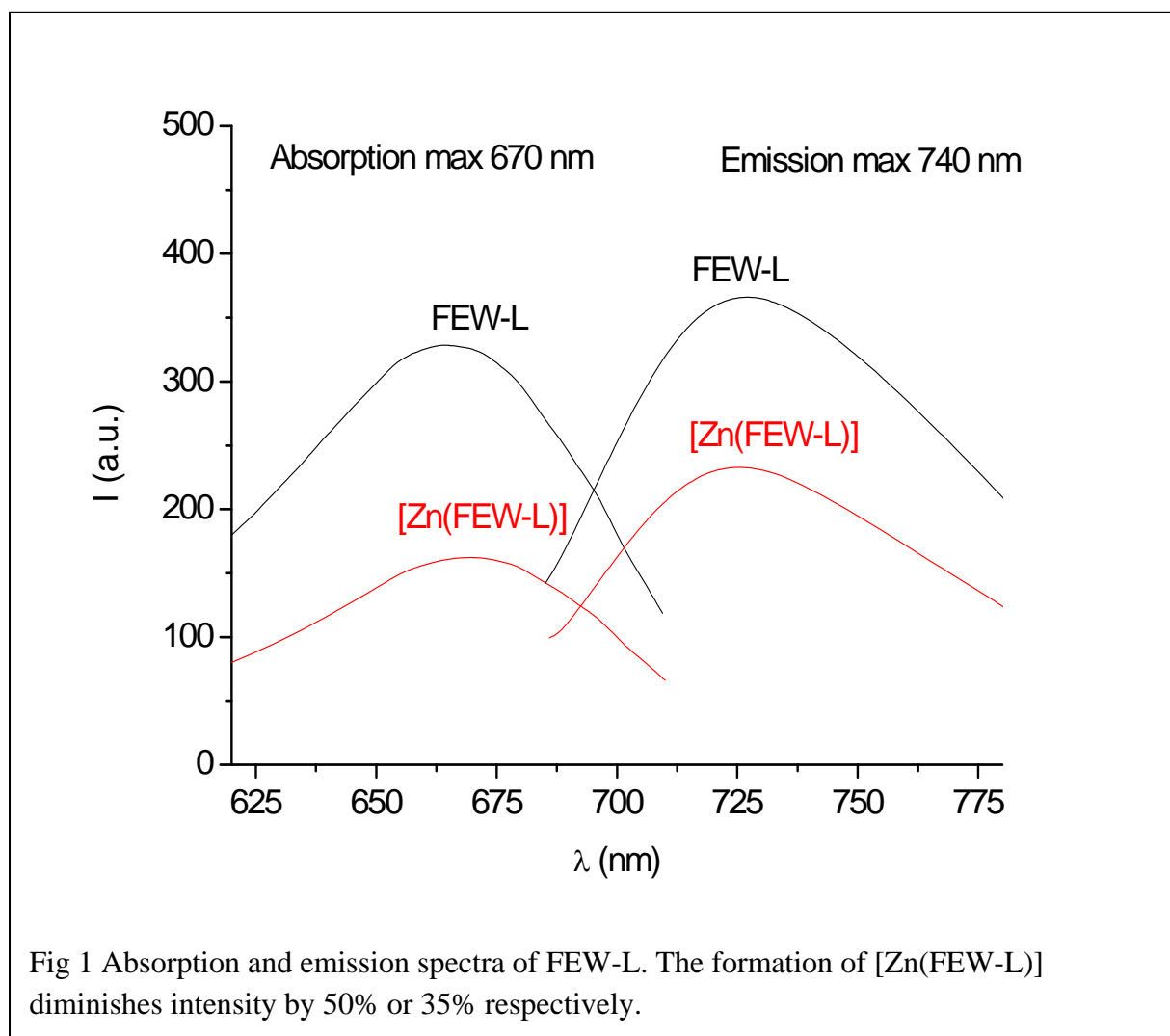
Table 4 Response of PQV and PQVI regarding different phosphate groups according to section 1.3

Notation	Phosphate Group	Phosphate	Recovery Rate	Response time
PQV	ATPase reaction	ATP	-	350 s
		ADP	54%	350 s
		P _i	54%	600 s
	Guanines	GTP	59%	350 s
		GDP	61%	350 s
		GMP	63%	350 s
		cGMP	54%	500 s
	AMP, cAMP, PP _i	AMP	59%	350 s
		cAMP	55%	350 s
		PP _i	53%	600 s
	Adenines	ATP	-	350 s
		ADP	54%	350 s
AMP		59%	350 s	
cAMP		55%	350 s	
PQVI	ATPase reaction	ATP	70%	700 s
		ADP	66%	300 s
		P _i	62%	600 s
	Guanines	GTP	62%	450 s
		GDP	60%	700 s
		GMP	63%	450 s
		cGMP	70%	300s
	AMP, cAMP, PP _i	AMP	61%	700 s
		cAMP	67%	700 s
		PP _i	66%	300 s
	Adenines	ATP	70%	700 s
		ADP	66%	300 s
AMP		67%	700 s	
cAMP		66%	300 s	

5. Cyanine-Type Probe for Phosphates

5.1 Results and Discussion

The spectroscopic properties of [Zn(FEW-L)] in the presence of various phosphates are investigated in this chapter. Fluorescence intensity, excitation and emission spectra were recorded in a quartz cuvette. The concentration of Zn^{2+} ($5 \mu\text{mol}\cdot\text{L}^{-1}$), FEW-L ($1 \mu\text{mol}\cdot\text{L}^{-1}$), and phosphates ($17.5 \mu\text{mol}\cdot\text{L}^{-1}$) was constant in buffered aqueous solution (see 2.2). The ratio Zn/FEW-L was optimized beforehand (see 2.3.3). For each sample, absorption at 670 nm and emission at 740 nm were recorded. Fig. 1 displays these spectra for FEW-L.



Absorption peaks at 670 nm, the emission reaches its maximum at 740 nm. Upon the addition of Zn^{2+} in the form of perchlorate, $[Zn(FEW-L)]$ was formed, the fluorescence intensity dropped, and the maxima of excitation and emission were slightly shifted. More importantly zinc dications exercised strong quenching on FEW-L causing a decrease of about 50% in intensity in case of absorption. A decline of about 35% in emission was recorded. This phenomenon is due to the fact that $[Zn(FEW-L)]$ is of a different 3 D structure than the free ligand. Moreover, the Lewis acid zinc in the tetrahedral complex is lowering electron density by coordinating one nitrogen atom that is part of the extended conjugated π -system of the dye. Several modes of interaction can take place between phosphates and $[Zn(FEW-L)]$. Zinc phosphate possesses a rather low solubility product [1] and will readily precipitate even in small concentrations as are dealt with here. The same behaviour can be expected for diphosphate [1] and partly the adenosine and guanosine compounds although the sugar should render them more soluble in water. Yet, the aromatic base is in position to interact with FEW-L through π -stacks or cation- π interactions as well as electrostatically. This reduces the concentration of phosphate that is available for binding to zinc dications. Thus, not enough phosphate to free and subsequently precipitate them might be available. Accordingly the aromatic bases are capable of quenching FEW-L or $[Zn(FEW-L)]$ even more by also reducing electron density, enabling relaxation via electron transfer instead of fluorescence.

The behaviour of $[Zn(FEW-L)]$ being exposed to phosphates is investigated. A like approach as in chapter 4 regarding the grouping of the investigated species is followed here. APTase decomposes ATP into ADP and P_i (*Phosphates involved in APTase reaction*). Thus these compounds constitute the first group of phosphates as acknowledging their importance in monitoring this particular enzyme.

The *Guanosine Phosphates* GTP, GDP, GMP, and cGMP are in the next group of phosphates as they all share a common base.

The next group is made up by other phosphates which were also subjected to this sensing scheme: *AMP, cAMP and PP_i* .

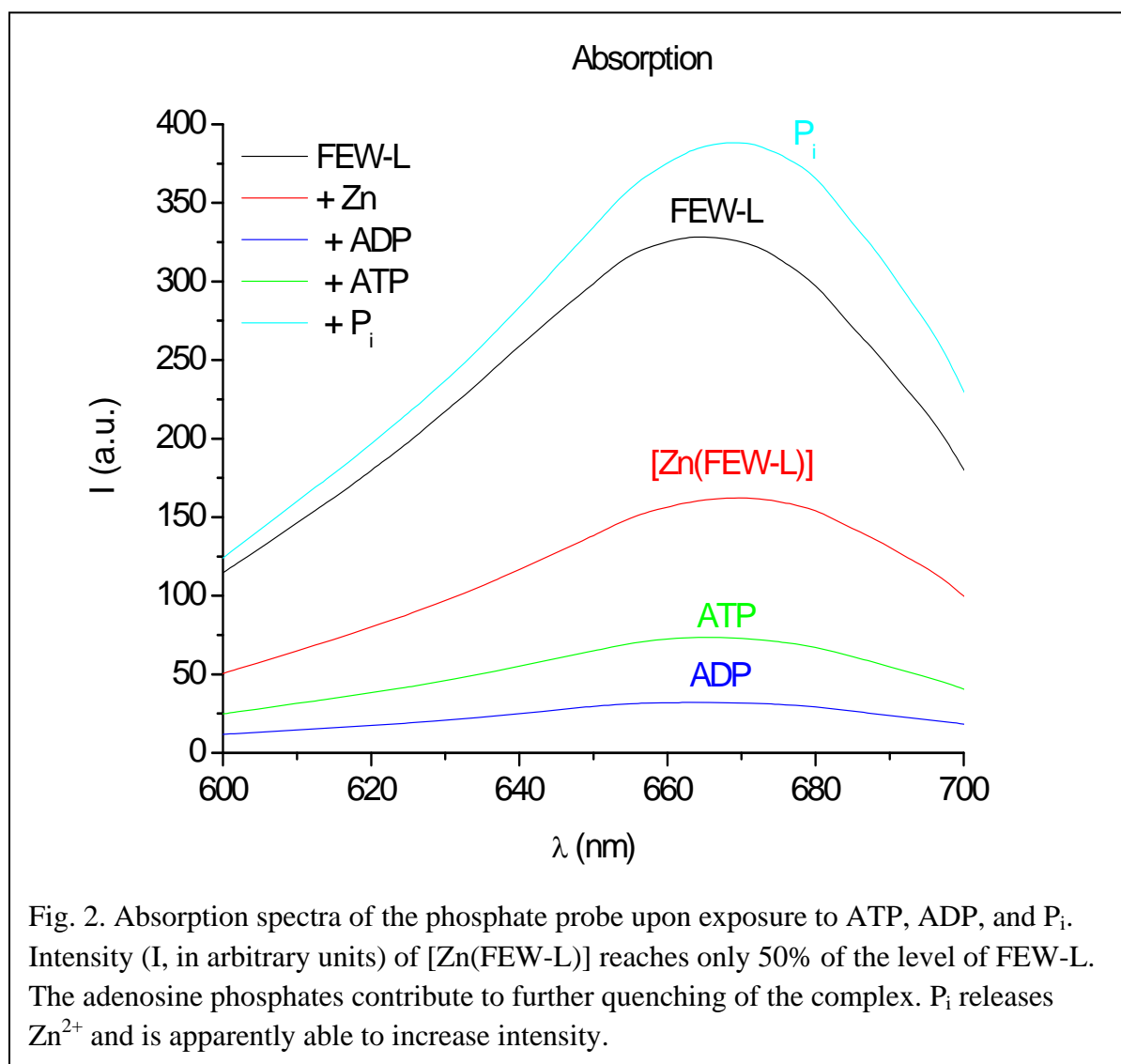
Finally the response of all *Adenosine Phosphates* is on display for a better comparison of these molecules.

[1] A. Hollewan, E. Wiberg, F. Wiberg, *Lehrbuch der Anorganischen Chemie*, de Gruyter, 2007

5.1.1 [Zn(FEW-L)]: Absorption-Based sensing of ATP and other phosphate species

Phosphates in ATPase Reaction

Fig. 2 reveals the absorption spectrum of [Zn(FEW-L)] being exposed to ATP, ADP



and P_i. The complex [Zn(FEW-L)] yields a intensity of 50% of the reference FEW-L only. P_i enhances the signal, according to the assumptions lined out above. Intensity is even surpassing that of the FEW-L. A possible explanation can be sought in the form of an increase in pH. A concentration of roughly 14 $\mu\text{mol}\cdot\text{L}^{-1}$ P_i remains in solution if it is assumed that

Zn^{2+} , in the form of $Zn_3(PO_4)_2$, will precipitate completely. This equals a pH of above 10. The buffer contains TRIS at $24 \text{ mmol}\cdot\text{L}^{-1}$, a concentration overwhelmingly higher than $14 \mu\text{mol}\cdot\text{L}^{-1}$. Yet it should exercise a considerable impact on pH as it was adjusted to pH 7.8 by HCl prior to all experiments. Thus a rise in pH can be observed lowering the rate of protonation on the secondary amino group or any basic moiety of FEW-L notably.

ATP exercises an additional quenching effect on $[Zn(\text{FEW-L})]$ and reduces the signal to below 25%. A further decrease can be observed in the case of ADP that lowers the response to roughly 10%. As was surmised above, this is most likely due to interaction of the aromatic base and the conjugated π -system of the FEW dye, opening electron transfer as an alternative pathway to relaxation.

A clear distinction can be drawn between all phosphates involved. Thus this probe is well suited for application in the monitoring of ATPase, for instance, considering the good resolution. It might even be more advantageous that the sensing scheme based on viologens (see 2.2) as P_i only enhances intensity while all phosphate species inhibit the bipyridinium quenchers to a certain degree.

Guanosine Phosphates

Fig. 3 yields the response of all guanine carrying phosphates. GDP is decreasing the low signal of $[Zn(\text{FEW-L})]$ to 10% of the level of FEW-L. All other guanosine phosphates raise absorption intensity again. Addition of cGMP entails to a recovery of the signal to about 55%. In the case of GMP, a response of around 63% of FEW-L could be recorded. The signal for GTP recovered at about 66%. Only GDP exercised a quenching effect on the probe, this deviates from the behaviour of the adenosine phosphates investigated so far. Previously, a rise in fluorescence intensity could be recorded for P_i only.

It seems reasonable that cGMP, GMP, and GTP should exhibit a response in that particular order, regardless of the nature of the reaction or mode of interaction with $[Zn(\text{FEW-L})]$. This is due to the bulky structure of cyclic phosphates, while the others only differ in length of phosphate groups, and thus in number of negative charges and size. Accordingly a weaker interaction takes place in the former case, an increasingly better one in the latter case. Surprisingly, the behaviour of GMP and GTP cannot be extrapolated to GDP although its only element of distinction lies in the length of the phosphate chain.

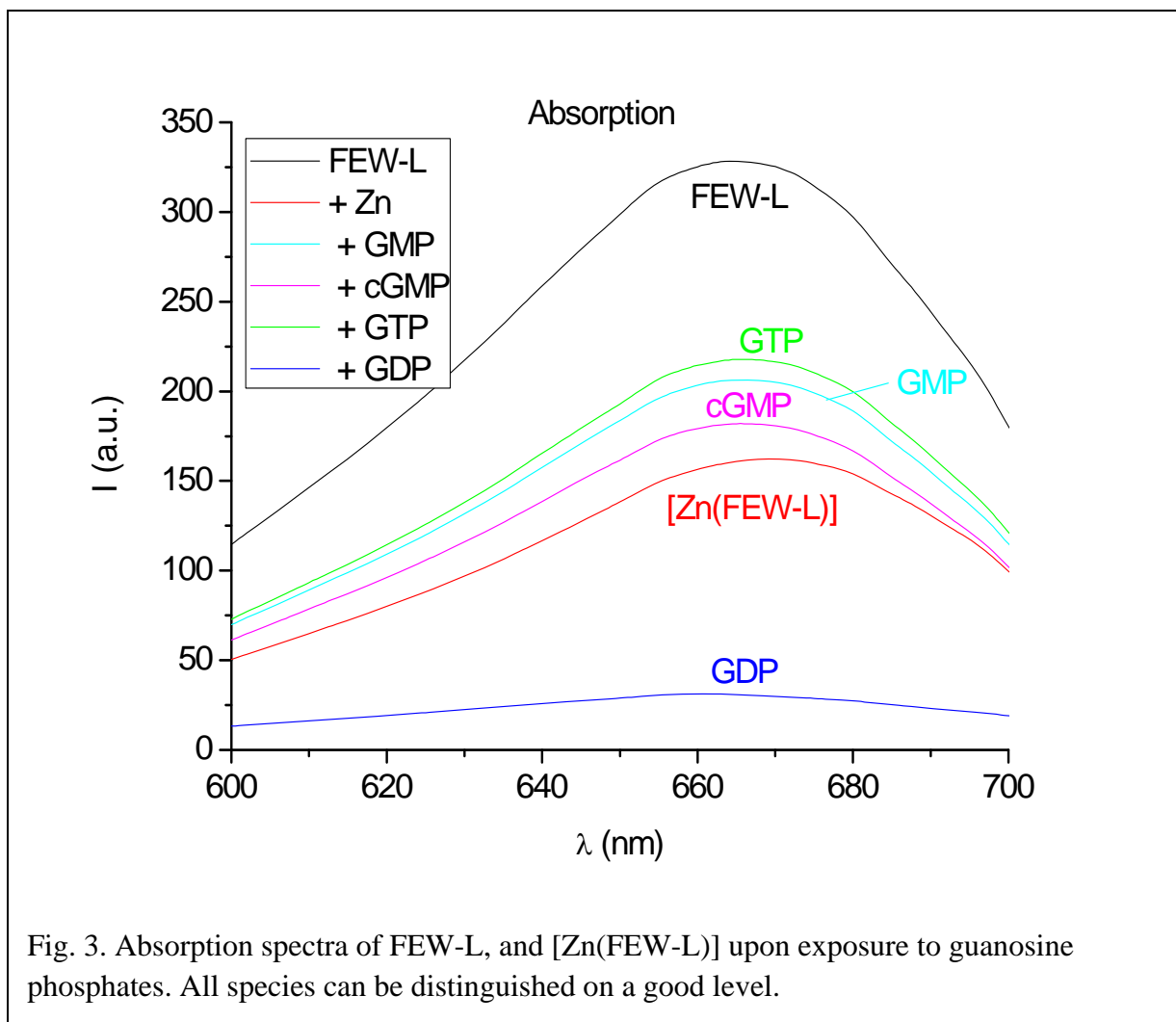


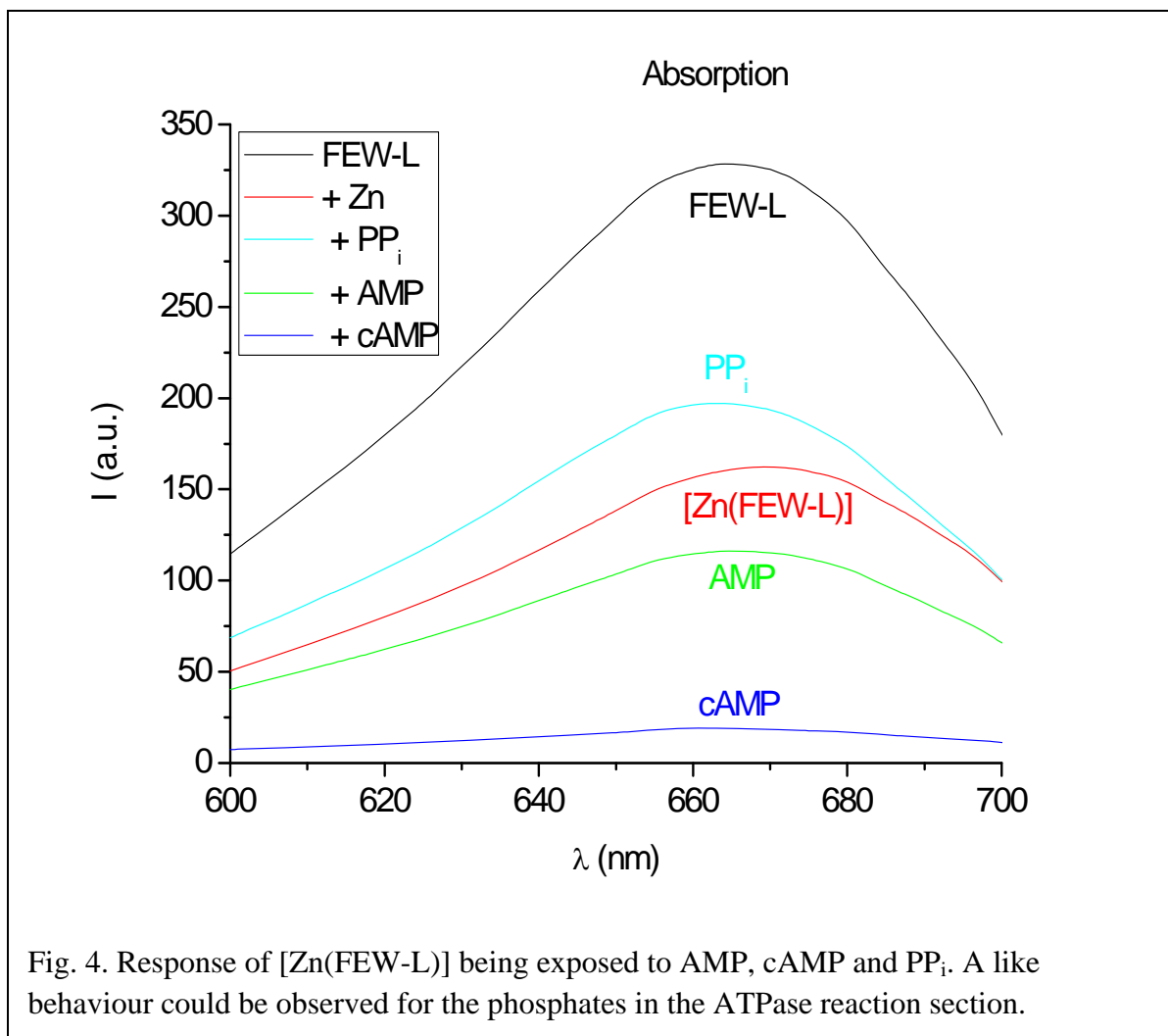
Fig. 3. Absorption spectra of FEW-L, and [Zn(FEW-L)] upon exposure to guanosine phosphates. All species can be distinguished on a good level.

All guanosines can be distinguished albeit on a smaller scale as in the case of the ATP, ADP and P_i.

AMP, cAMP and PP_i

Fig. 4 shows the response of AMP, cAMP and PP_i. PP_i recovers absorption intensity. Similar results were obtained for P_i. The signal of PP_i, however, does not exceed that of FEW-L. It reaches 60% only. Diphosphoric acid is a stronger acid than phosphoric acid. The fourth hydroxyl group features a pK_a of 9.25 while HPO₄²⁻ is of a pK_a of 12.32 [1]. Thus PP_i is less acidic by a factor of 1,000. Obviously a much lesser impact on pH is expected. Hence intensity is not enhanced but recovered to a certain degree upon the addition of PP_i.

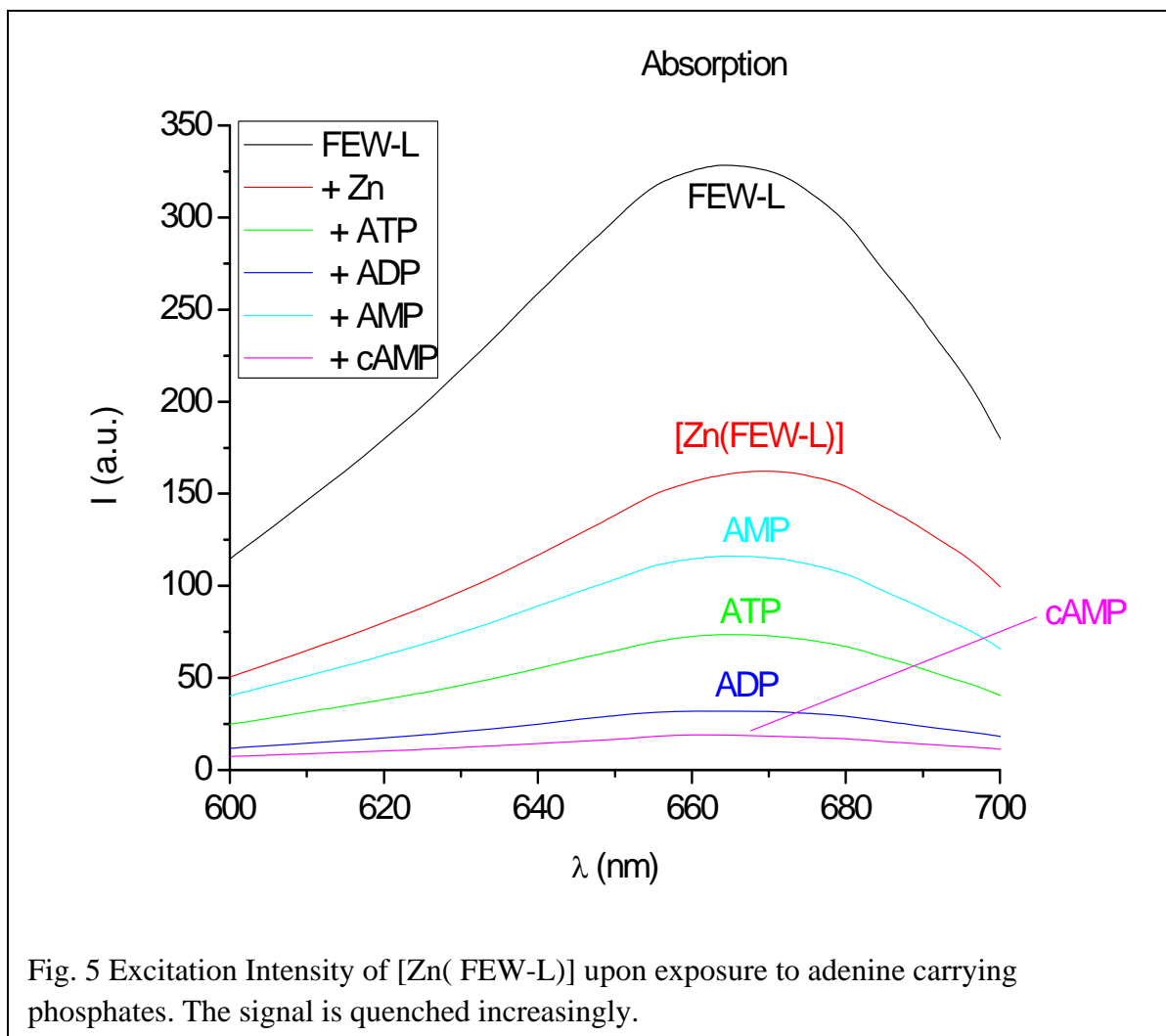
[1] A. Hollemann, E. Wiberg, F. Wiberg, *Lehrbuch der Anorganischen Chemie*, de Gruyter, 2007



AMP decreases the response of [Zn(FEW-L)] by 15% to 35% of FEW-L. cAMP reduces the signal to a mere 5%. Apparently it exercises the strongest impact on [Zn(FEW-L)] despite its demanding structure.

Adenosine Phosphates

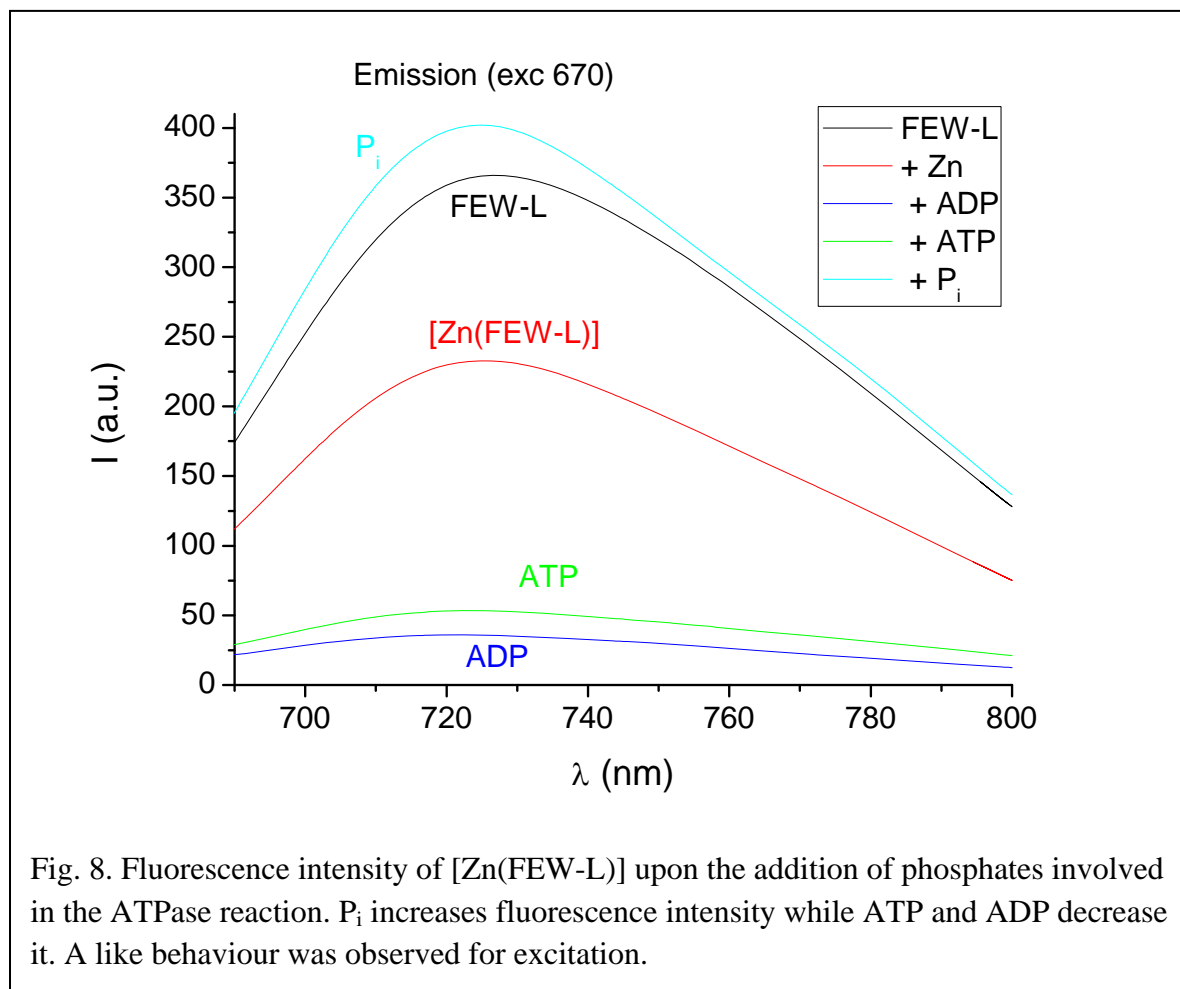
Fig. 5 reveals the response of all adenosine phosphates. Decreasing absorption intensity can be observed, from 35% in the case of AMP to 5% in the case of cAMP. All species can be clearly distinguished. This behaviour corresponds well with theoretical concepts that a change in charge and in size entails to a substantial change in signal intensity. Hence, [Zn(FEW-L)] constitutes a convenient probe for phosphate sensing.



5.1.2 [Zn(FEW-L)]: Emission-based sensing of ATP and other phosphate species

Phosphates in ATPase Reaction

Fig. 8 reveals the emission spectrum of [Zn(FEW-L)] being exposed to ATP, ADP,



and P_i . [Zn(FEW-L)] quenches the fluorescence intensity of FEW-L by over 35%. ATP reduces the signal even further to about 15%. ADP decreases fluorescence intensity to below 10%. A higher signal was recorded for P_i and [Zn(FEW-L)] than for FEW-L. This behaviour is similar to that of the absorption and can be likewise explained. A good resolution could also be observed.

Fig. 9 shows the fluorescence intensity of the guanosine phosphates upon exposure to

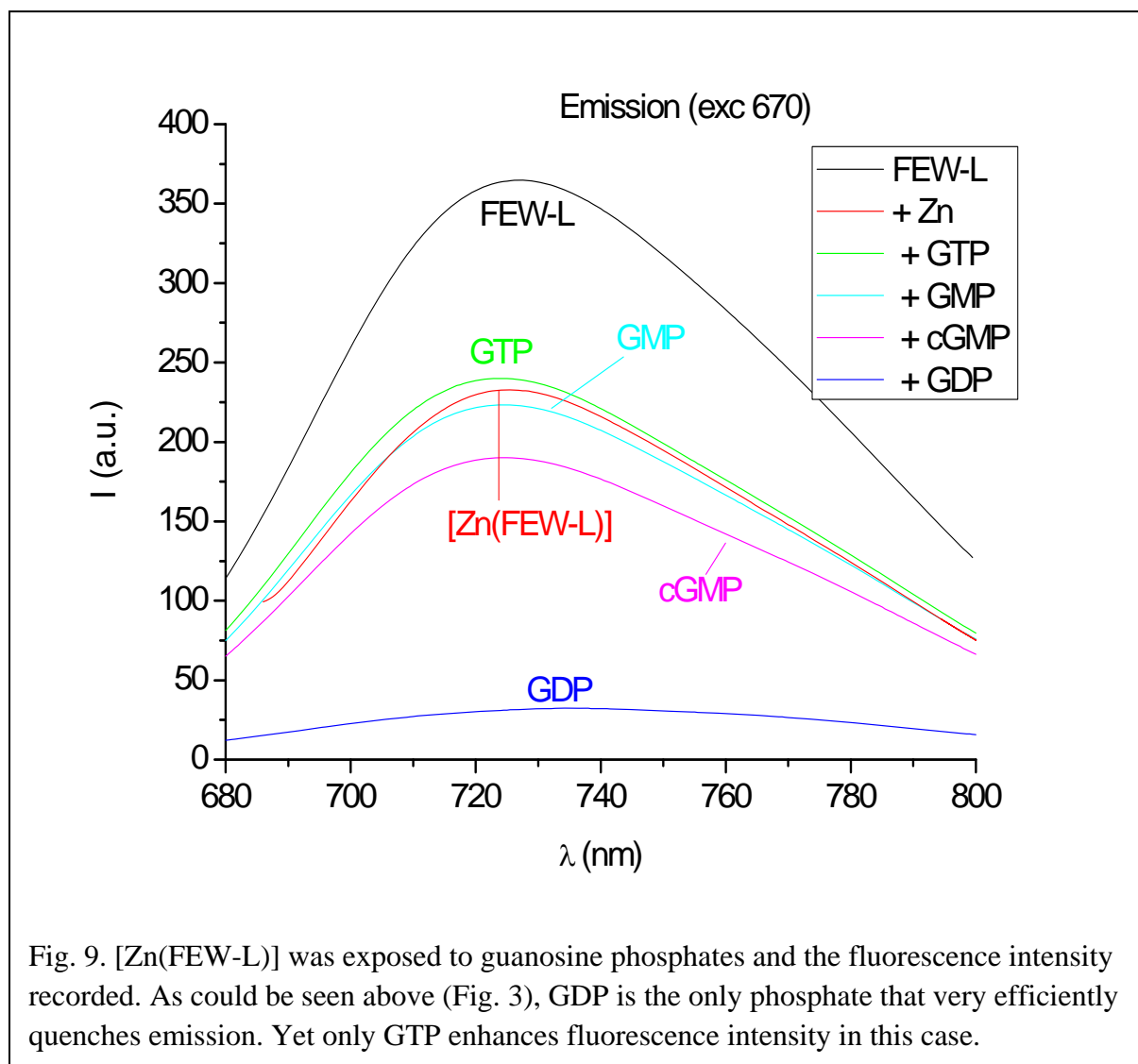
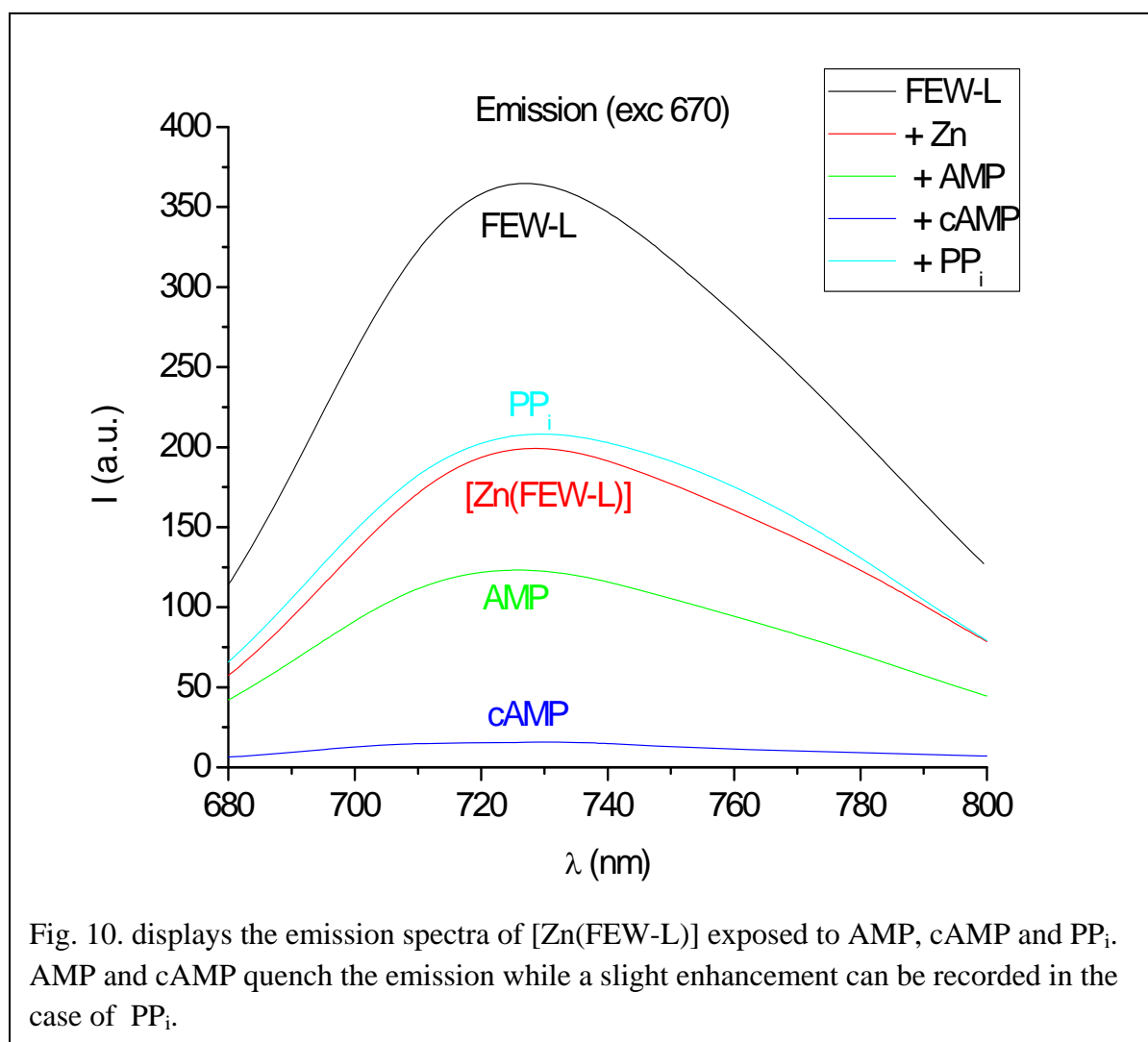


Fig. 9. [Zn(FEW-L)] was exposed to guanosine phosphates and the fluorescence intensity recorded. As could be seen above (Fig. 3), GDP is the only phosphate that very efficiently quenches emission. Yet only GTP enhances fluorescence intensity in this case.

[Zn(FEW-L)]. GDP quenches fluorescence intensity dramatically, lowering the signal to around 12%. This observation is in line with that of the absorption spectrum. cGMP reduces the signal to roughly 50% from 65% by [Zn(FEW-L)]. The response after the addition of GMP (around 60%) can often merely be distinguished from that of the probe. GTP slightly enhances fluorescence intensity to approximately 67%. GMP and cGMP deviate in their behaviour regarding emission from their absorption spectra. This can be explained by similar considerations as before (see 2.3.1).

Fig. 10 reveals the emission spectra of [Zn(FEW-L)] upon the addition of AMP, cAMP and



PP_i. The adenosine phosphates quench the emission of the probe. Some increase in fluorescence intensity (approximately 58%) occurs when PP_i is added. A like behaviour was attest to [Zn(FEW-L)] in the absorption spectra. AMP reduces the signal of FEW-L by roughly 20% more than zinc. cAMP reduces fluorescence intensity to below 5%. Similar considerations apply here as in section 2.3.1 for a possible explanation. A fair resolution could be achieved as well.

Fig. 11 depicts the fluorescence intensity of [Zn(FEW-L)] being exposed to adenosine

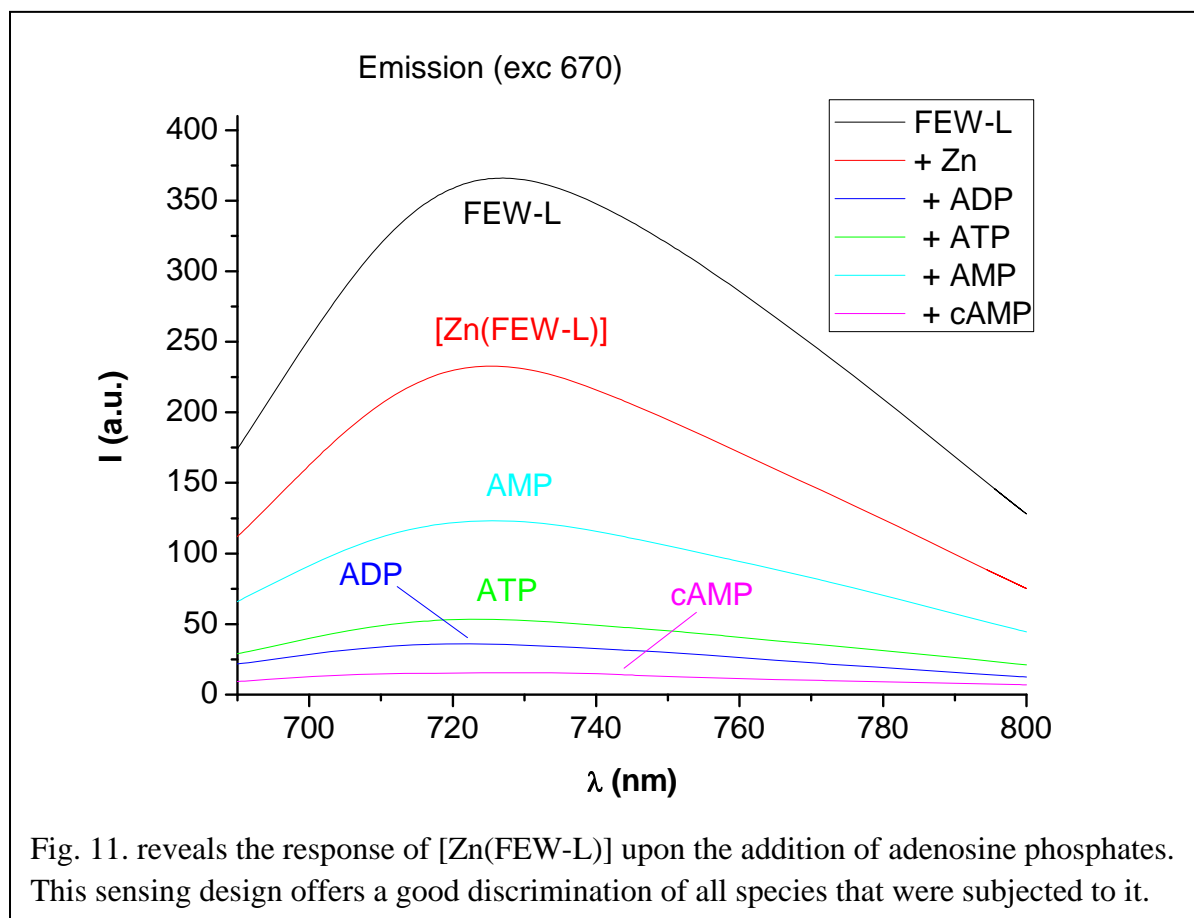
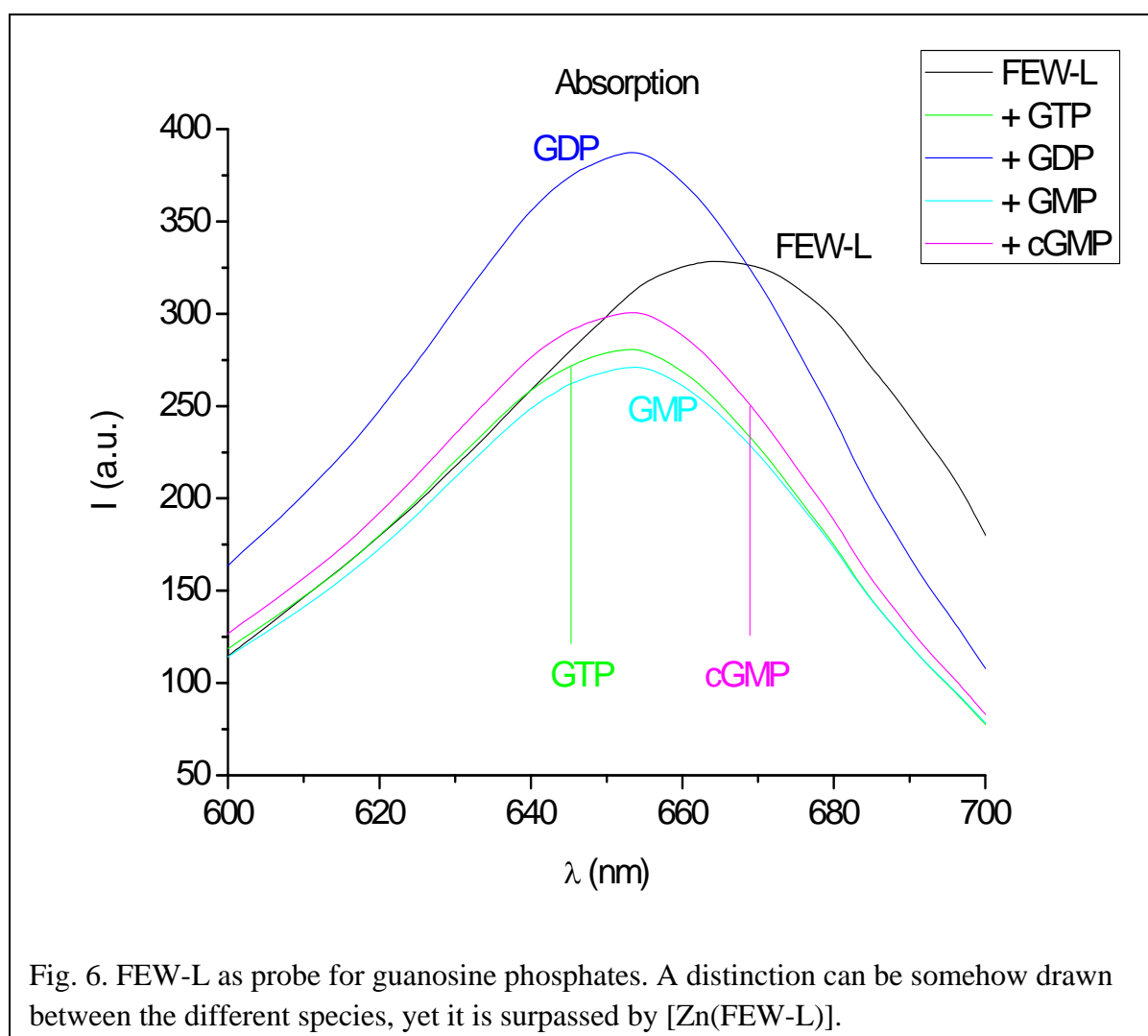


Fig. 11. reveals the response of [Zn(FEW-L)] upon the addition of adenosine phosphates. This sensing design offers a good discrimination of all species that were subjected to it.

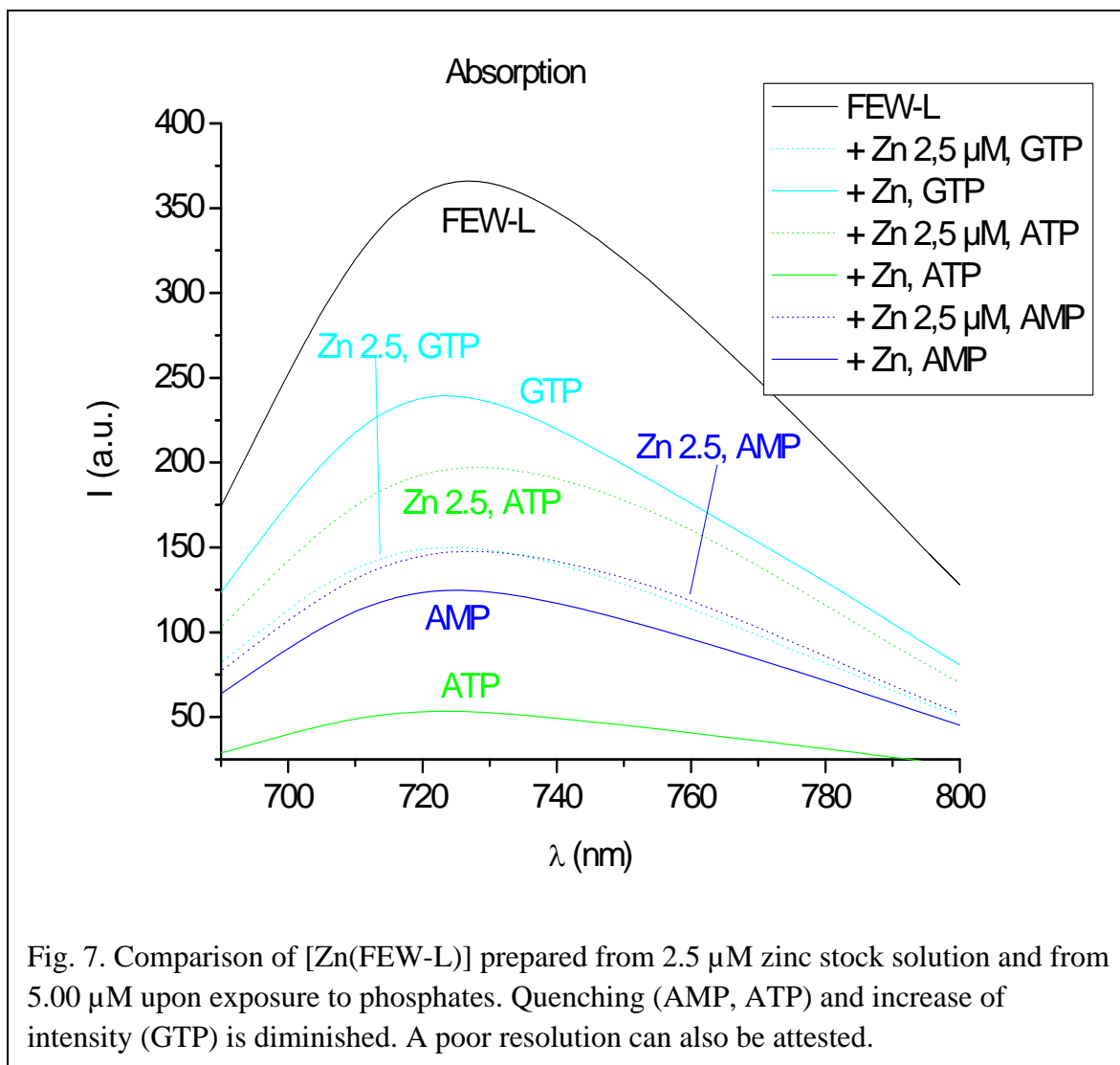
phosphates. All species quench fluorescence intensity. A distinction can be drawn between all phosphates, thus rendering this sensing design suitable for further applications in probing phosphates.

5.1.3 [Zn(FEW-L)]: Optimization of composition of the complex

This section deals with the optimization of the composition, the ratio of Zn^{2+} /FEW-L, in the probe used herein. For this purpose the zinc content was varied and similar experiments as lined out above were carried out. GDP, for instance, and adenosine phosphates were found to quench [Zn(FEW-L)]. The fluorescence intensity of FEW-L is lowered upon the addition of zinc cations. Thus it is reasonable to investigate whether the addition of a metal to form a complex is essential for this sensing scheme. This was subsequently studied. Fig. 6 displays



the response of FEW-L being exposed to guanine phosphates. Resolution is much poorer than for [Zn(FEW-L)] as probe. Furthermore, it was studied if a lower concentration of zinc ions might suffice for this sensing scheme to be realized. Hence, a solution of $2.5 \mu\text{mol}\cdot\text{L}^{-1}$ zinc was used to form [Zn(FEW-L)] instead of $5 \mu\text{mol}\cdot\text{L}^{-1}$. Fig. 7 offers a comparison of



[Zn(FEW-L)] prepared from different concentrations of zinc stock solution. A better resolution can be achieved if the concentration of zinc stands at $5 \mu\text{mol}\cdot\text{L}^{-1}$. A signal of virtually the same intensity can be recorded for GTP and AMP. ATP can be discriminated, though, albeit on a rather small scale. Hence, it is expedient to choose $5 \mu\text{mol}\cdot\text{L}^{-1}$ zinc stock solution to apply [Zn(FEW-L)] as a phosphate-sensitive probe.

5.2 Summary

This chapter offers a summary of the results obtained from the investigation of [Zn(FEW-L)] as a phosphate-sensitive probe. Table 1 lists the different phosphates that were probed herein and their response. All adenines prompt signals that can clearly be distinguished from one another. This is in line with theoretical considerations pertaining to their structure and number of charge. While all species possess the same aromatic, nucleic base, they are distinct by their size. Moreover, cAMP is rather sterically demanding, even more so than the already bulky AMP, ADP, and ATP. The number of negative charges needs to be taken into account as well. Thus many modes of binding to FEW-L are possible, i.e. electrostatically or through π - π or cation- π interaction. Yet free zinc cations and these in [Zn(FEW-L)] need to be considered as well. Phosphates can precipitate zinc. The sugar and base should increase solubility though. Thus the dominating factor is interaction with FEW-L and not that with zinc dications. While all adenosines decrease intensity, P_i and PP_i increase it. P_i is in position to precipitate $Zn_3(PO_4)_2$. A like behaviour can be expected of PP_i . In both cases not enough zinc is available to precipitate all phosphate. While PO_4^{3-} will impact pH substantially, $P_2O_7^{4-}$ will only be capable of doing so by a much smaller degree as the pK_a values differ by a factor of 1000. Most guanines increase intensity while only GDP lowers it. The same considerations as for the adenosines apply here, regarding structure etc. Yet interaction with zinc seems to be the driving force here as the low signal from [Zn(FEW-L)] is recovered mostly.

Table 1 Change of Absorption of [Zn(FEW-L)] upon being exposed to these various phosphates. They are grouped according to the experiments from section 2.3.

	Phosphate	Intensity (a.u.)	% of FEW-L
FEW-L	-	328	0
[Zn(FEW-L)]	-	164	50
ATPase reaction	ATP	77	23
	ADP	33	10
	P _i	392	120
Guanines	GTP	222	68
	GDP	31	9
	GMP	206	63
	cGMP	184	56
AMP, cAMP, PP _i	AMP	118	36
	cAMP	20	6
	PP _i	200	61
Adenines	ATP	77	23
	ADP	33	10
	AMP	118	36
	cAMP	20	6

Table 2 lists the fluorescence intensity of all phosphates probed by [Zn(FEW-L)]. All adenines cause a further quenching of the signal of the probe. Their response can clearly be discriminated. The explanation for this behaviour is parallel to that offered for the absorption spectra. PP_i and P_i have been found to enhance fluorescence intensity. Again, this is due to a change in pH and the solubility product, and thus precipitation, of these zinc phosphates. The responses of the guanosine phosphates are also clearly distinct, for an explanation see above (Table 1 and text).

It could be proved that [Zn(FEW-L)] is a convenient probe for numerous phosphates. NIR probes hold advantages over other fluorescent probes. These include deep penetration of tissue, non-destructive measurements, inexpensive set-ups among others. The [Zn(FEW-L)] probe offers features most convenient for a sensing scheme, i.e. a good resolution and sensitivity, up to 1 μ M and below. Yet LOD needs to be validated. Thus [Zn(FEW-L)] can be applied in probing phosphates and can possibly be used for monitoring enzyme activity. It remains to be seen whether or not two or more phosphate species can be examined simultaneously. Initial experiments have pointed in that direction though. Thus, further studies should be carried out regarding limit of detection and reproducibility. Different phosphate concentrations need to be probed which so far could not be discriminated. Moreover interference from other metal ions needs to be taken into account.

Table 2 Intensity of Emission of [Zn(FEW-L)] upon being exposed to these various phosphates. They are grouped according to the experiments from section 2.3.

	Phosphate	Intensity (a.u.)	% of FEW-L
FEW-L	-	364	0
[Zn(FEW-L)]	-	231	63
ATPase reaction	ATP	54	15
	ADP	35	10
	P _i	405	111
Guanines	GTP	222	61
	GDP	31	9
	GMP	206	57
	cGMP	184	51
AMP, cAMP, PP _i	AMP	118	32
	cAMP	20	5
	PP _i	200	55
Adenines	ATP	77	21
	ADP	33	9
	AMP	118	32
	cAMP	20	5

6. Summary

6.1 English

Phosphate-sensitive probes have been synthesized and characterized. The focus was on the (bio)phosphates ATP, ADP, AMP, cAMP, GTP, GDP, GMP, cGMP, P_i and PP_i. One design is utilizing the quenching of APTS or HPTS by viologen derivatives which is reversed upon addition of phosphates. Three viologens were tested for their applicability. The compound TEAPB in combination with HPTS yielded the most promising results. The probe allows for discrimination between all phosphate species investigated. This analytical design offers good resolution and sensitivity. It may be applied to monitoring enzyme activity, especially enzymes dealing with adenosines (PQI) or guanosines (PQII). LOD is above 1 μM. More experiments and further characterization is required for future applications though. It is disadvantageous for probing two phosphate species simultaneously.

The second detection scheme is based on a complex of zinc (2+) and a NIR dye FEW-L. The probe [Zn(FEW-L)] is quenched by all phosphates (same species as above). Excitation and emission spectra were recorded. In both cases all phosphates pertaining to possible biological applications could be sensed. A good resolution coupled with good sensitivity could be attested. Hence, this concept can be harnessed for future applications in monitoring enzyme activity in general or ATPase in particular. It is most suitable for P_i and adenosines. LOD is 1 μM and lower. Further characterization is needed in order to apply this sensing scheme to the determination of enzyme activity. It remains to be seen if two or more phosphate species can be probed simultaneously.

6.2 Deutsch

Phosphatsensitive Sonden wurden synthetisiert und charakterisiert. Der Fokus lag dabei auf Biophosphaten ATP, ADP, AMP, cAMP, GTP, GDP, GMP, cGMP, P_i und PP_i . Eine Messanordnung macht sich das Quenchen von APTS oder HPTS durch Viologenderivate zu nutzen welches bei Zugabe von Phosphaten umgekehrt wird. Drei Viologene wurden auf ihre Verwendbarkeit getestet. Die Verbindung TEAPB in Kombination mit HPTS lieferte die vielversprechendsten Resultate. Die Sonde ermöglicht eine Unterscheidung zwischen allen getesteten Phosphaten. Dieser analytische Aufbau bietet gute Auflösung und Sensitivität. Es könnte möglicherweise dazu benutzt werden, Enzymaktivitäten zu verfolgen, besonders solche Enzyme die mit Adenosinen (PQI) oder Guanosinen (PQII) zu tun haben. LOD ist größer $1 \mu\text{M}$. Mehr Experimente und eine weitere Charakterisierung sind für zukünftige Anwendungen nötig. Es ist unvorteilhaft damit zwei Phosphatspezies gleichzeitig zu detektieren.

Die zweite Messanordnung basiert auf einem Komplex aus Zink (+2) und einem NIR Farbstoff FEW-L- Die Sonde $[\text{Zn}(\text{FEW-L})]$ wird von allen Phosphaten gequencht (die gleichen wie oben wurden untersucht): Anregungs- und Emissionsspektren wurden aufgenommen. In beiden Fällen konnten alle Phosphate die in biologischem Kontext wichtig sind erkannt werden. Eine gute Auflösung zusammen mit einer guten Sensitivität konnte attestiert werden. Deshalb kann dieses Konzept für zukünftige Anwendungen beim Verfolgen von Enzymaktivität im Allgemeinen, oder ATPase im Besonderen, genutzt werden. Es ist am besten geeignet für P_i und Adenosine. LOD ist $1 \mu\text{M}$ und kleiner. Weitere Charakterisierung ist vonnöten um dieses Modell für die Bestimmung von Enzymaktivität zu nutzen. Es muß noch gezeigt werden, ob zwei oder mehr Phosphatspezies nebeneinander bestimmt werden können.

7. CURRICULUM VITAE

Personal Data

Name: Thomas Lang
Nationality: German
Date of birth: 17th June 1983

Education and Training

Sep 1989 – July 1993: Elementary School Hirschau
Jan 1993 – March 2002: Gregor-Mendel-Gymnasium Amberg
Oct 2003 – April 2009: University of Regensburg, Chemistry (diploma),
Nanostructured Surfaces for DNA Hybridisation
with V.M. Mirsky, O. S. Wolfbeis
May 2009 – May 2012: PhD at University of Regensburg, Institute of
Analytical Chemistry, Chemo- and Biosensors

Professional experience

Aug 1999 – Sep 2004: Three to six week stints at Depot of Amberger
Kaolinwerke, Eduard Kick GmbH & Co. KG
Aug 2005 – Sep 2007: Six week stints at Kaolin Refinement at Amberger
Kaolinwerke, Eduard Kick GmbH & Co. KG

21st - 28th of Jul 2011:

Participation in Advanced Study Course on Optical
Sensors (ASCOS), Ireland

Languages

German: native language

English: fluency

Latin: basic knowledge

Greek: basic knowledge

8. List of Publications

Journal Papers

- I. R. Ali, T. Lang, S. M. Saleh, R. J. Meier, O. S. Wolfbeis, *Optical Sensing Scheme for Carbon Dioxide Using a Solvatochromic Probe*, *Anal Chem*, **2011**, 83, 2846-2851
- II. T. Lang, T. Hirsch, C. Fenzl, F. Brandl, O. S. Wolfbeis, *Surface Plasmon Resonance Sensor for Dissolved and Gaseous Carbon Dioxide*, submitted
- III. C. Spangler, T. Lang, M. Schäferling, *Spectral response of an Methylimidazolium-Derived Polythiophene to ATP and other Phosphates*, *Dyes and Pigments*, accepted, available online ahead of print
- IV. X. D. Wang, J. A. Stolwijk, T. Lang, R. J. Meier, J. Wegener, O. S. Wolfbeis, *Ultra-Small, Highly Stable and Sensitive Dual Nanosensors for Measuring Intracellular Oxygen and pH Directly in Cytosol*, in preparation

Poster Presentations

12th International Conference on Methods and Applications of Fluorescence: Spectroscopy, Imaging and Probes, September 2012, Straßburg, France: “ATP sensitive fluorescence based turn-on probe based on a pyrene-bipyridinium complex”

Oral Presentation

6th International Students Conference “Modern Analytical Chemistry”, September 2010, Prague, Czech Republic: “Luminescent ATPase Assay Using a Phosphate-sensitive Lanthanide Probe” (Print in Book of Abstracts)

6. Deutsches BioSensor Symposium, March/April 2009, Albert-Ludwigs-Universität, Freiburg, Germany: “A Technology of Molecular Tacking: A Control of Surface Density of Immobilized Oligonucleotides to Optimize Hybridization“ (Print in Book of Abstracts)

Erklärung

Hiermit versichere ich, daß ich die vorliegende Arbeit selbst verfaßt und keine anderen Hilfsmittel und Quellen verwendet habe.

Regensburg, den 09.05.2012